MQF_MQP 2045

Engineering Solutions for Ghana E-Waste Problems

A Major Qualifying Project

Submitted to the Faculty of the

WORCESTER POLYTECHNIC INSTITUTE

in partial fulfillment of the requirements for the degree of

Bachelor of Science

by

Lauren Handel
Electrical and Computer Engineering

Sarah Strazdus
Mechanical Engineering

Development Design Lab, March 18, 2021

Approved by:

Professor M. Amissah, PhD

Systems Engineering, Electrical and Computer Engineering Department

Professor M. S. Fofana, PhD

MIRAD Laboratory, Mechanical Engineering Department

Professor Robert Krueger, PhD

Development Design Lab, Department of Social Sciences and Policy

Abstract

The Engineering Solutions for Ghana E-Waste Problems MQP provides a mechanical means to pulverize electronic waste in Agbogbloshie, a roughly 20-acre scrap yard in the heart of Accra, Ghana. Current electronic waste practices have dangerous consequences, including environmental toxicity and relatively far less economic benefit for site workers. The Engineering Solutions for Ghana E-Waste Problems MQP plans to provide a low-cost grinder that will easily integrate into the current recycling process in Ghana. To ensure the grinder can be used in Agbogbloshie, local Ghanaian expertise guided the project's focus on manufacturing and sustainable maintenance. To allow for a multitude of design visualizations, SOLIDWORKS and ANSYS simulation tools were used to build and test several iterations of the design. The grinder is constructed using steel that is plasma cut and welded together. The crushing mechanism pulverizes material upon impact. At the bottom of the crushing mechanism, the material escapes through a mesh with holes that determine the size the material is ground to. The drive system includes a V-belt pulley system to transmit power from an AC motor. Future revisions of the Engineering Solutions for Ghana E-Waste Problems MQP could scale a manufacturing plan based on the final design, design the shredding and separation processes, and determine a grinder integration plan for Agbogbloshie.

Acknowledgements

We would like to thank the following people for all their help on our project:

- Our advisors **Robert Krueger, Mustapha Fofana, and Matthew Amissah** for their help, advice, and guidance throughout the project.
- **Meron Tadesse, Anita Mattson, and Mohammed Mohammed** who provided helpful insight and feedback in our weekly meetings and worked on the Chemistry aspect of the project.
- **Hector Boye**, who visited Agbogbloshie and provided insight on what the waste processors want and need.
- Washburn lab managers, **Torbjorn Bergstrom and Ian Anderson,** who gave feedback on the prototype design and taught us how to use the tools needed for manufacturing.
- **Liam Hemmerling**, who showed us how to use the handheld and table plasma cutter.
- **Barbara Furhman and Alice Clark**, who helped us order the necessary parts and materials.
- **Robert Kirch**, who taught us how to use the Instron for our PCB testing.

Authorship

This list states the primary authors of each section, though many sections were edited by both authors. Any photo without credit was created by the authors of this report. The final report was revised by both team members.

Section	**Author**
Abstract	Lauren
Acknowledgements	Sarah
Problem Statement	Lauren, Sarah
Executive Summary	Lauren
1.1	Lauren
1.2	Lauren
1.2.2	Lauren
1.2.3	Lauren, Sarah
1.3	Sarah
1.3.1	Sarah
1.3.2	Lauren
1.3.3	Lauren
1.4	Sarah
1.4.1	Sarah
1.4.2	Sarah
1.4.3	Lauren
1.5	Lauren
2.1	Sarah
2.2	Lauren, Sarah
2.3	Lauren, Sarah
2.4	Lauren, Sarah
2.5	Lauren
3.1	Lauren
3.2	Lauren

3.2.1	Sarah
3.2.2	Sarah
3.2.3	Lauren
3.2.4	Sarah
3.2.5	Lauren, Sarah
3.3	Lauren
3.3.1	Lauren
3.3.2	Lauren
3.3.3	Sarah
3.4	Lauren
3.4.1	Lauren
3.4.2	Lauren
3.5	Lauren
3.5.1	Lauren
3.5.2	Lauren
3.6	Lauren
4.1	Lauren
4.2	Sarah
4.2.1	Lauren, Sarah
4.2.2	Lauren, Sarah
4.2.3	Lauren, Sarah
4.3	Sarah
4.3.1	Sarah
4.3.2	Sarah
4.3.3	Sarah
4.3.4	Sarah
4.3.5	Sarah
4.3.6	Lauren
4.3.7	Sarah
4.4	Sarah

4.4.1	Sarah
4.4.2	Sarah
4.4.3	Sarah
4.5	Sarah
4.5.1	Sarah
4.5.2	Lauren
4.5.3	Sarah
4.6	Lauren
5.1	Sarah
5.2	Sarah
5.3	Lauren
5.4	Lauren
Appendix A	Lauren, Sarah
Appendix B	Sarah
Appendix C	Sarah
Appendix D	Sarah

Table of Contents

List of Figures

List of Tables

List of Nomenclature

$Ah = battery\ capacity$

$D_1 = diameter\ of\ the\ drive\ shaft\ pulley$

$D_2 = diameter\ of\ the\ motor\ shaft\ pulley$

$D_r = deformation\ of\ the\ PCB\ at\ the\ rupture\ point$

$d = diameter\ of\ the\ drive\ shaft$

$F_B = force\ of\ one\ bearing$

$F_H = distributed\ load\ of\ centrifugal\ force\ exerted\ by\ the\ hammers$

$F_h = centrifugal\ force\ exerted\ by\ the\ hammers$

$F_Q = force\ of\ one\ bearing$

$F_P = force\ of\ the\ shaft\ pulley$

$F_r = rupture\ force\ of\ the\ PCB$

$H_h = height\ of\ the\ hammer$

$I = current$

$K_b = combined\ shock\ and\ fatigue\ factor\ applied\ to\ the\ bending\ moment$

$K_t = combined\ shock\ and\ fatigue\ factor\ applied\ to\ the\ torsional\ moment$

$L = length\ of\ the\ belt$

$M_1 = moment\ at\ first\ cut$

$M_2 = moment\ at\ second\ cut$

$M_3 = moment\ at\ third\ cut$

$M_4 = moment\ at\ fourth\ cut$

$M_b = maximum\ bending\ moment\ in\ the\ drive\ shaft$

$m_h = mass\ of\ the\ hammer$

$m_I = mass\ impacting\ the\ hammer$

$m_p = mass\ of\ the\ PCB$

$M_t = torsional\ moment\ in\ the\ drive\ shaft$

$N = number\ of\ hammers$

$N_1 = speed\ of\ the\ drive\ shaft$

$N_2 = speed\ of\ the\ motor\ shaft$

$N_h = velocity\ of\ the\ hammers$

$n = factor\ of\ safety\ for\ the\ drive\ shaft$

$P = power$

$r_1 = radius\ of\ the\ drive\ shaft\ pulley's\ pitch\ diameter$

$r_h = radius\ of\ the\ circle\ made\ by\ the\ hammers\ rotating$

$RE = rupture\ energy\ of\ the\ PCB$

$SE_h = specific\ energy\ of\ the\ hammer$

$S_s = allowable\ shear\ stress\ of\ the\ material$

$T_0 = initial\ kinetic\ energy$

$T_1 = tension\ in\ side\ one\ of\ the\ belt$

$T_2 = tension\ in\ side\ two\ of\ the\ belt$

$V = voltage$

$v = velocity\ of\ the\ drive\ shaft$

$V_h = velocity\ of\ the\ hammer$

$W_h = width\ of\ the\ PCB$

$W_p = weight\ of\ the\ shaft\ pulley$

$x = distance\ between\ the\ centers\ of\ the\ pulleys$

$\alpha = angle\ of\ wrap\ for\ the\ belt$

$\beta = half\ the\ groove\ angle\ of\ the\ pulley$

$\sigma_{yt} = yield\ strength\ of\ the\ material$

$\mu = coefficient\ of\ friction\ between\ the\ belt\ and\ pulley$

$\theta = belt\ wrap\ angle$

$\omega_h = angular\ velocity\ of\ the\ hammer$

Problem Statement

Ghanaian people working in Agbogbloshie, the largest electronic waste (e-waste) site in Africa, are not fully benefiting from the economic potential of the e-waste. Instead, it is often shipped back to original equipment manufacturers (OEMs) in Europe for recycling or reuse. WPI's Institute of Science and Technology for Development (InSTeD) is working to develop cost-effective, environmentally safe ways of processing the e-waste so that the benefits accrue to the Ghanaians processing it rather than the multi-national companies they sell to. The current techniques of E-Waste recovery, including burning it to recover precious metals or cannibalizing it to repair other machines, could be improved to fully realize the value of the processed waste in Ghana.

Executive Summary

Agbogbloshie, located in Accra, Ghana, is one of the largest electronic waste (e-waste) and scrap metal dumps in the world (Amoyaw-Osei, et al., 2011). Between 10,000 and 13,000 metric tons of e-waste are treated annually in Ghana and between 121,800 to 201,600 Ghanaians depend partially or fully on informal e-waste refurbishing and e-waste recycling for their livelihoods (Prakash & Manhart, 2010). Based on the total number of people employed in the refurbishing and e-waste recycling sector and their average salaries, it is estimated that the sector contributes between US $105 to 268 million indirectly to the Ghanaian national economy. Despite the huge impact on the Ghanaian economy, most of the people employed in refurbishing and e-waste recycling sector in Ghana continue to live in extreme poverty (Prakash & Manhart, 2010).

Waste processors offload, sort, dismantle, and incinerate e-waste items for reuse and recycling (Daum, 2017). In our interview with Hector Boye of the Ghana Institution of Engineering, he described several 20-40 foot trailers filled with secondhand electronic parts from fridges, TVs, and computers on site at Agbogbloshie. All parts have value because the waste processors can take them apart and use them to refurbish other equipment. This project focuses on pulverizing and recycling printed circuit boards, or PCBs. PCBs are platforms on which integrated circuits and other electronic devices and connections are installed and they are typically made of FR-4 plastic, copper, gold, and other precious metals (Donadkar & Solanke, 2016). Our project aims to develop a cost-effective, environmentally safe way of processing these PCBs in Agbogbloshie so that the benefits accrue to the Ghanaians processing it rather than the multi-national companies that sell it back to them.

Co-design was the guiding design principle for this project. Co-design refers to the collective creativity between designers and those not trained in design who are involved in the design development process (Sanders & Stappers, 2008). As co-design has become a more widely used process, the roles in the design process have changed. In the classical design process, the user would be a passive object of study, the researcher would bring knowledge from theories, observation, and interviews, and the designer would passively receive this knowledge and use their creativity to develop ideas and concepts. In the co-design process, the roles are much more intertwined. The user now plays a role in the knowledge, idea, and concept development, using their expertise from experience. The researcher and designer support the user by providing tools

for ideation (Sanders & Stappers, 2008). We investigated several design processes such as Norman's Human Centered Design (HCD) and variations of the Engineering Design Process to develop our project's co-design process, as shown below in *Figure 1*. The e-waste processors in Agbogbloshie can provide critical creativity and knowledge to the design development process to ensure the e-waste grinder can be manufactured and maintained in Agbogbloshie. This project presents a design idea for others to absorb and build upon to improve the co-design.

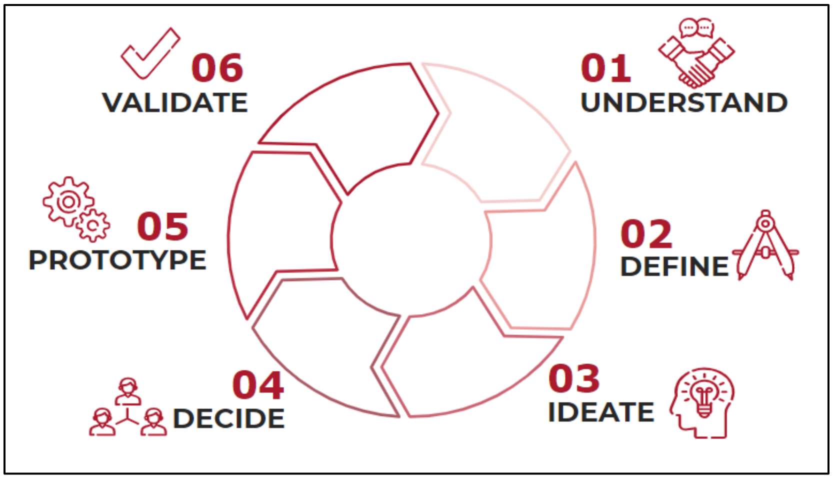

Figure 1: Co-design process for the Engineering Solutions for Ghana E-Waste Problems MQP

Typically, the PCB recycling process can be described by shredding, grinding, and chemical separation to recover the precious metals from PCBs. First, the boards are shredded down to smaller chunks via a machine resembles a paper shredder, where the two sets of discs rotate and cut up the material (Prosino, 2020). Then the boards are grinded using a mill to create a very fine powder. Lastly, the fine powder can be used in a chemical separation process where the gold is extracted. This chemical process is being researched in our counterpart MQP by Mohammed Mohammed, who designed experiments to determine the best method for extracting the gold from the PCB powder. This project focused on the grinding step specifically to meet the waste processors' needs to fully pulverize the PCBs.

After focusing in on the grinding step, we researched different grinding methods and came up with unique designs through ideation. We used a decision matrix to choose between the cutting mill, hammer mill, ball mill, and sandpaper grinder. Each of these machines met the basic requirements, but it was important to consider the machines in the context of Ghana and the waste processors' needs. The decision matrix rated the safety, usability, cost, assembly, maintainability, and efficiency of the grinding methods. The hammer mill received the highest weighted score, so we chose to design a hammer mill that can be fully manufactured, built, and maintained in Agbogbloshie. Hammer mills work by crushing and pulverizing the material upon impact.

The prototype of our grinding mechanism includes the following main parts of the assembly: the funnel cover, upper crushing chamber, bearings, pulleys, stand, motor, bottom crushing chamber, hammers, rotor discs, and the mesh. The design works by adding the PCB through the top funnel, having the hammers rotate and grind the PCB in the middle crushing chamber, and then the grinded power exits through the mesh. The main body and rotor assembly of the grinding mechanism was manufactured from sheet metal at WPI. A manufacturing plan was developed and executed that included plasma cutting, drilling, bending, cutting with a table saw, welding, and assembling. Design improvements were made as we iterated through our co-design process and incorporated feedback from Hector Boye and shop managers in Washburn Shops at WPI to improve the usability and manufacturability of the machine. We used an Instron, or a Universal Test Machine, to conduct a three-point bending test on the PCB to prove that the hammers will be able to fracture and grind the PCB.

Based on our experience with codesign and building the prototype, we propose recommendations for the continuation of this project. Future MQP work could include testing the prototype and refining the design with more co-design input from waste processors. Another MQP could focus on designing an effective shredder for the first step of PCB recycling. Future IQP students could interview waste processors in Ghana to determine the best plan to integrate and maintain the grinder and future designs of the recycling process. Further future work involves interviewing The GRATIS Foundation of Ghana, an organization that manufactures grinding and milling equipment in Ghana, to source all materials and develop a plan for manufacture. This project represents the first step toward a fully codesigned, cost-effective, and environmentally safe way to process PCBs in Agbogbloshie to directly benefit Ghanaian waste processors.

Chapter 1: Background & Problem Definition

1.1 Introduction

This chapter will provide important background information for the understanding of the project. Section 1.2 will introduce the topic of electronic waste (e-waste), how it can be recycled, and its global environmental impact. It was important to investigate current e-waste recycling and refurbishing techniques so that the project could build upon other practices. The next section, 1.3, will introduce the area of Agbogbloshie, and dive into the current practices and health conditions of the workers. Next, in section 1.4 international development will be reviewed, looking into how co-design will affect the project. Finally, a summary will wrap up the most important topics leading into the next section.

1.2 E-Waste Overview

"E-waste," "electronic waste," "e-scrap," and "end-of-life electronics" are terms often used to describe used electronics that are nearing the end of their useful life, and are discarded, donated, or given to a recycler. Though "e-waste" is the commonly used term, the US Environmental Protection Agency (EPA) considers e-waste to be a subset of used electronics. E-waste specifically refers to materials that can be reused, refurbished, or recycled to minimize the waste that might end up in a landfill or improperly disposed of in an unprotected dump site either in the US or abroad (EPA, 2020). Printed circuit boards (PCBs), as shown in *Figure 2*, are often a desirable target for e-waste recycling.

PCBs are platforms on which integrated circuits and other electronic devices and connections are installed. The materials present in PCB are classified into three groups: organic, metals, and ceramics. PCBs contain many electric/electronic components (EECs), such as condensers, inductors, resistors, relays, diodes, capacitors, and IC chips. In general, PCBs consist of about 30% metals, including Copper (~16%), Tin (~4%), Iron (~3%), Nickel (~2%), Lead (~2%), Zinc (~1%), Silver (0.05%), Gold (0.03%), Palladium (0.01%), and other metals (<0.01%), and non-metals constitute the remaining approximately 70% (Goosey & Kellner, 2003). PCBs also contain hazardous metals such as chromium, lead, beryllium, mercury, and cadmium (Donadkar & Solanke, 2016). Most printed circuit boards use FR-4, a glass-reinforced epoxy laminate material, as the substrate for manufacture. FR-4 functions well as an electrical insulator, has a good strength-to-weight ratio, and is flame resistant (Azar & Graebner, 1996). PCBs vary in thickness, ranging from 0.032" to 0.062", depending on whether they are single our double sided.

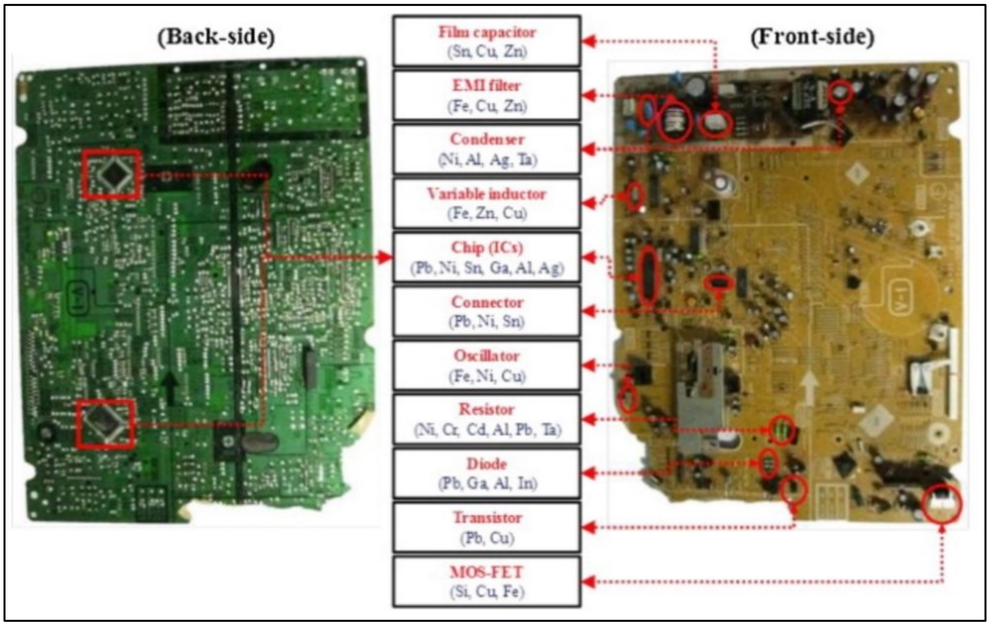

Figure 2: PCB with categorized electric/electronic components (EECs) (Lee, Kim, & Lee, 2012).

Desktop computers are rich sources of e-waste – including everything from iron to plastics to gold and other precious metals in the printed circuit boards and connectors. More than 80% of the weight consists of silica (glass), plastics, iron, and aluminum. According to the Microelectronics and Computer Technology Corporation (MCC), "Precious and scarce materials account for only a small percentage of the total weight. Nevertheless, the concentration of such metals, e.g., gold, is higher in a desktop computer than found in naturally occurring mineral ore" (MCC, 1996). This detailed breakdown of the metals found in desktop computers can inform the e-waste separation process, especially at the chemical separation step, so that the most precious metals are preserved.

1.2.2 E-Waste Recycling Process

The foundation of electronics recycling is the efficient separation of materials. As shown in *Figure 3*, the typical process for industrial e-waste recycling includes the following steps: course crushing, fine-pulverizing, and electrostatic separating into metals and non-metals (Donadkar &

Solanke, 2016). Shredding the e-waste facilitates the sorting and separation of plastics from metals and internal circuitry, and waste items are shredded into pieces as small as 100mm to prepare for further sorting (Haque, 2019). In some manufacturing settings, a powerful overhead magnet separates iron and steel from the waste stream on a conveyor belt. Further mechanical processing separates aluminum, copper, and circuit boards from the material stream—which now is mostly plastic. Water separation technology is then used to separate glass from plastics. Chemical separation technology can also be used to locate and extract any remaining metal remnants from the plastics to purify the stream further (Haque, 2019).

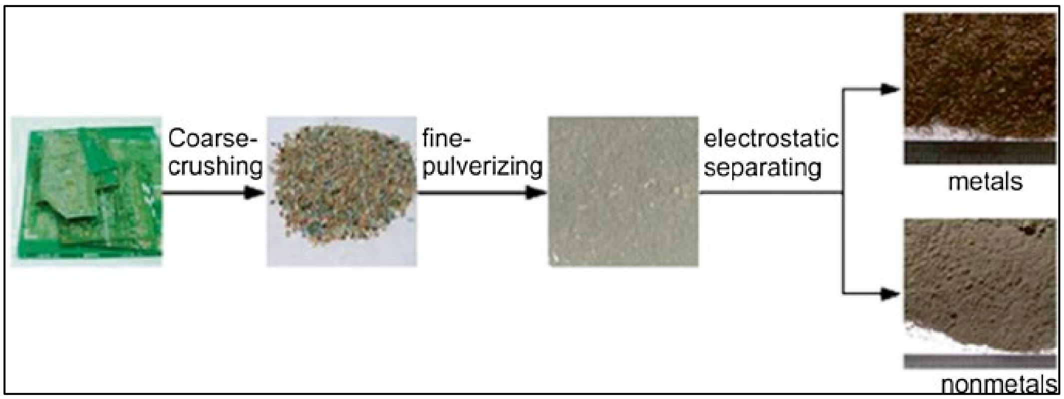

Figure 3: Typical process for industrial e-waste recycling (Donadkar & Solanke, 2016).

In *Figure 3*, above, the course crushing step is typically accomplished with a shredder, the fine pulverizing is typically done with a grinder, and electrostatic separating can be referred to as chemical separation. The typical separation methods have several obstacles to use as an industrial process for recycling waste PCBs, such as their limited processing capacity, high energy consumption, toxic gas leakage, and the used hot fluid medium and chemical reagent disposal (Lee, Kim, & Lee, 2012). In an effort to avoid these obstacles, Lee, Kim, & Lee (2012) designed and manufactured one effective apparatus for removing EECs from PCBs, as shown in *Figure 4*.

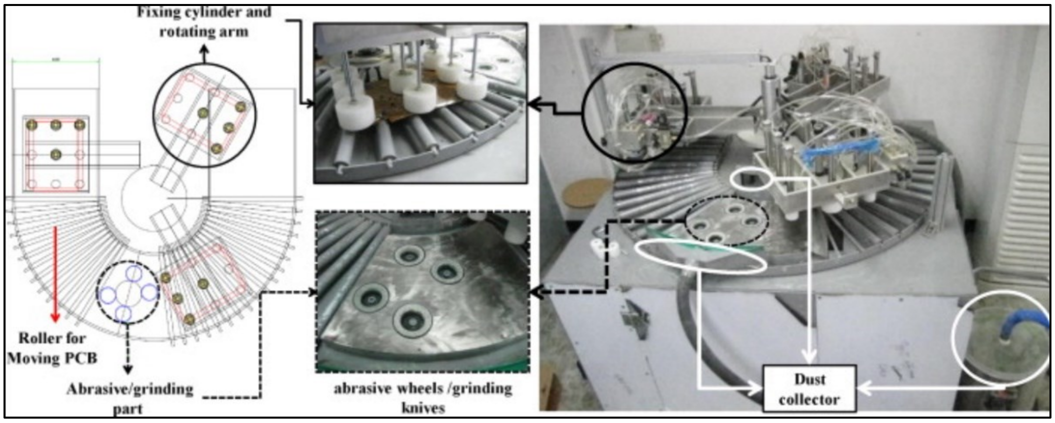

Figure 4: A schematic diagram for one method for disassembling EECs from WPCBs, including a feeding method and diamond grinders (Lee, Kim, & Lee, 2012).

This apparatus primarily consists of three units with different roles. The first unit is a feeding unit with three rotating arms, one of which has nine pressing cylinders to fix and move the PCB. The second unit removes the EECs from the PCB with four diamond grinders that wear down the solder joints on the back-side of PCBs at a speed of ~5500 rotations per minute (rpm). The third unit collects the separated EECs and the abrasion powders, which contain substantial metals, using a vacuum and back-filter system. The EECs were disassembled under several treatment conditions with variations in the speed of grinder between 2500 and 5500 rpm, the height of grinder (0.5, 1.5 mm) and the moving speed of the PCB on the apparatus (1, 3, 5 cm/s) (Lee, Kim, & Lee, 2012). *Figure 5*, below, shows an example of the PCBs as received, followed by the results of this study.

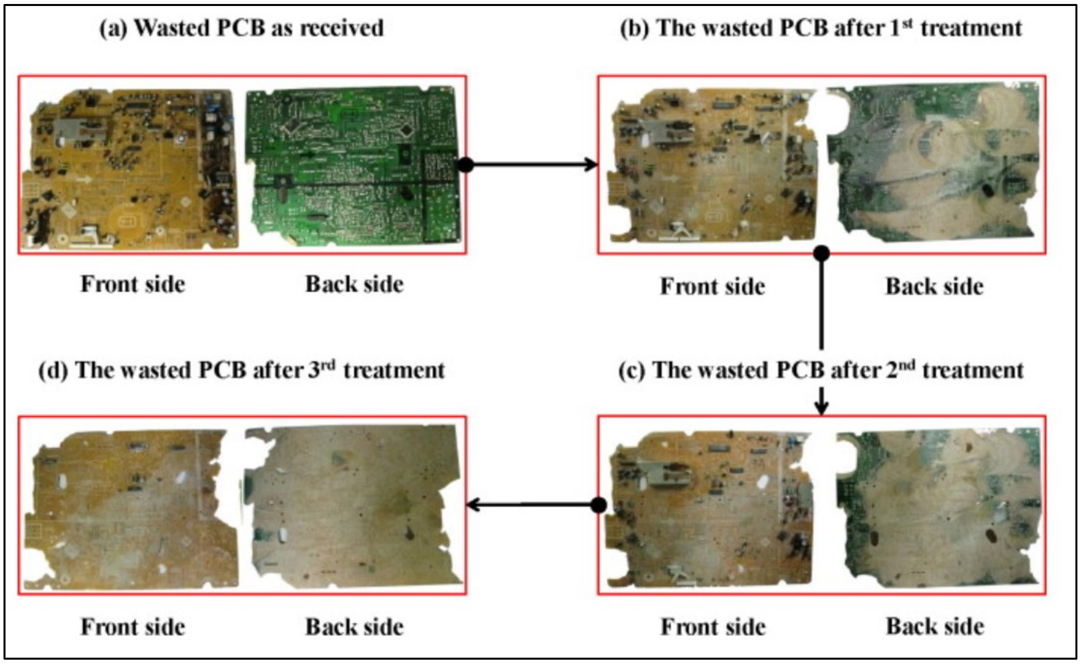

Figure 5: WPCB breakdown following repeated physical treatment (Lee, Kim, & Lee, 2012).

At the lower grinder speed of 2500 rpm, the efficiency of e-waste recovery increased gradually with a decrease in the PCB moving speed. For a grinder height of 1.5 mm, e-waste recovery for the 1 cm/s moving speed was lower than that for the 3 cm/s moving speed. According to Lee, Kim, & Lee (2012), the reason for this result (i.e., higher efficiency in spite of a faster moving speed) may be explained by the complicated structure of a PCB, especially the presence of EECs on the back side of the PCBs. For the treatment of PCBs at the speed of 5500 rpm and the height of 1.5 mm, the efficiency increases dramatically with repeated treatments and reaches the maximum efficiency values of 97.7% recovery at the 3 cm/s moving speed and 98% recovery at the 1 cm/s moving speed (Lee, Kim, & Lee, 2012).

1.2.3 Global Environmental Impact of E-Waste

According to McFadden (2020), approximately 50 million tons of e-waste is discarded globally every year. The USA alone creates about 11 million tons of e-waste every single year. Of that, a negligible 12.5%, or so, is actually recycled or reprocessed. In many cases, e-waste is simply shipped to Asia and Africa to be recycled. Once there, it is usually sorted and sold for scrap, or simply burnt to either dispose of it or attempt to extract valuable materials (McFadden, 2020). Many Western nations have implemented e-waste regulations to attempt to curb the more dangerous aspects of disposing of old electronics because e-waste contains extremely toxic chemicals like lead, cadmium, dioxins, gurans, arsenic, mercury, DDT, PCB, chromium, vinyl chloride, antimony, beryllium, etc. (McFadden, 2020).

The recycling of e-waste can have a very negative impact on the environment. These harmful recycling methods typically include open burning of PCBs, cables, and plastics, burning wires for copper recovery, harmful chemical processes to recover gold from PCBs, plastic chipping and melting, and dismantling of cathode ray tubes. These processes release toxins into the air. Sépulveda & Schluep (2009) conducted a study to review the effects of poor waste electrical and electronic equipment (WEEE) recycling techniques and developed a diagram to show how they affect the environment, seen in *Figure 6*. They determined that the toxins released in these processes could be separated into three groups: original substances, auxiliary substances, and by-products. These substances can be found in the following types of emissions: leachates from dumping activities, particulate matter from dismantling, ashes from burning activities, wastewater from dismantling and shredding, effluents from cyanide and other leaching activities or mercury amalgamation, and fumes from mercury amalgamate "cooking," de-soldering, and other burning activities. The soil is then affected by the dumping of heavy metals and flame retardants, where substances leach through the soil and form inorganic and organic complexes. The effluents can also leach into bodies of water as seen in *Figure 6*. Dismantling activities cause pollution as the dust can get into the air, water, and soil. The thermal and metallurgical processes, such as the burning of copper wires, release some of the most hazardous pollutants, poly-halogenated dioxins and furans, into the environment. As *Figure 6* depicts, there are many different pathways for these toxins and pollutants to get into the environment, impacting ecosystems and human health (Sépulveda & Schluep, 2010). In *Figure 6,* the Ovals represent the types of emission substances, the Continuous Bold Lines represent the fate of the original and auxiliary substances, the Dotted Bold Lines represent the fate of the by-products, the Black Arrows with a Bold Dot represent material transport fluxes between treatments, and the Fine Dashed Arrows represent general environmental pathways (Sépulveda & Schluep, 2010).

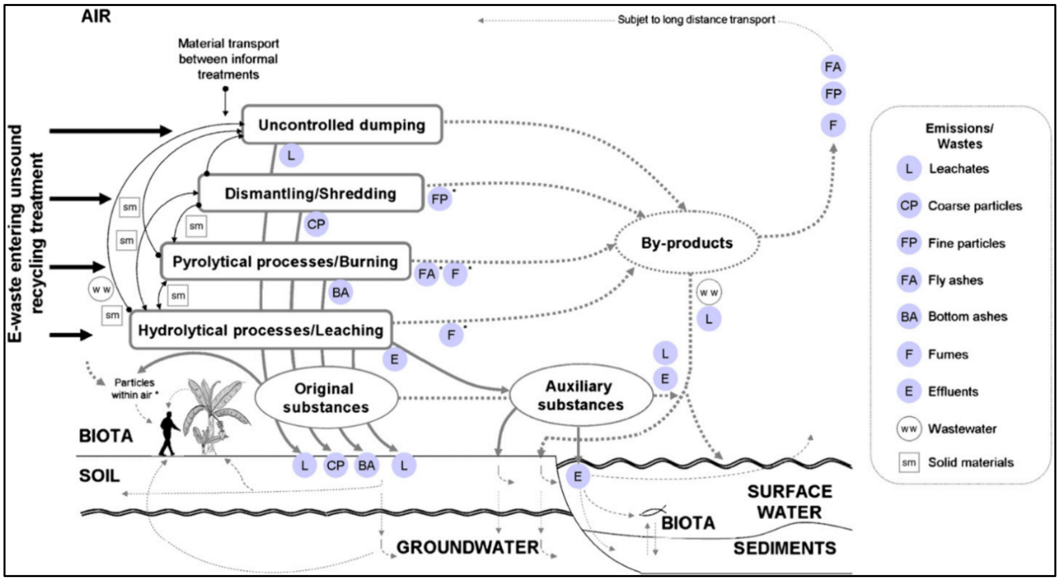

Figure 6: Types of produced emissions and environmental pathways (Sépulveda & Schluep, 2010).

With these pollutants, there are concerns about the effect it has on human health. A study done by Sépulveda and Schluep (2010) showed that the most vulnerable groups affected by the pollutants are pregnant women and children. In Guiyu, a large e-waste site in China, it was found that eighty percent of children suffered from respiratory diseases and are at a higher risk for lead poisoning. Guiyu residents were also shown to be exposed to PBDEs and dioxins, with levels twice as high in dismantling workers than normal. While the fine particulate matter tends to affect human lungs, the larger coarse particulate matter can irritate the eyes, nose, and throat (Sépulveda & Schluep, 2010).

Hazardous toxins from improper WEEE recycling can also have indirect effects on people, as shown by Sépulveda and Schluep's (2010) study. There is evidence to suggest that hazardous dust from the WEEE recycling can be transported into surrounding areas, causing a risk of secondary chemical exposure. Dust samples from a schoolyard and open-air food market in Guiyu showed high concentrations of lead, copper, nickel, and zinc. Toxins in the open-air food market are a huge concern as this means the food items sold can easily be contaminated. Soil contamination proves to be another concern for food contamination. In Guiyu, there was evidence to show that there is slow uptake of these harmful compounds over an extended period. Consumption of food contributes to approximately 90% of exposure to dioxins and furans. Dismantling and shredding residues are also entering the rivers, which can pose a huge threat to the ecosystem and human health. Using these contaminated waterways for agriculture and aquaculture, or even drinking water, poses an even bigger threat (Sépulveda & Schluep, 2010). Improper WEEE recycling not only affects the workers there, but surrounding areas.

While the main portion of this study was conducted in one e-waste site in Guiyu, there is strong evidence to show that all informal WEEE practices can harm the environment and human health (Sépulveda & Schluep, 2010). Another study was conducted in Agbogbloshie and Koforidua by Amoyaw-Osei et. al. (2011), and that showed high levels of copper, lead, tin, antimony, cadmium, and zinc in the soil and ashes. In Agbogbloshie, the market can become flooded, causing contaminated dusts and soils to flow into the lower-lying lagoons, the Odaw River, and ultimately the ocean. The burning of copper wires plays a large role in the pollutants at Agbogbloshie, where approximately 200 kg of cable are burned in one hour, leading to a high amount of dioxin emissions. Other sources of pollutants to the air and soil in Agbogbloshie comes from the burning of solid waste such as plastic, CRT glass, PCBs, batteries, etc. (Amoyaw-Osei, et al., 2011). When designing our e-waste grinder, we must be considerate of the toxins that could be released from our process. It will be very important that our e-waste grinder is safe and does not lead to further pollutants. While we cannot solve all the current pollution, we can work to ensure we do not add to it.

1.3 Agbogbloshie: The Largest Electronic Waste Site in Africa

Agbogbloshie, also referred to as Old Fadama, is one of the largest e-waste and scrap metal dumps in the world (Amoyaw-Osei, et al., 2011). It consists of approximately 30,000 people in the upper region of the Korle Lagoon in Accra. What started as a food stuff market, has now developed into a slum of electronic waste (Amoyaw-Osei, et al., 2011).This is due in part to the world's increasing demand for electronic equipment. The enormous amount of e-waste is produced by consumers continually upgrading their devices and tossing out the old ones. The e-waste arrives in Ghana at the Port of Tema before being brought to Agbogbloshie. The waste mainly comes from Western Europe and the United States in huge shipping containers (Yeung, 2019). Hundreds of tons of e-waste end up in Agbogbloshie every month where they are broken apart to salvage copper and other valuable metallic components (Amoyaw-Osei, et al., 2011). *Figure 7* shows the extent of what this site looks like and the vast amount of e-waste.

Figure 7: E-waste piles in Agbogbloshie (Yeung, 2019).

These valuable components are the motivation behind e-waste recycling in Agbogbloshie. Prakash and Manhart (2010) reviewed the way these metals are recovered using tools such as hammers, chisels, and stones. Cables and wires are also often burned to recover the copper. Currently, printed circuit/wiring boards are traded from Ghana to Asia, instead of Ghanaians performing the wet chemical leaching processes necessary to recover these precious metals. The e-waste recovery process has become popular because it requires little previous skills and can provide easy cash. Many poor people from Northern Ghana have turned to e-waste recycling and moved to Agbogbloshie, despite the environmental and health hazards associated with it (Prakash & Manhart, 2010).

1.3.1 Health and Safety of Workers

There is a huge concern about the exposure to toxic chemicals at informal e-waste recycling sites, as Prakash and Manhart (2010) describe. These risks are from improper recycling techniques, such as the open burning of cable and wires. Sometimes PCBs are burned as well to help reduce the amount of e-waste. Other toxins are produced from the burning of insulating foam and tires that help sustain the fires. You can see in *Figure 8*, the open fires at the scrapyard. The dismantling techniques also add to the spread of toxins as the dust is inhaled by the worker. Without proper techniques and protective gear, these toxins become very harmful to the workers (Prakash & Manhart, 2010).

Figure 8: Interview with site workers (Boye & Amoako-Gyimah, 2020)

Some of the toxic elements produced are arsenic, lead, mercury, and copper. These harmful elements have been found in soil, water, ash, sediment, and dust (Srigboh, et al., 2016) Yeung (2019) describes how these toxins have enormous negative effects on the nearly 10,000 workers at Agbogbloshie. Most workers also live at Agbogbloshie, meaning they are continually exposed to these harmful toxins, making their health issues even worse. Some of these problems include burns, back problems, infected wounds, respiratory problems, chronic nausea, and debilitation headaches (Yeung, 2019). Srigboh et. al. (2016) did a study with urine samples taken from men and women who work and live at Agbogbloshie, to better understand their exposure to toxins. It showed high levels of elements in their urine and blood, but more studies are needed to fully understand how bad the health concerns at Agbogbloshie are (Srigboh, et al., 2016). Another concern is that these toxins may be entering the food chain, as the livestock roam and graze on the dumpsite. Recently, a chicken egg from Agbogbloshie was found to exceed the European Food Safety Authority limits on chlorinated dioxins which cause cancer and immune system damage, showing how bad the issue is (Yeung, 2019). These pollutants have also put pressure on the ecosystem and completely destroyed the Odaw River, a place that once was an important fishing ground (Amoyaw-Osei, et al., 2011).

The toxins present at the Agbogbloshie have also had a severely negative effect on neonatal health of Ghanaian infants. According to Daum (2017) of the International Journal of Environmental Research and Public Health, breast milk samples from women residing near the Agbogbloshie Market contained abnormally high concentrations of polychlorinated biphenyls and other brominated flame retardants like PBDE and hexabromocyclododecane (HBCD). While adults endure persistent exposure to e-waste toxins through air, dust, water, and food, nursing infants face an additional potential exposure via breast milk (Daum, 2017). The many exposure routes make infants highly susceptible to metal and chemical toxins from the e-waste site in Agbogbloshie.

1.3.2 Current E-Waste Practices

When e-waste arrives at the Agbogbloshie scrapyard, it gets either sent away to Nigeria or European OEMs for recycling or broken down and burned on site. Second-hand e-waste items, which arrive in containers from Europe and North America in the port in Tema, are offloaded, sorted, dismantled by breakers. A substantial portion of shipments that end up in Accra are rerouted from various African ports, so other African nations also share the blame for Accra's growing e-waste piles (Daum, 2017). The recovered parts are often traded to scrap metal dealers from India and China who are based in Tema (Rapezzi, 2020). The parts that cannot be sold are taken to the dump site where workers light flammable, industrial by-products to burn rubber tires and the plastic off electrical wires to retrieve the valuable metals for resale (Rapezzi, 2020).

According to Hector Boye and Kofi Gyimah Amoako-Gyima's 2020 Initial Field Report from visiting Agbogbloshie, current e-waste practices are carried out by the following key players: collectors, repairers, dismantlers, technicians, component harvesters, burners (Boye & Amoako-Gyimah, 2020). The collectors search for any faulty or obsolete items, including car parts, electronic appliances of all kinds, metals, and cables. They earn close to about $35 a day from buying, collecting, and selling electronic parts. Dismantlers, as shown in *Figure 9*, buy the items from the collectors and either dismantle them for parts or hand them over to repairers who can fix them. The dismantlers seek out cables, circuit boards, transformers, coils, and electric motors so that they can sell them to those who are interested in processing these parts further for copper, brass, and other metals - even gold and titanium. When collectors realized that an item, especially computers, looked in good conditions, they send it to the technicians, or repairers. One repairer that Boye and Gyimah Amoako-Gyima interviewed had some training by a German organization called GIZ in collaboration with the Ministry of Environment Science and Technology of the Republic of Ghana. Without any formal education, he tests these electronic wares to see if they can be worked on and replaces parts with salvaged ones from the dismantlers. Some other repairers had apprenticeship training in repairing computers. Components harvesters are a small group, who are knowledgeable in electronics, who collect rare parts during the dismantling process. Burners collect the wires and any other components which have copper, brass or other expensive metals in them for burning. The burning removes insulations and other materials from the items gathered and the copper is sold at US $3 per kilogram (Boye & Amoako-Gyimah, 2020).

One of the most powerful conclusions from to Hector Boye and Kofi Gyimah Amoako-Gyima's 2020 Initial Field Report was that boards are purchased by the Nigerian immigrants in Ghana who work in the yard. The Nigerians buy the boards at a negotiated, and often low, price from the Ghanaian collectors, then sell kilograms of e-waste to OEMs in Europe. Ghanaian collectors expressed grievances towards the fact that computer manufacturers in Europe buy the boards for the micro-processors to develop new computers and sell them back at full price (Boye & Amoako-Gyimah, 2020).

Figure 9: Waste processors dismantling PCBs (Boye & Amoako-Gyimah, 2020)

The Ghanaian government has done little to manage the informality of the e-waste trade in Agbogbloshie. International regulatory frameworks are partially responsible for overseeing the Ghanaian system, but non-compliance with existing regulations is the norm (Daum, 2017). In 2019, a German development agency GIZ spent €5 million on a health clinic and education program intended to promote sustainable recycling practices with the Agbogbloshie workers. The health clinic is supplemented by a technical training center where workshops on safe dismantling and recycling are held as well as training on activities like soap making, baking and hairdressing, all to support alternative jobs (Rapezzi, 2020). The training center also houses two machines that can shred bunches of wires and cables to enable workers to extract the metals without burning them. The initiative set up by the non-profits Pure Earth and Green Advocacy Ghana are said to process up to 30 percent of the wires and cables that come to Agbogbloshie. However, the shredding machines may not be sustainable as a full solution because they do not always work and they cannot process the full volume of scrap available at the market (Rapezzi, 2020). For now, the burning continues because there is not an end-to-end solution to solve the excessive e-waste problem at Agbogbloshie. Despite significant international attention to Accra's e-waste problem, loopholes within international environmental regulations and treaties provide few incentives and resources for Ghanaians to strengthen protections for its local economy and human health (Daum, 2017).

1.3.3 Economic Impact of E-Waste Industry

According to Prakash and Manhart (2010), in their Socio-Economic Assessment and Feasibility Study on Sustainable E-waste Management in Ghana, with the lack of proper recycling infrastructure in Ghana, metals present in the e-waste are partly lost from the closed loop recycling management. The results of the socio-economic assessment, which took place primarily at the Agbogbloshie metal scrap yard and the Greater Accra region, show that between 10,000 and 13,000 metric tons of e-waste are treated annually in Ghana by the informal sector (Prakash & Manhart, 2010). This assessment also revealed that between 121,800 to 201,600 people in Ghana depend partially or fully on informal e-waste refurbishing and e-waste recycling as a livelihood option. This represents about 1.04% to 1.72% of the total urban population in Ghana, or 0.50% to 0.82% of the total Ghanaian population. Prakash and Manhart (2010) noted that the true value of e-waste recycling is not reflected in the national GDP due to the informal nature of refurbishing and e-waste recycling sector. Based on the data on the total number of people employed in the refurbishing and e-waste recycling sector and their average salaries, it is estimated that the sector contributes between US$ 105 to 268 million indirectly to the Ghanaian national economy (Prakash & Manhart, 2010).

Despite the huge impact on the Ghanaian economy, most of the people employed in refurbishing and e-waste recycling sector in Ghana continue to live in extreme poverty (Prakash

& Manhart, 2010). This socio-economic study revealed that collectors earn between US$70 and $140 monthly, refurbishers earn between US$ 190 to $250 monthly, and recyclers between US$175 to $285 monthly. If the regular supply or collection of e-waste is hindered, these incomes could also go even lower. Most of the people related to refurbishing and e-waste recycling activities, including partial and full dependents, live below nationally and internationally defined poverty lines. *Figure 10,* below, shows a nine-year-old child, Adjoa, who sells small water bags, for drinking and extinguishing fires, to the workers. Many young people, like Adjoa, believe this is just a temporary situation (McElvaney, 2014).

Figure 10: Adjoa, nine, sells small water bags to the workers (Rapezzi, 2020)

1.4 International Development

International development came about after World War II when poverty was discovered on a large scale in Asia, Africa, and Latin America (Escobar, 1995). Escobar (1995) said the solution to poverty, as seen by "developed" or First World countries, was to provide economic growth and development. At this time, the First World was interested in developing Third World countries to ensure they did not fall to communism and would keep access to their resources (Escobar, 1995). Today, international development is defined as the process of working to improve the lives of people through various areas of needs and interests and to provide them with more opportunities. Many of the large international development projects work to end poverty, AIDs, and discrimination against women (The Ultimate Guide for International Development, 2020). The grinder is part of an international development project that focuses harnessing the value of the precious metals found in PCBs to benefit the waste processors at Agbogbloshie.

Beginning development approaches often involved a developed country going to an undeveloped country and providing a solution without fully understanding the problem or their needs. Hulse (2007) described how developers often failed to fully define specific objectives and criteria and followed the concept that "one solution satisfies all needs." These early developers did not consider the traditions, cultures, climates, resources, etc. of the country and how that impacted the problem and solution (Hulse, 2007). It is important for us to not act on this naive belief and understand that we can learn just as much from the workers at Agbogbloshie as they can learn from us. To avoid creating a solution that does not fix the problem, we will use a co-design approach to develop an e-waste grinder that fits the needs of the workers at Agbogbloshie.

1.4.1 The Co-Design Approach

When developing an e-waste grinder for the workers in Agbogbloshie, it is important to work with them and develop something they would use. Oftentimes, solutions are brought to a group of people without fully understanding what the problem is and what their needs are. This is where development can go very wrong. To avoid this, it is important to use a co-design approach to develop our e-waste grinder.

Co-design is defined by Elizabeth B.-N. Sanders and Pieter Jan Stappers (2008) as the "collective creativity as it is applied across the whole span of a design process." This refers to the collective creativity of designers and those not trained in design who are also helping in the design development process (Sanders & Stappers, 2008). In our process, co-designed alongside our WPI project advisors and workers at Agbogbloshie in Ghana. Because we co-designed an e-waste PCB grinder to be used by the workers in Ghana, it was imperative that we designed with them and got their input on what their needs are and how much to design the grinder.

As co-design becomes a more widely used process, the roles in the design process are changing. In the classical design process, the user would be a passive object of study, the researcher would bring knowledge from theories, observation, and interviews, and the designer would passively receive this knowledge and use their creativity to develop ideas and concepts. In the co-design process, the roles are much more intertwined. The user now plays a role in the knowledge, idea, and concept development, using their expertise from experience. The researcher and designer support the user by providing tools for ideation. Similar to the old process, the designer still plays a large role in developing the final designs (Sanders & Stappers, 2008). We will act as the researcher and designer, working alongside the stakeholders, the workers at Agbogbloshie. Our WPI advisors will act as additional researchers to provide more insight from their experiences working on projects.

1.4.2 Benefits of Co-Design

Marc Steen, Menno Manschot, and Nicole De Koning (2011) conducted a literature review to determine the benefits of co-design in service design projects. They organized the benefits into those for the service design project, those for the service's customers or users, and those for the organization. The service design project benefits from better ideas from the users, better knowledge about users' needs by working directly with them, and better idea generation by using the creativity of multiple groups. It can also lead to higher quality of service definition and more successful innovations. And the project management can benefit from better decision making, lower development costs, reduced development time, and continuous improvements. In the benefits for the service's customers or users, there is typically a better fit of the users' needs and the service provided, a higher quality of service, and more differentiated services. These will also lead to a higher satisfaction and loyalty rate of the users. And lastly, in the benefits for organizations categories, co-design leads to improved creativity, improved focus on the users' needs, and better cooperation between different people, organizations, and disciplines. It also often leads to more successful innovations, improved innovation practices with more support and enthusiasm for innovation and change, and better relations between the service provider and customers (Steen, Manschot, & De Koning, 2011). These benefits of co-designs will help to make our project successful.

1.4.3 Co-Design in the Context of the Project

The ideal co-design scenario for this project would have involved engineering a solution alongside the community in Agbogbloshie. Ideal co-design was not realistic for this project because travel to Ghana was not permitted and the pandemic prevented building a close relationship with community members. Instead, a representative from the Ghana Institution of

Engineering visited the e-waste site and communicated their experiences using video chat and email. These mediums helped improve the codesign, however, there was not any direct contact with waste processors or other community members, so it was impossible to truly understand the full perspective. Emotions and experiences can get lost over digital platforms. This begs the question of if we are violating codesign by moving forward with the design despite these limitations. The answer is no because we present this design as an idea for others to absorb and build upon through more extensive codesign. This project lays a foundation for collaboration between community members and future WPI students when circumstances allow for travel.

A co-design process was developed for this project with the following steps: understand, define, ideate, decide, prototype, and verify, as shown earlier in *Figure 1*. In the understand phase, the context of the problem and the targeted outcomes expected from our counterparts in Ghana were thoroughly researched. In the define stage, the team members worked together with the Ghanaian contact, advisors, and each other to collectively define the proposed problem from the cross-cultural perspective. In the ideation phase, team members brainstormed ideas of how to efficiently approach the current problem defined in the understand stage. This stage consisted of individual team brainstorming, followed by a cross-team brainstorming session with the Chemistry focused MQP. In the decide stage a decision matrix was used and cross-functional input across teams to allow the team members to agree upon a prototype idea. An e-waste grinder that could easily be manufactured, assembled, and maintained within the local context of Agbogbloshie was decided upon as the project goal. In the prototype stage, a steel prototype of a grinder design was manufactured in Washburn Shops at WPI. In the validate stage, team members to verified that the prototype worked and to ensured that all designers and contributors felt heard and given the opportunity for feedback. In this stage, our team presented the prototype to all contributors and those interested in this project, including members the WPI Design Development Lab and our contact in Ghana. The audience was encouraged to ask questions to challenge the design for further improvements.

1.5 Summary

Waste processors in Agbogbloshie are continually exposed to harmful toxins produced by incinerating e-waste. Nearly 10,000 site workers suffer from burns, back problems, infected wounds, respiratory problems, chronic nausea, and debilitating headaches to maintain the e-waste site. Many waste processors must rely on the informal e-waste refurbishing sector for their livelihoods. Waste processors can improve their recycling processes to further realize the value in PCBs. We developed a PCB grinder that allows the waste processors to pulverize the PCBs to a powder, where the gold can be extracted and reused or sold. The following section describes the functional, performance, and interface requirements for the grinder as informed by our co-design partners in Ghana.

Chapter 2: System Requirements Specification

2.1 Introduction

In this chapter, the stakeholder needs are refined and used to develop system requirements for the design. First, the project objectives are introduced in section 2.2. Section 2.3 then begins by introducing the stake holders, and how they might influence the design. The next section, 2.3, develops the system requirements. These were broken up into functional, performance, and interface requirements. Finally, the concluding section summarizes the stakeholders and subsequent requirements.

2.2 Research Question and Project Objectives

The research question this project aimed to solve was:

> How might we co-design and co-produce, with local expertise in Ghana, a technical grinder to improve the e-waste processing techniques in Agbogbloshie?

The following objectives were then developed to solve this research question:

1) Design and build a prototype grinder with a crushing chamber that can pulverize PCBs into a fine powder
    a) Understand the current e-waste recycling practices, limitations, and desires of the Agbogbloshie community.
    b) Understand the manufacturing capabilities, including tools, local knowledge, and feasibility in Agbogbloshie
2) Co-design, with local experts in Ghana, a PCB grinder to improve the e-waste processing techniques in Agbogbloshie
    a) Collaborate with WPI Chemistry & Biochemistry (CBC) student and WPI graduate student on the chemical separation aspects of the project

2.3 Stakeholders

The waste processors at Agbogbloshie are the stakeholders in this project. This includes the recyclers, dismantlers, manufacturers, and subsequent users of the grinder. Through an interview with Hector Boye, Director of Operations at the Ghana Institution of Engineering, it was determined that the stakeholders value safety, low cost, and appropriate integration into current e-waste refurbishing techniques. As well, ease of manufacturability, maintainability, and assembly will be important for the longevity of the grinder. The summary of important stakeholder needs is shown below in *Table 1*.

Table 1: Summary of Stakeholder Needs

SUMMARY OF STAKEHOLDER NEEDS	
Priority 1	The system must be safe to use. There should be no accessible motorized pinch points, no exposed high voltage wiring or connectors, no accessible sharp edges, and no risk of creating a projectile.
Priority 2	The design can be manufactured and built at a low cost for use in Agbogbloshie
Priority 3	The design can be easily maintained with readily available parts
Priority 4	The design should easily integrate into the current recycling process in Ghana
Priority 5	Design works for computer PCB boards, typical size 25 by 30 cm
Priority 6	After grinding, PCB size should be at least 0.5 x 0.5 cm

2.4 System requirements

The system requirements were developed based on the stakeholders' needs, limitations, and opportunities. First, are the functional requirements, or high-level statements on what the grinder system does, to reflect the stakeholder values. These requirements refer to the high-level parts of the grinder, shown in the block diagram in *Figure 11*. Next, are performance requirements, or statements on how well the grinder must execute its functions. Finally, interface requirements were developed based on what systems and components will connect to execute the grinding. The requirements are shown in *Table 2.*

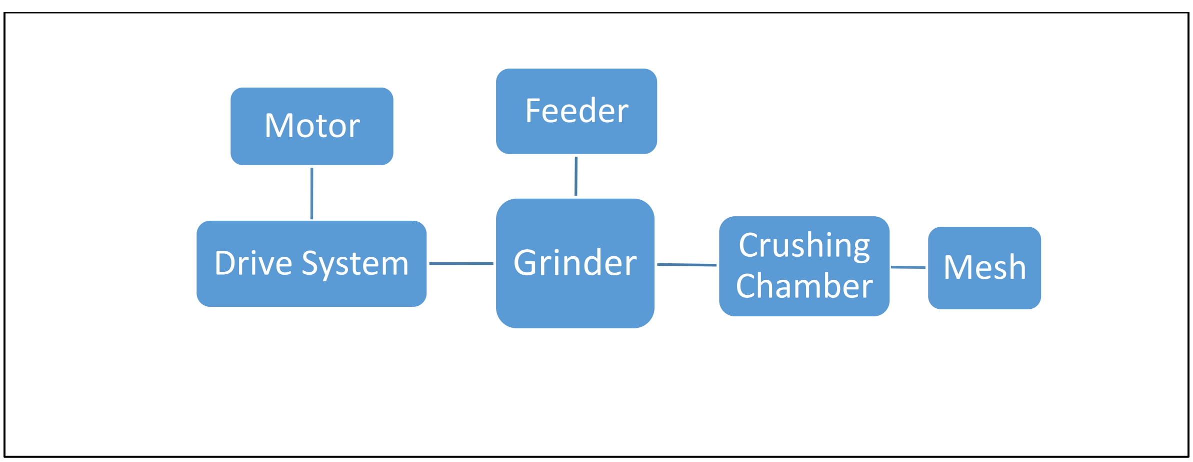

Figure 11: Block diagram of grinding system

Table 2: Summary of system requirements

Type	Requirement	Description
Functional	1	The grinder shall be safe for the operators
	2	The grinder shall be easy for the operators to build and maintain
	3	The grinder shall be built to minimize failure
	4	The motor will be powered in a way that works best for the operators in Agbogbloshie
	5	The drive system shall transmit power from the motor to the grinder
	6	The feeder shall allow for easy and safe input of the PCBs to the grinder
	7	The crushing chamber shall be powerful enough to grind PCB and be accessible for maintenance
	8	The mesh shall determine the size the PCB is grinded to
Performance	1	Design works for computer PCB boards, typical size 25 by 30 cm and material of FR-4 plastic and various metals
	2	After grinding, PCB size should be smaller than 0.5 x 0.5 cm
	3	Grinder drive system shall minimally support breaking of the PCB, determined by PCB rupture energy
Interface	1a	If grid-powered, the grinder shall interface with the grid specs in Ghana at 240 V, 50 Hz (Bank, 2016).
	1b	If battery powered, powered grinding machine will require a DC motor and an ADC converter attachment.
	1c	If fuel powered, motor shall use a fuel that is available in Agbogbloshie.
	2	The motor shall interface with the main shaft rotor using a pulley, gear, or direct connection to spin the rotor at 1500 – 2000 rpm
	3	There shall be a feeding mechanism that will improve safety and ease of use for the operator
	4	The outer casing shall be secured shut during operation and easily removable for cleaning or other maintenance
	5	There shall be a removable mesh to allow for different sizes of PCB fragments to fall through
	6	There shall be an easily removable collection bucket

2.5 Summary

Stakeholders involved in the Agbogbloshie e-waste recovery process are more likely to adopt this grinder if their local expertise, engineering insights, and feedback on manufacturing are incorporated. After understanding their needs, specific functional, performance, and interface requirements were developed. These requirements will guide the next chapter, which explores system design options through the lens of the following criteria: safety, usability, cost, assembly, maintainability, and efficiency. A safe and efficient grinder is chosen by understand the current practices, limitations, and desires of the stakeholders.

Chapter 3: Design Options

3.1 Introduction

A grinder was chosen as the system design for our project because the Ghanaian stakeholders desired a mechanical method for grinding PCBs into finely ground powder. The shredding step was not as important to the stakeholders because they can use a saw or other manual methods to cut PCBs into smaller pieces. The separator step, an entirely chemical process, has been investigated by the related Chemistry & Biochemistry (CBC) MQP. Although the separation step was not the primary focus, this project to ensured we designed a grinder that would break down PCBs into small enough pieces for chemical separation.

In the following section 3.2, the ideation for different grinders and mills including a cutting mill, hammer mill, tumbling ball mill, and a sandpaper grinder is described. A decision matrix was designed to organize the benefits and risks of each grinding method to determine the best method in the local context of Agbogbloshie. After a grinding method was chosen, a few key elements of the grinding method were described. Section 3.3 reviews the drive system, 3.4 revies the feeding mechanism, and 3.5 revies the mesh.

3.2 Grinding Process Overview

To choose a grinding method, typical industrial e-waste recycling centers were reviewed. These industrial grinders are typically cutting mills, or hammer mills. Other types of mills were reviewed, and it was determined a ball mill could be applicable to this application. Finally, design ideation was done where a sandpaper grinder was developed. Each design brings their own advantages and disadvantages. A detail review of each was conducted before choosing the best design through a design matrix.

3.2.1 Cutting Mill Grinder

Cutting mills use cutting and shearing forces to grind materials. The material is fed through a hopper and then to the grinding chamber. In the grinding chamber, there is a rotor with sharp blades that spins around to grind the material, as seen in *Figure 12*. There can also be teeth or stationary cutting boards on the housing that improve the grinding process. On the bottom of the grinding chamber is a mesh or sieve. The holes in this mesh will determine how small the material is grinded. Once the material is small enough, it will exit the grinding chamber through this mesh (Cutting Mills, 2021).

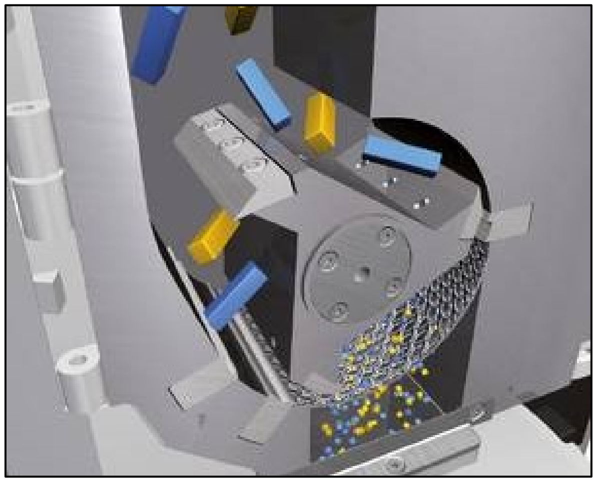

Figure 12: Retsch cutting mill, showing a material being grinded (Cutting Mills, 2021).

3.2.2 Hammer Mill Grinder

Hammer mills are a type of crushing machine that reduces the size of materials. It is often used to crush materials such as asphalt, brick, coal, grains, and even PCBs. Hammer mills use an impact or striking force to fracture and break down materials. The hammer mill has a rotor with a series of hammers that swing outward due to the centrifugal force of the spinning rotor, as you can see in *Figure 13*. These hammers spin rapidly to crush the material (What is a hammermill and what can it do for you?, 2018). These hammers can swing freely to absorb the shock of hitting the hard materials. The number, size, style, and material used for the hammers vary depending on the situation. The material to be processed is fed through a hopper, typically on the top of the hammer mill (Princewell, 2017).

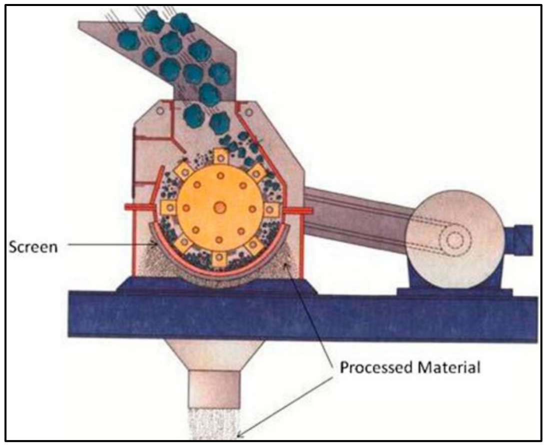

Figure 13: Typical design of a hammer mill to crush materials (Ezurike, Osazuwa, Okoronkwo, & Okoji, 2018).

Hammer mills must be operated at high speeds to pulverize and disintegrate the materials. The high speed of the rotating hammers help strike and grind the inputted material. The material will break down from the impact of the hammers and the collisions with the screen, walls, and other particles. At the bottom, there is a mesh or screen that varies in size to determine how small the material is grinded to. The material will exit the grinder through the mesh once it is small enough to fit through (Princewell, 2017).

3.2.3 Tumbling Ball Mill Grinder

Tumbling ball mills use a cylindrical shell with steel balls to grind materials into fine pieces, as seen in *Figure 14*. The grinding process depends on the impact of steel balls on the material. This design is often used to grind and blend materials for use in mineral dressing processes, paints, pyrotechnics, ceramics, and selective laser sintering (Kakuk, Zsoldos, Csanády, & Oldal, 2009). The inner surface of the shell is coated with abrasion-resistant material in order to protect the shell from the constant impact from the steel balls. The cylindrical shell rotates around its own axis, and once the material gets to the desired size, it is discharged from the opening at the bottom (Intro Into Ball Mill, 2014). In commercial tumbling ball mills, speeds up to 2000 rpm allow for ultra-fast pulverization of the sample, and water-cooling permits continuous operation without cool down breaks (Ball Mills, 2020).

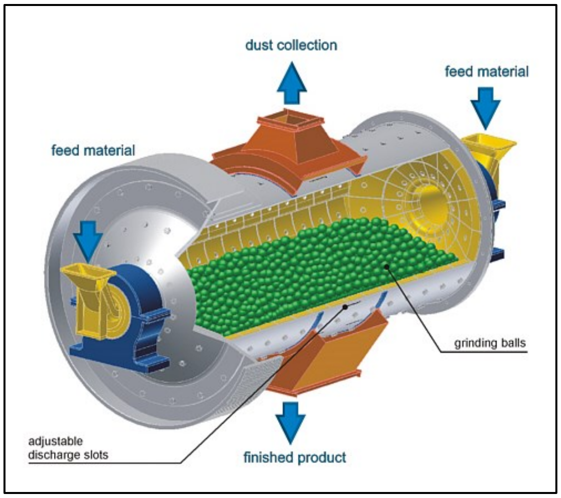

Figure 14: Tumbling ball mill design (Intro Into Ball Mill, 2014)

3.2.4 Sandpaper Belt Grinder

Through our own ideation, we came up with the idea of a sandpaper belt grinder. This would work like the belt sander seen in *Figure 15* with a few adjustments. There would be two vertical sandpaper belts very close together to grind the PCB. A mesh or screen would be placed at the bottom of the belts. The basics of how this sandpaper grinder would work is like some of the mills. First, the material is loaded through the hopper. It would then be squeezed and ground between two pieces of sandpaper belts that rotate. Once the material is grinded small enough, it would be fine enough to exit the grinding chamber through the mesh on the bottom.

Figure 15: Belt sander for sandpaper grinder (Belt Disc Sander, 2021)

3.2.5 Grinding Method Selection

To choose between the cutting mill, hammer mill, ball mill, and sandpaper grinder, a decision matrix was used. Each of the machines above meets basic requirements, but it is important to consider the machines in the context of Ghana and the stakeholder's needs. The decision matrix rated the safety, usability, cost, assembly, maintainability, and efficiency of the grinding methods. A number from one to five was assigned to each category based on how important it was to consider, with one being the least important and five being the most important. Each grinding method was then assigned a value for the six categories on a scale of one to four, with one being poor and four being great. A weighted score was then calculated. The option with the highest weighted score is the best choice. Each score is described below, with the final decision matrix shown in *Table 3*. The scores were determined for each method and category through research, except for the sandpaper grinder where we used our best judgement on how we hoped the design would work. Each decision is described below in more details to give an understanding of the scores were made.

For the cutting mill, it received a safety score of 3 because drive belts on pumps can slip badly enough to burn and create toxic fumes and smoke (Michaud D. , 2015). Any of the designs that rely on a drive belt run the risk of the belt snapping and injuring the operators. Usability was scored a 3 because cutting mills can have a wide selection of accessories that allow for easy adaptation to different application requirements (Cutting Mills, 2020). Cost was rated a 2 because the parts must be machined from high-speed steel or cemented carbide. Assembly was scored a 2 due to its complicated design. There are many bolts and screws to hold it together and sharp blades make it difficult to manufacture and assemble. Maintainability was scored a 1, due to the number of parts and the sharp blades that will need to be replaced often. And finally, the efficiency of the cutting mill was scored a 4, because the sharp blades use cutting and shearing forces to grind the PCB and other materials down to very small sizes (Cutting Mills, 2021).

For the hammer mill, the safety was rated a 4 because the enclosed center rotor discs provide a low risk for a projectile. Sometimes in commercial hammer mills, oil is the primary fluid that is used in torque converters and couplers. If for some reason the equipment must be started up and shut down three or four times, in rapid succession, this oil may become hot, producing pressure (Michaud D. , 2015). Usability was scored a 2 because the user must learn about process requirements, such as production capacity, product particle size, and particle-size distribution in order to get started with a hammer mill (Liu, 2017). Cost was rated a 3, because similar to the cutting mill, the parts must be machined from steel or other high strength metals. Assembly was scored a 3 for the hammer mill. While the design has many moving pieces, it uses simple and common parts such as rods, washers, and rectangular hammers. These simple parts make it easier to understand (Ezurike, Osazuwa, Okoronkwo, & Okoji, 2018). Maintainability was scored a 2, due to the many parts in this design that increase the chances of something breaking and can make it more complicated to repair. For example, if a couple washers or screws break, the design will not work well but because it is tedious to replace the operators may choose to not fix it. Finally, the efficiency of the hammer mill was scored a 3. Hammer mills are often used to grind PCBs due to its high productivity and flexibility to grind many different materials. This was not a perfect four, however, because sometimes a second grinding step is needed after the hammer mill to grind the material further (Princewell, 2017).

The safety of the ball mill was scored a 2 because there is a risk of explosion from the extremely high vibration rate, but there are no belts that may fail on the design and otherwise low risk of creating a projectile (Ball Mills, 2021). Usability was scored a 4 because ball mills have large applicability in the mining industry and many of our stakeholders are miners (Francioli, 2015). Cost was scored a 1 because they may be made of chrome steel, stainless steel, ceramic, or rubber. The inner surface of the cylindrical shell can be lined with an abrasion-resistant manganese steel or rubber lining (Ball Mills, 2020). The variation in materials and the precious metals make for a high cost to our stakeholders. Assembly of the ball mill was scored a 3. Ball mills are typically very large and heavy, which makes it difficult to put together with limited tools and machines. However, it is a simple and easy to understand design as it is just a large cylinder filled with metal balls that rotates. For maintainability, it was scored a 2. Ball mills are typically easy to service, but again the number of bolts and parts in the design bring down the maintainability, specifically the metal balls, which need to be replaced after so much wear. It is likely that the operators in Agbogbloshie would run the system far past the capabilities. And lastly, the efficiency of the ball mill was a 2. While ball mills are often used for grinding materials and work very well, we did not find any cases of them being used for PCB grinding (Neikov, 2009).

For the sandpaper grinder, the safety was scored a 1 because this design creates a high risk for a projectile if the PCB gets jammed between the two sandpaper belts. There is an unnecessary risk to the operator because their fingers could get injured when they manually feed the PCB into the hopper. Usability was scored a 1 because there is no precedent for use of this original design. Cost of the sandpaper grinder was scored a 4 because there is no machining required for most parts, no expensive metals for blades, and sandpaper belts are a low-cost material. Assembly was given a score of 4 because of the simplicity of the design. The main working features are two rotating sandpaper belts, which are easy to understand and assembly. For maintainability, it was scored 3 because there are not a ton of screws or moving parts to maintain, however the sandpaper belts would likely have to be replaced frequently. Lastly, the sandpaper grinder was rated a 1 for efficiency. Because this was a design we created, we do not have any proof that it will work well to grind the PCB. We also suspect the sandpaper may not be strong enough or have enough force to grind the PCB.

Table 3: Grinder design decision matrix

	Safety	Usability	Cost	Assembly	Maintainability	Efficiency	
CRITERIA DESCRIPTION	Safest design includes no pinch points, exposed high voltage wiring, accessible sharp edges, or risk of creating a projectile	Usability means the grinding method can be easily understood by a new user or with few barriers to learn	A lower cost is better	Assembly refers to a design that is easy to put together using parts and methods in the local context of Agbogbloshie	Maintainability refers to a design that requires little maintenance and can be easily repaired over time by the operators	Efficiency refers to a well-researched method that can process PCB in the shortest and most efficient time	
WEIGHT	5	4	2	4	3	4	22
	23%	18%	9%	18%	14%	18%	100%
CRITERIA	Safety	Usability	Cost	Assembly	Maintainability	Efficiency	WEIGHTED SCORE
Cutting Mill	3	3	2	2	1	4	2.636
Hammer Mill	3	2	3	3	2	3	2.682
Ball Mill	2	4	1	3	2	2	2.455
Sandpaper Grinder	1	1	4	4	3	1	2.091

The hammer mill received the highest weighted score, as shown in *Table 3*, so this grinding method was chosen as the final method. The hammer mill will be designed to specifically meet the stakeholder criteria in Chapter 2 and can be fully manufactured, built, and maintained in Agbogbloshie.

3.3 Drive System of Grinder Overview

For the power and electrical system, power and other specifications based on commercially will be scaled down from what is typically used in hammer mills. The drive system consists of the motor and the motor drive, or the mechanism for moving of energy from the motor to the hammer mill rotor shaft location, where it is applied to perform useful work (Carvill & Cullum, 1994). Motor drives can come in the form of pulleys, and gears, or a combination of those elements. The motor shall interface with the main shaft rotor using a pulley, gear, or direct connection to spin the rotor at 1500 – 2000 rpm to pulverize PCB e-waste in Agbogbloshie.

3.3.1 Motor Selection

Electric motors work by converting electrical energy to mechanical energy in order to create motion. Alternating (AC) or direct (DC) current interacts with a magnetic field to generate force within a motor. As the strength of a current increases so does the strength of the magnetic field. Ohm's Law, $V = IR$, states that voltage must increase in order to maintain the same current as resistance increases (How to Choose the Right Motor, 2020). The most important characteristics to pay attention to when selecting a motor are:

- Voltage
- Current
- Torque
- Velocity (rpm)

Voltage keeps the net current flowing in one direction to overcome back current. The higher the voltage, the higher the torque. The voltage rating of a DC motor indicates the most efficient voltage while running. If you apply voltage below the rating, the motor will not work. If you exceed the voltage rating, you can short windings resulting in power loss or complete destruction (Csanyi, 2011).

Operating and stall current are important to consider for all motors. Operating current is the average amount of current the motor is expected to draw under typical torque. Stall current applies enough torque for the motor to run at stall speed, or 0 rpm. This is the maximum amount of current the motor should be able to draw, as well as the maximum power when multiplied by the rated voltage.

Operating torque is the amount of torque the motor was designed to give and stall torque is the amount of torque produced when power is applied from stall speed (How to Choose the Right Motor, 2020). Velocity represents the speed at which the motor spins and is most often measured in rpm. Torque and velocity must be considered together with the drive system because adding pulleys and gears will impact the efficiency of the motor. For safety reasons on this prototype, we plan to spin the rotor between 1500-2000 rpm. The number of hammers used for a hammer mill of 1,800 rpm, should be one for every 2.5 to 3.5 horsepower, and for 3,600 rpm, one for every 1 to 2 horsepower (Hammer Mills, 2020). The horsepower-to-hammer ratio declines with heavier hammer patterns and tough to grind materials. For example, the typical ratio is 1:1 for normal applications or even 1:2 for very fine or difficult grinding with ¼" thick hammers (Advantages & Disadvantages in Particle Reduction Techniques, 2021).

3.3.2 Power Source and Voltage Selection

In our literature review, we discovered a hammer mill setup with a one horsepower (0.75 kW) electric motor that achieves approximately 2,000 rpm with a drive power of 300 W (Ezurike, Osazuwa, Okoronkwo, & Okoji, 2018). In this case, the hammer mill used a pulley and the drive power transmitted by the belts is obtained from adding the tensions in the tight, T_1, and slack, T_2, side of the belt and then multiplying by the velocity, V, of the electric motor. The drive power of 300 W may have been adequate for this hammer mill because it was milling maize, a much softer material than FR-4 PCB. Our design may require a higher drive power transmitted by the belts in order to efficiently break down the PCBs.

Another hammer mill from our literature review of crushing and grinding machines found that a 1-kilowatt single-phase AC electric motor transmitting power to a main shaft speed of 2,000 rpm is suitable to mill effectively (Mohamed, Radwan, & Adly, 2015). For our project, an AC motor must be paired with an inverter and a battery pack because the Agbogbloshie site currently only has access to grid electricity on the far outskirts of the site (Boye & Amoako-Gyimah, 2020). Pairing a single-phase AC motor with an inverter will cause a failure because the inverter creates a virtual alternating current with high-speed switching. If the inverter is connected to a single-phase capacitor-start induction motor, the capacitor will overheat and burn due to repetitive charging and discharging. Also, if the inverter is connected to a split-phase-start induction motor or repulsion-start induction motor, the motor's internal centrifugal switch will not operate, and the starting coil may overheat (Omrom Industrial Automation, 2021). Based on these system limitations for inverters, we will move forward with recommending a three-phase motor for use in Agbogbloshie.

3.3.3 Motor Drive Overview

Next, the connection of the motor to the shaft must be reviewed. There are a couple ways to do this: belt, chain, and gear drives. Each option was explored in detail to determine which would best fit a hammer mill design for Agbogbloshie.

3.3.3.1 Belt Drive

Belt drives use a belt or rope to transfer power from the motor to the shaft using pulleys. Belt drives can either rotate at the same speed or different speeds. Because they are flexible, the belts absorb shock loads and isolate vibrations. Belt drives are simple, inexpensive, and can be used in dirty and hazardous environments (Jindal, 2010). There are three different types of belts that are commonly used, flat, V, and circular, shown in *Figure 16*. Flat belts are used when a moderate amount of power needs to be transferred and the pulleys are no more than eight meters apart. V-belts are used to transfer a large amount of power when the pulleys are close together. Circular belts are used to transfer a larger amount of power when the pulleys are more than eight meters apart. Because our system will not require the pulleys to be more than 8 meters apart, we decided not to use a circular belt and only reviewed the flat and V-belts in more detail (Khurmi & Gupta, 2005).

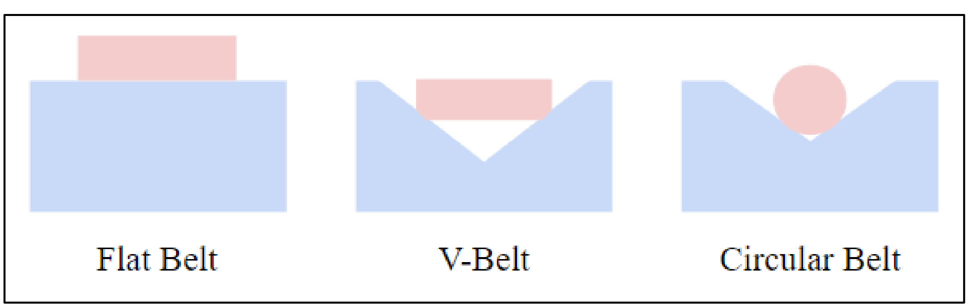

Figure 16: Diagram showing the flat, V-, and circular belts

Flat belts are typically cut from a roll and joined together by cement, laces, or a hinge, while v-belts are made endless by molding fabric and cords in rubber in a trapezoidal shape and covering it in more fabric and rubber. This shape of the v-belt provides some advantages over the flat belt. The power of a V-belt is transmitted by the wedging action between the belt and groove in the pulley. This wedging effect gives a negligible slip between the belt and pulley, giving the V-belt system a positive drive. Compared to a flat belt, V-belts are easier to install and are better suited for small distances between the center of the pulleys. They also have a life of approximately 3-5 years, operate quietly, and can be operated in any direction. It is also important to note that the speed of the V-belt must be between 5 m/s and 50 m/s due to the centrifugal tensions, while flat belts do not have this constraint. The V-belts unique shape does make them more complicated to construct and less durable than flat belts (Khurmi & Gupta, 2005).

3.3.3.2 Chain Drive

Steel chains can be used as an alternative to belt drives, to prevent slipping. The chain is made up of rigid links connected with pin joints. The chains are wrapped around sprocket wheels, which have teeth that fit in the links of the chain. An example of what a chain drive looks like can be seen in *Figure 17*. Chain drives are often used in bicycles, motorcycles, and conveyors. A chain drive is particularly advantageous because no slip occurs, a perfect velocity ratio is obtained, has up to a 98% transmission efficiency, and it can transmit more power than belts. Chain drives can also be used for any distance and one chain can transmit motion to several shafts. A downside to using a chain drive is that there is a high production cost. As well, the chain drive needs to be mounted very accurately and requires routine maintenance for lubrication and slack adjustment (Khurmi & Gupta, 2005).

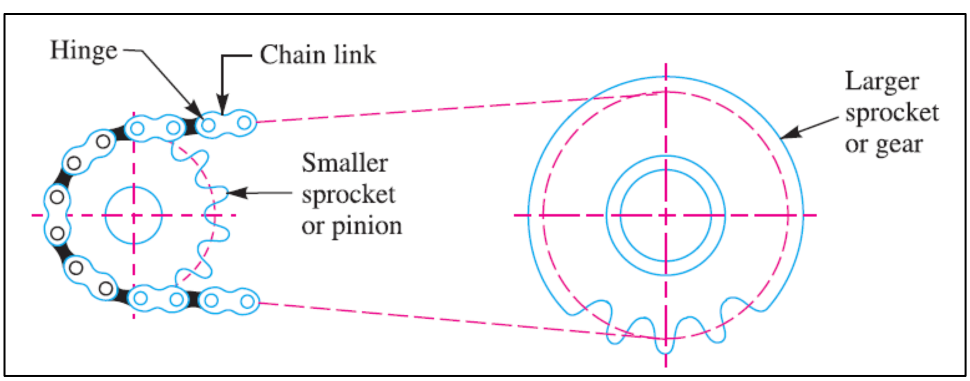

Figure 17: Diagram of a chain drive (Khurmi & Gupta, 2005)

3.3.3.3 Gear Drive

Gear drives are another alternative drive system that reduces slip. These systems consist of two toothed wheels that interlock with each other and spin to transfer the motion, as seen *in Figure 18*. Gear drives are used in situations where a positive velocity ratio is necessary, and a lot of power must be transmitted. They also work well for small center distances between the shafts. Gear drives also have high efficiencies and are very reliable. However, the gears are hard to manufacture and must be very precise, making them expensive. If the gears are not cut precisely, the small errors in the teeth can cause vibrations and noise. Another thing to consider with gears is that they require frequent lubrication (Khurmi & Gupta, 2005).

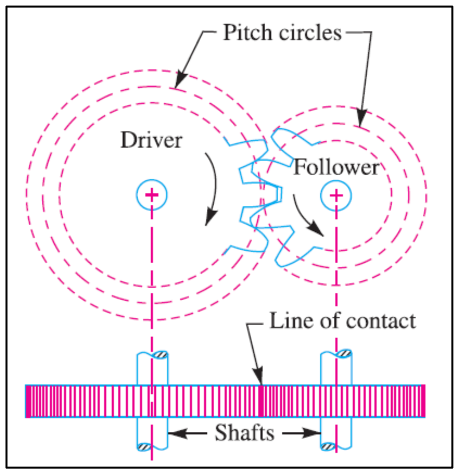

Figure 18: Diagram of a gear drive (Khurmi & Gupta, 2005)

After reviewing the various types of drives, we chose to use a belt drive. One advantage of using the belt drive over the chain or gear drives is that it does not need to be lubricated. Belt drives also tend to be cheaper than chain and gear drives. They also give us more control over the motor distance in comparison to a gear drive (Khurmi & Gupta, 2005). In addition to researching each possible drive method, we reviewed several journal articles on hammer mill design that also used a belt drive. Ibrahim et.al. (Ibrahim, Omran, & Abd Elrhman, 2019), Ezurike et. al. (Ezurike, Osazuwa, Okoronkwo, & Okoji, 2018), and Mohamed et. al. (Mohamed, Radwan, & Adly, 2015) all used belt drive to attach the shaft to the motor.

More specifically, a V-belt was chosen for the final design, similar to Ezurike et. al. (Ezurike, Osazuwa, Okoronkwo, & Okoji, 2018) and Ibrahim et. al. (Ibrahim, Omran, & Abd Elrhman, 2019). The V-belt provides some advantages over a flat belt, such as being a positive drive, the ease of installation, and the endless design of the belt without a joint which could lead to failures. V-belts typically have a long life than flat belts as well, about 3-5 years. It is also advantageous to have a belt that can operate in any direction, so that the motor can be mounted horizontally or vertically.

3.4 Feeding Mechanism Overview

A feeding mechanism was chosen to maximize safety and grinding efficiency in our design. Proper feeding of a hammer mill allows for maximum grinding efficiency with the lowest possible cost per ton. Uneven or inconsistent feeding can lead to surges in the motor load. Fixed hoppers and belt feeding mechanisms were explored to determine the best fit for our design.

3.4.1 Gravity Hopper Feeder

A gravity hopper refers to a stationary feeder that eases the intake of materials using only the force of gravity. Full width top feeders commonly achieve maximum efficiency and minimize the cost of operation (Advantages & Disadvantages in Particle Reduction Techniques, 2021). A full width top feeder ensures the entire screen area can be utilized and that the work being done on the PCB fragments will be evenly distributed across the full hammer pattern. These types of hoppers can also be easily manufactured, as steel plates can be marked, cut to sizes, and then welded together (Mohamed, Radwan, & Adly, 2015). Most well-designed modern hammer mills have a flow director or diverter in the top of the hammer mill and to prevent any materials that are circulating within the grinding chamber from getting pushed back out (Advantages & Disadvantages in Particle Reduction Techniques, 2021). *Figure 19*, below, show a gravity hopper with a flow director at the top of the hammer mill.

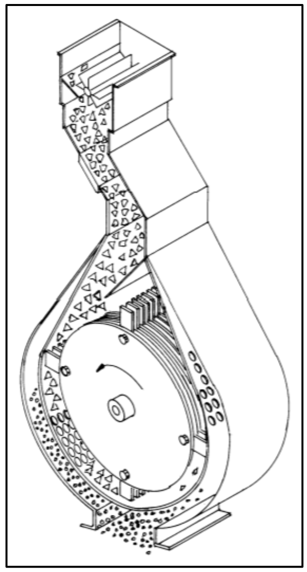

Figure 19: Gravity hopper with flow director (Advantages & Disadvantages in Particle Reduction Techniques, 2021)

The hopper must be able to accommodate enough PCB fragments to achieve the operators' desired throughput capacity, or feed rate (Ibrahim, Omran, & Abd Elrhman, 2019). *Figure 20*, below, shows an elongated, angled gravity feeder that can hold a significantly higher volume of PCB than a typical full-width top-feeder. The advantage of this design is an increased feed rate and the lowered risk of a projectile due to the long, covered hopper. However, this design uses more steel than a typical top feeder, this increasing the hammer mill cost for our stakeholders.

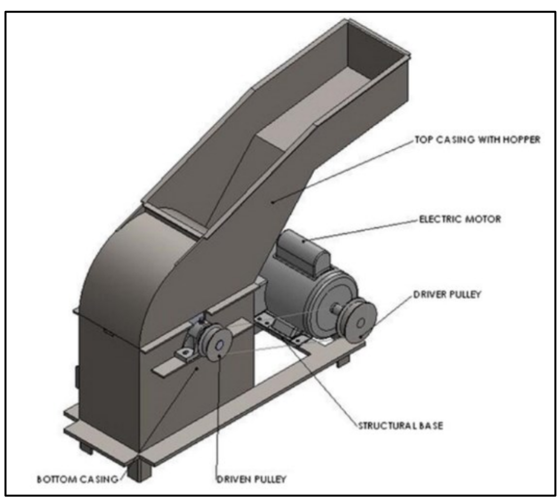

Figure 20: Gravity feeder with elongated, angled design (Ezurike, Osazuwa, Okoronkwo, & Okoji, 2018)

Some gravity feeders have a sieving component to only allow materials to enter the grinding chamber if they are of a particular size. In the grinder shown below in *Figure 21*, the sieving component is attached to an outlet of the main feeder. In this process, the part of the product which can pass through the screen is separated out instantly. The sieve method can lower energy consumption and prevents material from being over ground and heated (Xuan, Cao, Wu, Ma, & Han, 2012). However, one disadvantage to the sieve is it slows down the feed rate significantly and it may negatively affect the overall efficiency.

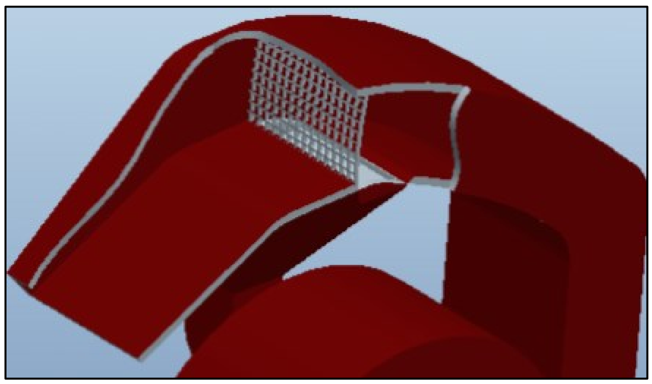

Figure 21: Feeder with sieve CAD model (Xuan, Cao, Wu, Ma, & Han, 2012)

3.4.2 Rotary Pocket Feeder

Rotary pocket feeders utilize a rotor mechanism much like a rotary airlock to evenly distribute the feed to the hammer mill, as shown in *Figure 22*. In most cases, the rotor is segmented, and the pockets are staggered to improve the distribution of the feed and to reduce surges in the feed rate. These feeders are best suited to granular materials with a high density, such as whole grains and coarsely ground meals (Advantages & Disadvantages in Particle Reduction Techniques, 2021). FR-4 PCBs have an even higher density than whole grains and coarsely ground grains, so it is likely the PCB would flow freely in the rotary pocket feeder. In our design, the same motor we use for the rotor shaft could power a rotary pocket feeder. The primary advantage for this feeder is that our operators will use conventional inverter technology to control the feed rate. One of the disadvantages of this method is it creates an extra moving part for our stakeholders to maintain. The rotary piece will require re-alignment when the capacity of the mill drops by 20-30% or when finished product quality is no longer acceptable (Advantages & Disadvantages in Particle Reduction Techniques, 2021).

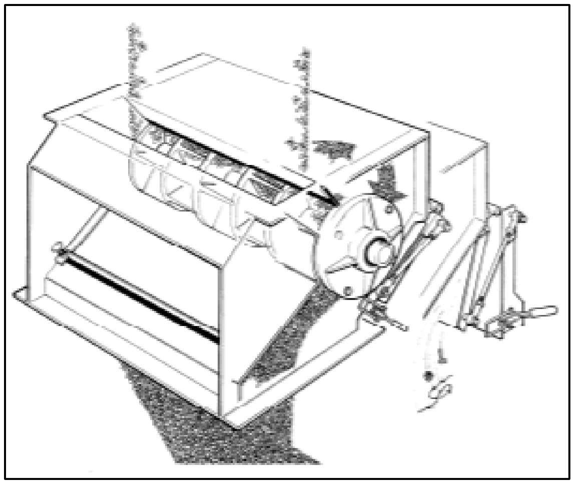

Figure 22: Rotary pocket feeder (Advantages & Disadvantages in Particle Reduction Techniques, 2021)

3.5 Mesh Design Overview

The stakeholders aim to collect small and uniform PCB fragments from this grinder design. Curved and flat meshes were explored so that 0.5 cm x 0.5 cm PCB pieces shall be released from the grinder while the rest of the pieces continue to be ground up.

3.5.1 Curved Mesh

Most industrial hammer mills have a circular bottom casing and a semi-circular screen, as shown in *Figure 23*. The major problems associated with the conventional machine are longer milling time and low efficiency because of the material moving alongside the circular screen. This screen shape can cause re-crushing of carried products by the hammers, thereby reducing the feed rate (Ezurike, Osazuwa, Okoronkwo, & Okoji, 2018). As a result of wear and corrosion, the sieve screen holes enlarge or burst thereby allowing larger than desired particles to pass through. After several hours of hammer mill operation, the sieve screen holes can get clogged thereby reducing its efficiency and capacity (Adekomaya & Samuel, 2014).

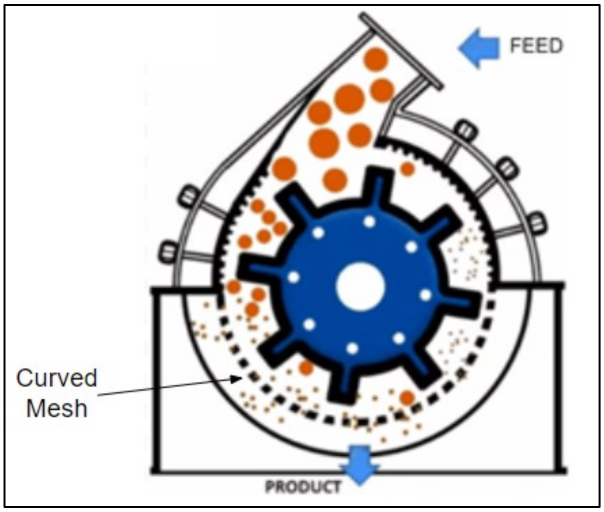

Figure 23: Curved mesh hammer mill (Michaud L. , 2016)

3.5.2 Flat Mesh

The flat mesh design, as shown in *Figure 24*, does not carry the uncrushed product and provides a larger open area for intake. Other advantages of the proposed design include low clogging of materials and higher feed rate (Ezurike, Osazuwa, Okoronkwo, & Okoji, 2018). The tested results showed that the newly designed machine gave a satisfactory performance in productivity and energy consumption while maintaining feed quality. The designed machine also has room for easy maintenance activities such as replacement of screen, hammers, and cleaning of the bottom casing. (Ezurike, Osazuwa, Okoronkwo, & Okoji, 2018) To prevent this wear and corrosion, we are interested in providing our stakeholders with a removable mesh. This design is favorable for our operators because they may be interested in collecting the larger PCB fragments and then running them through the grinder again to achieve the smallest possible fragments or dust.

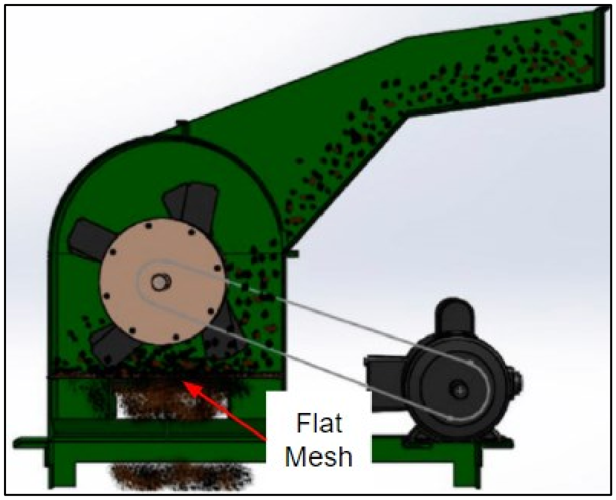

Figure 24: Flat mesh for agricultural hammer mill (Ezurike, Osazuwa, Okoronkwo, & Okoji, 2018)

3.6 Summary of Design Selections

After research into different grinding methods, a design matrix was used to choose a hammer mill as the best design for PCB grinding in Agbogbloshie. The hammer mill design has been shown to work on materials such as PCB before and has good usability and maintainability. After choosing a hammer mill as the grinding method, the individual parts of a hammer mill were researched. This researched showed that if a 2 HP, 3500 rpm, 60Hz, 208-230V motor was used, it is best paired with an inverter, a battery bank, and pulley system for use in Agbogbloshie. As well, a V-belt pulley system will work best for the hammer mill as it is commonly used and would be the cheapest method of power transmission. Different types of feeders were reviewed, where a simple gravity hopper was chosen as best for the design. This simple design helps make the overall design of the hammer mill easier to build, use, and maintain. And finally, types of meshes used in hammer mills was researched. An interesting article by Ezurike et. al. (2018) showed the benefits of flat mesh hammer mills. A flat mesh design was chosen based on his research and that it would be easier to manufacture. Many decisions for the prototype hammer mill design were chosen. These informed designs then led into the development of the first prototype designs and then the final hammer mill design to be manufactured as described in the next chapter.

Chapter 4: Prototype Ideation, Manufacturing, & Testing

4.1 Introduction

After conducting thorough literature on the background, determining the stakeholder's needs, and making key design decisions, the first prototype was developed. Through several rounds of feedback and continued researched, the design was improved to create the final prototype design in SolidWorks, detailed in section 4.2. Because the prototype is being built in the US, the final design followed Imperial System units to ensure the correct parts could be purchased. Then, a manufacturing plan to create the prototype was developed as described in section 4.3. This included tools such as a plasma cutter, drill press, table saw, welder, sheet metal brake, and more. Following the manufacturing steps, testing was conducted on an Instron and with ANSYS to ensure the design would work, as shown in section 4.4. Finally, in section 4.5, recommendations on how to implement the grinder and manufacturing plan in Ghana were given.

4.2 Prototype Design and Working Drawings

After choosing a hammer mill grinder and researching its parts, a prototype design was made. The design went through several iterations, described below. The design changes were informed by continued research, advisor feedback, and manufacturing experience.

4.2.1 First Design Iteration

Design one was developed using the research and design decisions from Chapter Three. This research impacted the development of the design in the ideation process. The design was first drawn on paper, shown in *Appendix A,* and then converted into a computer aided design (CAD) model using SolidWorks, shown in *Figure 25*. *Table 4* shows the cross-section of the design, with its corresponding parts.

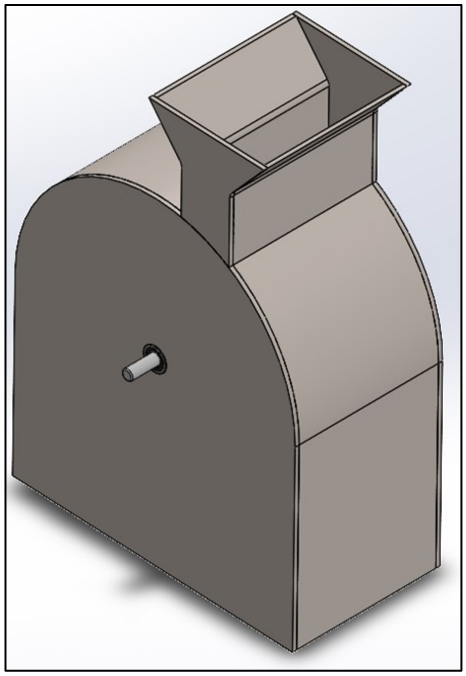

Figure 25: CAD model of design one

Table 4: Design 1 Cross-Section List of Parts

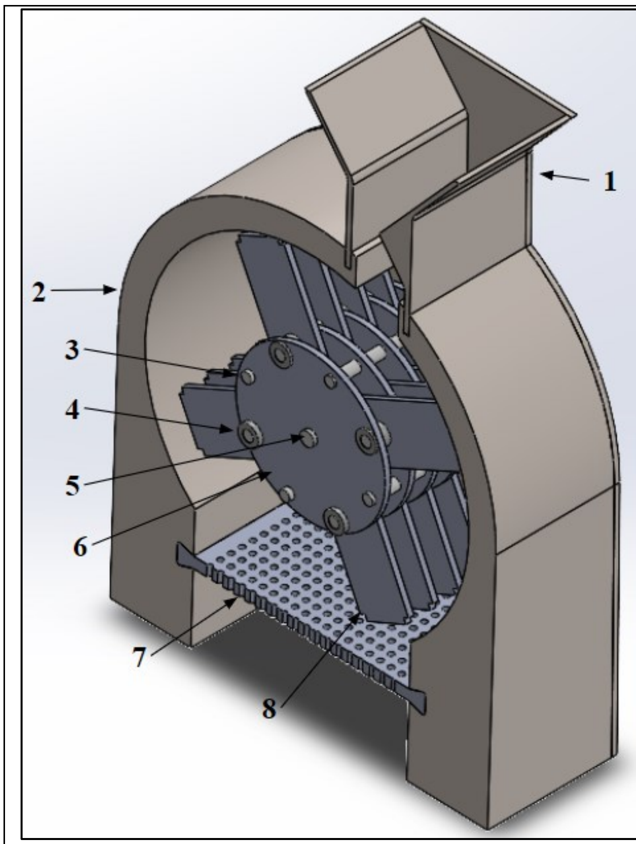

1	Funnel
2	Outer Casing
3	Hammer Pin
4	Washer
5	Drive Shaft
6	Rotor Disc
7	Mesh
8	Hammer

At this point in the design, there was not a clear method for what the grinder would be made of or how it would be machined. However, the original thought here was to use steel since it is very strong and is often used in hammer mill designs such as those by Ibrahim et. al. (2019), Mohamed et. al. (2015), and Ezurike et. al. (2018). The drive shaft, hammer pins, spacers, bearings, and pulleys would all be purchased online. The outer casing, mesh, hammers, and rotor discs would be cut out of steel using the machines in WPI's Washburn Labs. The following sections will call upon each part in more detail.

4.2.1.1 Crushing Chamber

A simple gravity feeder was chosen for the feeding mechanism. The preliminary design includes four pieces that would connect to form a funnel shape. The hopper is approximately 4.8" tall and sits slightly off center with a triangular opening, as seen in *Figure 27.* The opening on the bottom is approximately 6.7" x 2.3" and the opening on the top is approximately 6.7" x 5.7" to allow more space to add the PCBs. There is a small triangular piece sticking out of one side, which helps to prevent any splash back of pieces and prevents a hand from entering the crushing chamber, like the hoppers on the Retsch cutting mills (Cutting Mills, 2020).

The outer casing was designed to protect the operator from the high-speed spinning hammers and to support to rotor. In the ideation phase, an outer casing with teeth or blades on the inner curved pieces was considered. Instead, the inside surface was kept smooth because this will be easiest for our stakeholders to manufacture. The outer casing diameter is approximately 14" across. There is an approximately 6.7" x 2.3" slit at the top of the outer casing so that the funnel can easily fit on top and be secured via welding or other methods. The bottom of the outer casing is rectangular and hollow to allow the maximum amount of PCB to flow freely beneath the shaft assembly and above the mesh. We designed a 17 cm diameter hole for the shaft bearings on the front and back face of the hammer mill to support the shaft assembly.

Our preliminary design for the mesh is flat and fits into the outer casing with a dovetail joint on each end. The mesh is approximately 16.71 cm long and 12 cm wide. The grid pattern for the first mesh allows 0.5 x 0.5 cm PCB pieces to fall through the bottom of the outer casing.

4.2.1.2 Shaft Assembly

The shaft assembly is comprised of the drive shaft, rotor discs, hammers, spacers, and hammer pins. The parts are assembled onto the drive shaft, which rests on the bearings embedded in the outer casing. This drive shaft will be approximately 1 cm in diameter and 13 cm long. There are then total of seven rotor discs welded onto the drive shaft, 11 cm in diameter and 0.5 cm thick. Eights hammer pins, 0.7 cm in diameter and 15.12 cm long, are then placed through the rotor discs. Every other pin for a total of four pins will include six hammers wedged between two spacers and two rotor discs, as can be seen in the CAD model in *Figure 26*. These hammers are 9.25 cm long, 5 cm wide, and 0.5 cm thick. The hammers swing back and forth freely to reduce the risk of material getting stuck between the shaft assembly and the outer casing. This also reduces the risk of causing the motor to stall. The hammers are designed with a notch in the upper corners to allow for material to flow freely as the hammers impact the material (Ezurike, Osazuwa, Okoronkwo, & Okoji, 2018).

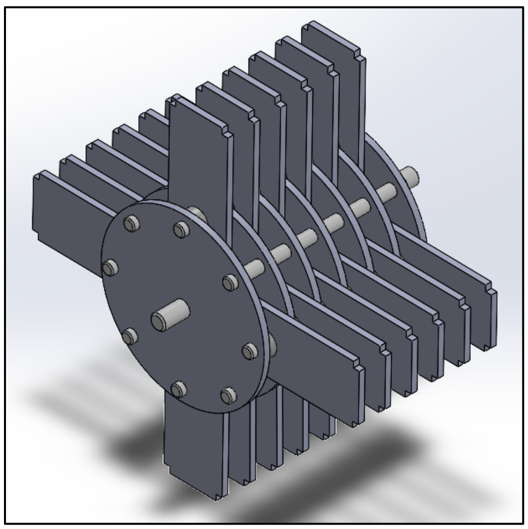

Figure 26: Design One Shaft Assembly CAD Model

4.2.1.3 Power Transmission Unit

A one horsepower (HP),1725 rpm motor would be used to drive the system to meet our drive requirement. To transfer power to the shaft, a V-belt pulley system was chosen based on the research above. A 3-inch pulley for the motor and drive shaft would be used to transfer all 1725 rpm from the motor to the shaft assembly.

4.2.2 Second Design Iteration

Changes were made to design one to reflect feedback from our advisors, new research, and further review into the stakeholder’s needs. As seen in *Table 5 and 6* of the second design, the major changes were to the outer casing, the mesh, the bearings, and the addition of a stand.

Table 5: Design 2 Full Assembly Parts List

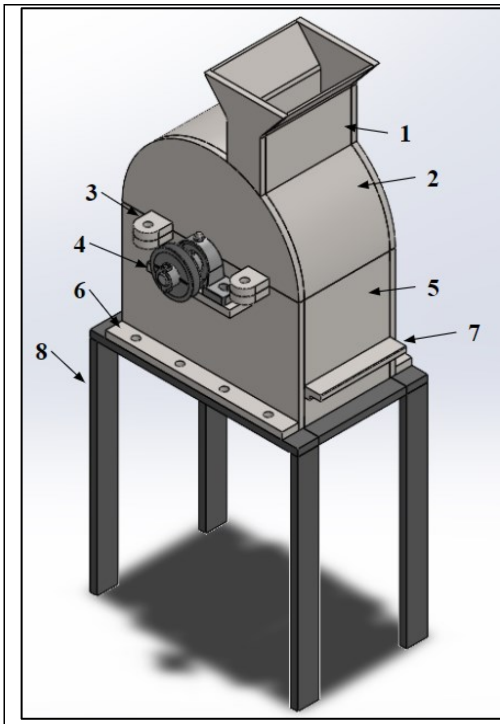	1	Funnel
	2	Upper Outer Casing
	3	Crushing Chamber Connection Flange
	4	Bearing Base
	5	Lower Outer Casing
	6	Crushing Chamber-Stand Connection Flange
	7	Mesh
	8	Stand

Table 6: Design 2 Shaft Assembly List of Parts

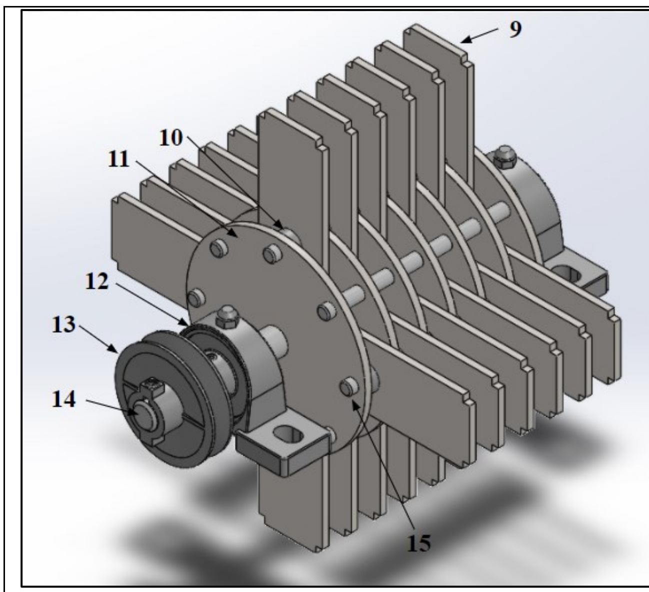	9	Hammer
	10	Spacer
	11	Rotor Disc
	12	Bearing
	13	Pulley
	14	Drive Shaft
	15	Hammer Pin

4.2.2.1 Crushing Chamber

In Design 2, the fixed flat mesh was replaced with a removable flat mesh. The outer casing was updated to include a small tab for the mesh to rest on top of. A horizontal slit, slightly wider than the mesh thickness, was added on the outer casing so that the operator can easily slide the mesh out for maintenance or replacement. This feature also allows the operator to use meshes with larger or smaller hole diameters, depending on the desired size of PCB particles.

The outer casing was separated into two components, the top and bottom casings, as shown in *Table 5*. Four external tabs with ¾ inch screw holes were added to the top and bottom casings so that the stakeholders can easily bolt the two sections together. A nut and bolt connection were chosen so that our stakeholders can easily remove the top casing to access the shaft assembly for maintenance. The bottom casing was designed so that it can easily be screwed into and supported by the base of the stand.

In this design, the bearing is no longer embedded in the outer casing to account for the new two-piece design. Instead, a flange of steel will be welded to the outside of the casing on each side to hold a mounted bearing. This design change allows for the hammer mill to be put together and taken apart easier by the users. Now, the top outer casing can be unscrewed and removed from the bottom and then the bearing mounts can be unscrewed to remove the shaft assembly from the bottom outer casing.

4.2.2.2 Stand Assembly

The first rendering of the stand design was also added in this stage. It is a simple design, that includes steel bars welded together to make a basic stand design in the shape of a table. The stand is approximately 41 cm tall, so that a typical five-gallon bucket can be placed underneath to catch the grinded PCB. The hammer mill will sit on top and be bolted to the stand on two sides.

4.2.3 Final Design Iteration

In the final design, several changes were made to improve the manufacturability and efficiency of the hammer mill. This included changing the material and size of the parts to better reflect sheet metal sizes, the shape of the hopper, the design of the shaft assembly, the shape of the hammers, the shape of the mesh, the connection of the outer casing, and the motor for use at WPI and in Ghana. The major changes can be seen in the updated CAD model of design three, shown in *Table 7 and 8*.

Table 7: Design 3 Full Assembly List of Parts

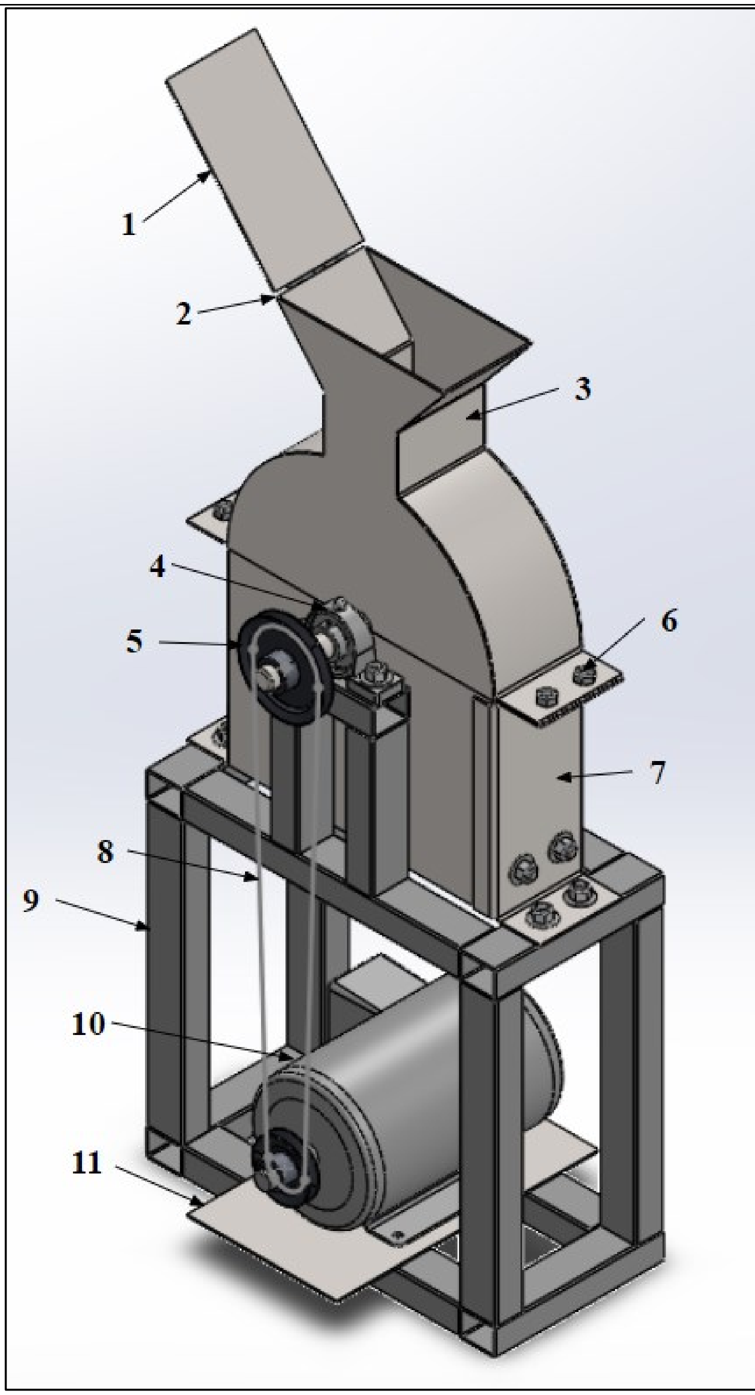

1	Funnel Cover
2	Hinge
3	Upper Outer Casing
4	Bearing
5	Drive Pulley
6	Nuts and Bolts
7	Lower Outer Casing
8	Belt
9	Stand
10	Motor
11	Motor Base

Table 8: Design 3 Cross-Section List of Parts

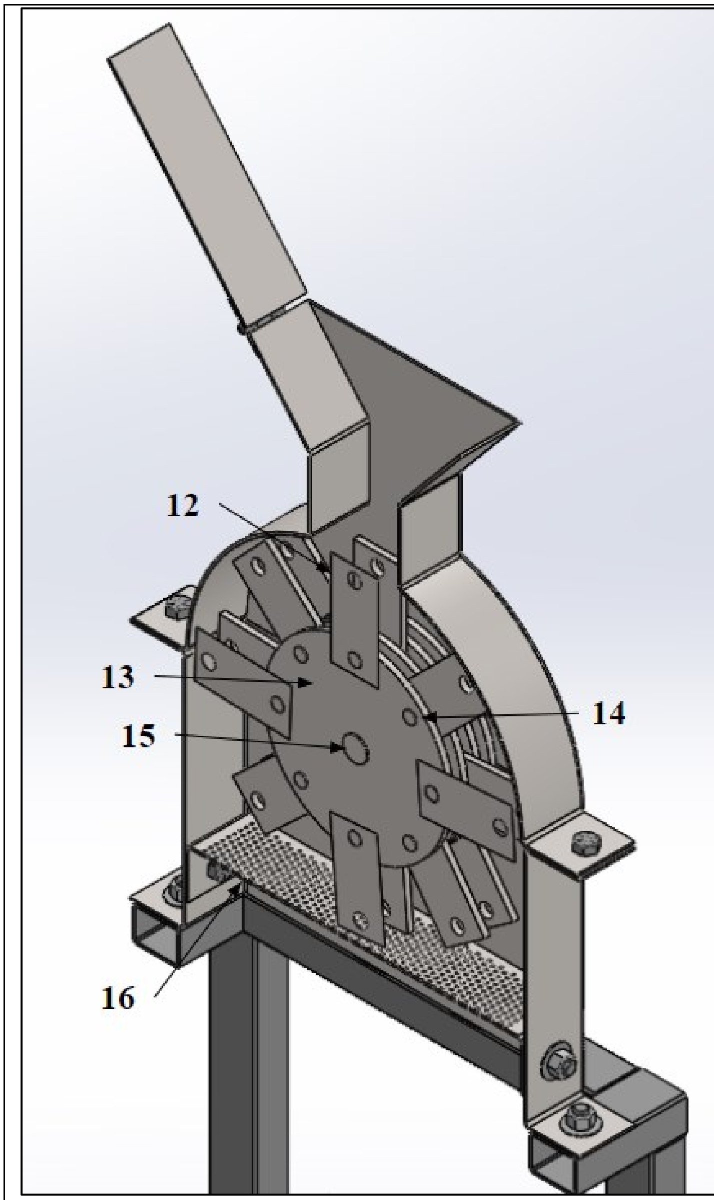	12	Hammer
	13	Rotor Disc
	14	Hammer Pin
	15	Drive Shaft
	16	Mesh

4.2.3.1 Crushing Chamber

First, the entire design was redone using the sheet metal feature on SolidWorks to better account for the size of the sheet metal available in the U.S., the curves that are made from bending sheet metal, and the method of cutting out the sheet metal. *Figure 27* shows how the SolidWorks sheet metal feature works by creating the curved piece and then flattening it out to determine what cuts to make. These changes came from recommendations made by WPI Washburn Lab's operational manager, Torbjorn Bergstrom, and senior instructional lab technician, Ian Anderson.

They recommended making the entire design out of sheet metal and using the Crossfire V1.1 CNC Plasma table to cut out the parts. It was also recommended to combine some of the pieces, so that there was less to cut out and less to weld together, making for easier manufacturing. From that recommendation, the hopper was combined with the top casing piece. There are now four pieces that will be welded to make up the top casing and hopper, a flat front and back piece and two curved and bent side pieces. The bottom casing was them combined into two pieces that are bent and welded together to create the four sides. The flanges to bolt the top and bottom casing was moved from the front and back to the sides. This allows the front and back to fit flush together around the drive shaft and prevent any particles from escaping. It was determined that a 12-gauge steel sheet would be used for the entire outer casing

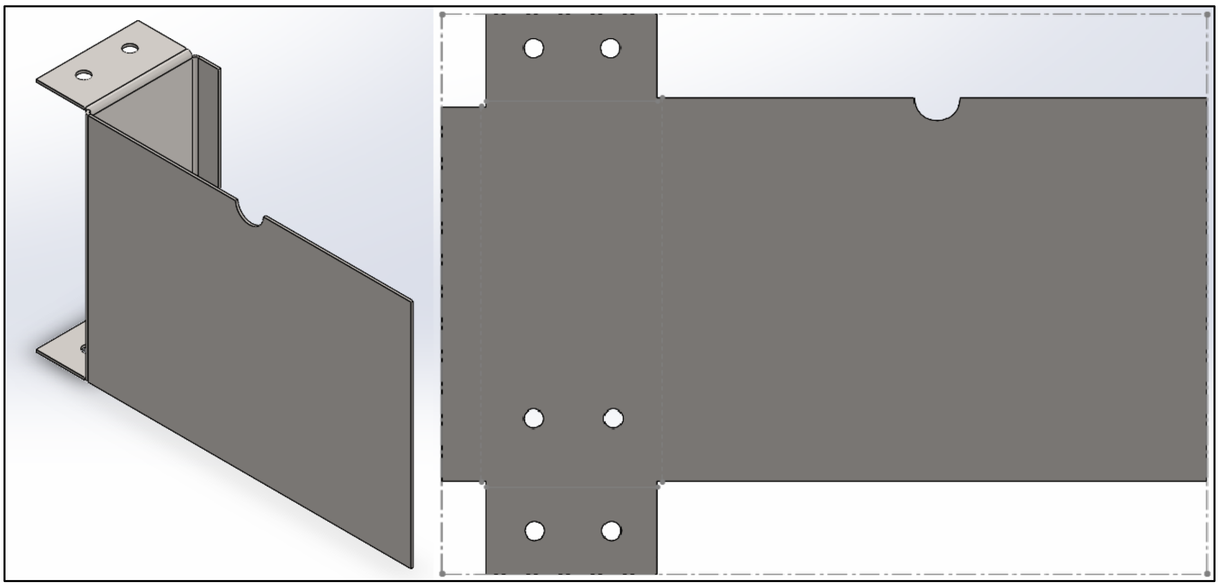

Figure 27: Side by side comparison of sheet metal feature in SolidWorks; the left shows the curved piece, and the right shows the flattened out sheet metal

In the previous design, the mesh was designed to rest on two bars on the bottom of the outer casing. In the final design, the mesh was bolted inside the lower casing so that operators can remove it without taking apart the top and bottom. The flat mesh follows a pattern of 60-degree triangles, with 1/8 in. diameter holes. Holes that are aligned in a 60-degree staggered pattern optimize open area while maintaining screen strength (Hammer Mills, 2020). The final mesh design meets the necessary requirements to ensure the system does not over heat and is efficient. First, to ensure the PCB will be ground properly, the mesh must never have less than 14 in^2 /HP of screen area, and typically more screen area is better. Then, to allow for cooling, the meshe should never have less than 4 in^2/HP of “open area” or holes (Advantages & Disadvantages in Particle Reduction Techniques, 2021). The amount of holes in the final mesh design ensures both of these requirements are met.

4.2.3.2 Stand Assembly

In the previous design, the bearings were bolted to a flange that was welded to the outside of the bottom casing. However, this is not very sturdy, and it was pointed out by Anderson that these welded flanges should never be load bearing. To accommodate this design flaw, the stand was designed to hold the bearings in addition to the hammer mill and motor. The stand is designed using 2” x 1 ½” x 0.083” rectangular tubing. The 2” width was chosen to fit the 2” width of the bearing mount. Originally, 1” height was preferred because it would be thick enough but also cheaper. However, Sullivan Metals, the steel warehouse, was out of this size so a 1 ½” height they had in stock was used. The basic stand design follows a box shape where the rectangular tubing would be welded together. Two sides on the top of the box shape would include holes to bolt the hammer mill bottom casing to. An additional part of the stand was built on the top of the box shape to hold the bearings. The top piece of this also included holes to bolt the bearing mounts to. On the bottom of the stand, a piece of sheet metal is welded that the motor can be bolted in to.

4.2.3.3 Power Transmission Unit

Initially in design one, a one HP motor was going to be used. With heavier hammer patterns, the HP/hammer ratio naturally declines so the HP was reevaluated. For tough-to-grind materials in small diameter mills, up to 28”, with 1/4” thick hammers, the ratio is roughly 1:1 (1 HP/hammer) for normal applications and 1:2 (1 HP/2 hammers) for very fine or difficult grinding (Advantages & Disadvantages in Particle Reduction Techniques, 2021). Too much HP/hammer will tend to “rock” the hammer each time the hammer swings through a bed of material on the screen, leading to rapid wear of the hammer hole and hammer mounting pin. Too little HP/hammer dramatically reduces hammermill efficiency by consuming motor horsepower simply to turn the rotor with its load of hammers (Advantages & Disadvantages in Particle Reduction Techniques, 2021). Therefore, a 1-2 HP motor would be the ideal range. The final motor chosen was a three-phase AC motor with the following specifications was used: 2 HP, 3500 rpm, 60Hz, 208-230V, as shown in *Table 9*. In the U.S., most commercial grinding machines plug into the grid, with specifications 120 V, 60 Hz. Grid power was used for the prototype in Worcester, MA because it’s the simplest and cheapest option for a proof-of-concept machine built in the U.S. The motor shown below, in *Figure 28*, was used for all calculations for the prototype.

Table 9: Prototype Motor Specifications

<table>
<tr><td rowspan="6">MOTOR SPECIFICATIONS FOR PROTOTYPE</td><td>Horsepower</td><td>2 HP</td></tr>
<tr><td>Rotor Speed</td><td>3500 rpm</td></tr>
<tr><td>Rotor Diameter</td><td>0.888 in</td></tr>
<tr><td>Frame</td><td>145T</td></tr>
<tr><td>Motor Type</td><td>3-Phase</td></tr>
<tr><td>Voltage</td><td>208-230 V</td></tr>
</table>

Figure 28: Three-phase, 2 HP AC Motor for Prototyping

Because a 2 hp and 3500 rpm motor were used, the pulley system was designed to reduce the drive shaft rpm to 1725 rpm. A 6-inch, or 15.24 cm, pulley diameter was used for the drive shaft. The following equation was then used to determine what size the motor shaft pulley should be:

$$N_1 D_1 = N_2 D_2 \qquad \text{Eq. 1}$$

Where, N_1 is the speed of the drive shaft in revolutions per minute (rpm), N_2 is the speed of the motor shaft in rpm, D_1 is the diameter of the drive shaft pulley in cm, and D_2 is the diameter of the motor shaft pulley in cm. Using 1725 rpm for N_1, 3500 rpm for N_2, and 15.24 cm as D_1, the diameter of the motor shaft pulley is calculated as 7.51 cm, or 2.96 inches. Therefore, a 3-inch diameter V-belt pulley was chosen for the motor shaft.

Next, the length of the belt was calculated. The distance between the center of the pulley's was estimated to be 58.564 cm. This distance allows a 15-inch tall five-gallon bucket to fit under the stand. Using equation 2, the length of the belt was calculated.

$$L = \frac{\pi}{2}(D_1 + D_2) + 2x + \frac{(D_1 - D_2)^2}{4x} \qquad \text{Eq. 2}$$

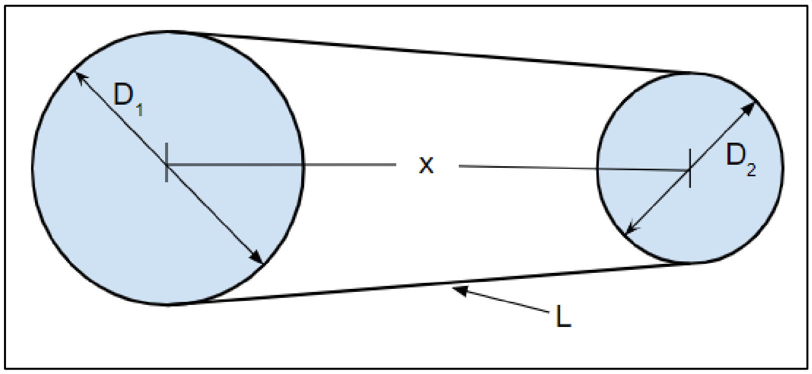

Figure 29: Set up of pulley and belt for power transmission

Where x is the distance between the centers of the pulleys in cm and L is the length of the belt in cm, all represented above in *Figure 29*. Here, the pitch diameter of the V-belts is used to calculate the belt length (Collins, 2017). Using 58.564 cm for x, 14.859 cm for D_1, and 7.239 cm for D_2, the length of the belt was calculated as 152.09 cm or 59.84 cm. A 60-inch A type V-belt was chosen for the system. The height of where the motor is attached can easily be adjusted to fix any tensioning issues.

To confirm a V-belt pulley is applicable, the speed is converted from rpm to the velocity in meters/second, in the following equation:

$$v = \frac{2\pi}{60} r_1 N_1 \qquad \text{Eq. 3}$$

Where v is the velocity of the drive shaft in m/s, r_1 is the radius of the drive shaft pulley pitch radius in meters, and N_1 is the speed of the drive shaft pulley in rpm. Using 0.0743 m as r_1 and 1725 rpm as N_1, the velocity is calculated as 13.421 m/s. This confirms a V-belt pulley will work for the design, because it is within the applicable 5 to 50 m/s range (Khurmi & Gupta, 2005).

4.2.3.4 Shaft Assembly

There were many changes made to the shaft assembly design. First, the entire design was increased slightly. To ensure the hammers had room to swing back and forth, the rotor disc diameter was increased to 7.75 inches, or 19.69 cm. It was also determined that the rotor disc would be made from a ¼” x 8” hot rolled steel flat. This is close to the thickness in design 2, and is a standard size of steel that can be easily purchased. This steel can also be used for the hammers, which will reduce the cost to purchase steel. The spacers between the hammers and rotor discs were also removed. These spacers were expensive to purchase, at approximately $8.00 apiece. After more research, it was found that these spacers are not always necessary. While there are several designs that do use spacers, there are many more that do not (Advantages & Disadvantages in Particle Reduction Techniques, 2021). So, to reduce the overall cost of manufacturing, the spacers were removed from the design.

The hammer design was further improved to increase the efficiency and maintainability. First, the diameter of the pins that go through the hammers and rotor discs was increased to ½”, to support the centrifugal force of the hammers. The maintainability of the hammers was then improved by adding holes to both sides of the hammer so that when one side wears down, the user can flip the hammer and use the other side for twice as long as a typical single-holed hammer (Hammer Mills, 2020). The layout of the hammers was then switched to a heavy hammer pattern, with hammers on all eight pins since FR-4 can be considered a tough-to-grind product (Advantages & Disadvantages in Particle Reduction Techniques, 2021). Placing hammers on all eight pins can reduce surging in the mill and improves screen coverage without overloading either hammer pins or rotor plates (Advantages & Disadvantages in Particle Reduction Techniques, 2021). The distance between hammer and screen should be approximately 1/2 inch for ideal size reduction of material, so the hammers were adjusted to meet his requirement (Hammer Mills, 2020).

As in design 2, two mounted ball bearings will be used to support the shaft. The chosen bearing is for a 1-inch diameter shaft, secured by two set screws. The bearing is self-aligning to compensate for shaft misalignment and sealed to block out contaminants. The bearing is lubricated using a lithium thickener. However, it is not permanently lubricated and will need to be periodically lubricated. A permanently lubricated bearing can be used instead for ease of use but will increase the cost. The chosen bearing has a max speed of 5,100 rpm, sufficient for the 1,725 rpm the shaft will rotate at. As mentioned earlier, the bearings will now be supported by the rectangular tubing stand.

The overall size of the shaft was then increased. This increase was determined through several calculations, following the method of Ibrahim et. al. (2019). First, the angular velocity must be calculated using:

$$\omega_h = \frac{2\pi r_h N_h}{60} \quad \text{Eq. 4}$$

Where ω_h is the angular velocity of the hammer in radian/seconds (rad/s), r_h is the radius of the circle made by the hammers rotating in meters, and N_h is the velocity of the hammer in rpm. Using 0.17325 m for r_h and 1725 rpm for N_h, the angular velocity of the hammer is 31.296 rad/s. Now, the centrifugal force from the hammers is calculated using (Ibrahim, Omran, & Abd Elrhman, 2019):

$$F_h = N_h m_h r_h \omega_h^2 \quad \text{Eq. 5}$$

Where F_h is the centrifugal force exerted by the hammers in Newtons (N), N_h is the number of hammers, and m_h is the mass of the hammers in grams (g). Using 24 hammers for N_h, 0.2486 g for m_h, 0.17325 m for r_h, and 31.296 rad/s for ω_h, the centrifugal force exerted by the hammers becomes 1012.35 N.

Next, the torsional moment is calculated to later be used in the pulley tension and shaft diameter calculations. This is found by using the power of the motor in the following equation (Ibrahim, Omran, & Abd Elrhman, 2019):

$$M_t = \frac{P * 60}{2\pi N_1} \quad \text{Eq. 6}$$

Where M_t is the torsional moment in Nm and P is the power in Watts. Using 1419.4 W for power and 1725 for N_1, the torsional moment is calculated as 8.256 Nm.

The tensions on the pulley are then be calculated to use in the bending moment calculations later. The tensions on each side of the belt are found from a system of equations using equation 7a and 7b below (Ibrahim, Omran, & Abd Elrhman, 2019).

$$2.3 \, log \frac{T_1}{T_2} = \mu\theta \, csc \, \beta \quad \text{Eq. 7a}$$

$$M_t = (T_1 - T_2) r_1 \quad \text{Eq. 7b}$$

Where T_1 is the tension on side one in N, T_2 is the tension on side two in N, μ is the coefficient of friction between the belt and pulley, θ is the belt wrap angle, β is half the groove angle of the pulley in degrees, and r_l is the radius of the drive shaft in m. Here, r_l is 0.0743 m and M_t is 8.256 Nm. The estimated coefficient of friction between a rubber belt and metal pulley is 0.3 (Khurmi & Gupta, 2005). The groove angle is estimated to be 32 degrees, so β is 16 degrees (Ibrahim, Omran, & Abd Elrhman, 2019). The belt wrap angle is calculated using equations 8a and 8b below.

$$\sin\alpha = \frac{D_1 - D_2}{2x} \qquad \text{Eq. 8a}$$

$$\theta = (180 - 2\alpha)\frac{\pi}{180} \qquad \text{Eq. 8a}$$

Where alpha is an angle of wrap in degrees to find the theta angle of wrap in radians. Using 14.859 cm for D_1, 7.239 cm for D_2, and 58.564 cm for x, alpha is calculated as 0.0651 degrees. Alpha is then used to find theta, which is calculated as 3.139 degrees.

Now going back to equation 7 and 8, the belt tensions are calculated using 3.139 degrees for θ. This gives T_1 as 114.913 N and T_2 as 3.787 N. The tensions are then used to calculate the F_P, the force of the pulley, using equation 9 (Ibrahim, Omran, & Abd Elrhman, 2019). The total force of the pulley is the sum of the two tensions, as shown in *Figure 30.*

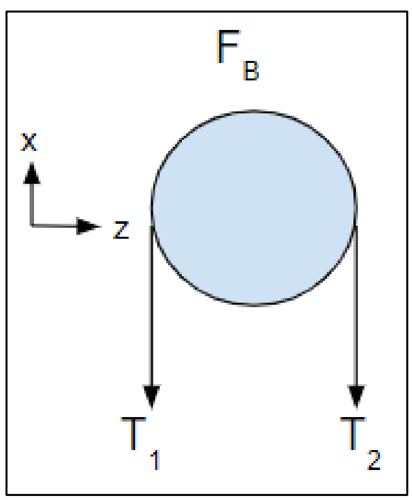

Figure 30: Forces acting on the drive shaft pulley

$$F_P = T_1 + T_2 \qquad \text{Eq. 9}$$

Using 114.913 N as T_1 and 3.787 N as T_2, the force of the pulley is calculated as 118.646 N.

Next, the maximum bending moment in the drive shaft must be calculated. To determine this, a bending moment diagram is created by looking at the loads on the shaft. Several cuts were made along the shaft to calculate the bending at various locations. *Figure 31* shows the loading on the shaft and where the cuts are made. F_h is the centrifugal force of 1012.35 N, shown as a distributed load acting upward F_H, of 10,369.36 N/m for the length of the rotor disc and hammer subassembly. F_P is the pulley force of 118.646 N. F_B and F_Q are the force of the bearings, both unknown. To calculate the unknown forces, a sum of forces equation, equation 10, and a sum of bending moments equation, equation 11, were created.

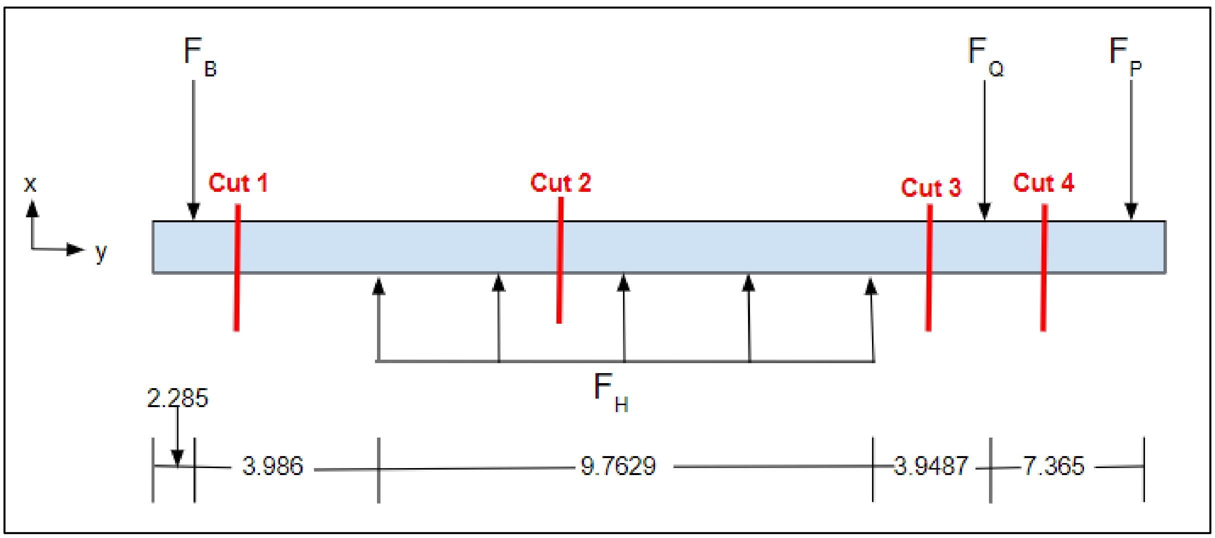

Figure 31: Forces acting on the drive shaft, with distances in cm. Red lines represent the arbitrary locations where cuts were made to calculate the bending in the beam.

$$\sum F = ma = 0 = F_h - F_B - F_P - F_Q \qquad \text{Eq. 10}$$

$$\sum M = 0 = -0.02285F_B + 0.1115F_h - 0.1998F_Q - 0.2735F_P \qquad \text{Eq. 11}$$

Using system of equations, F_B is calculated as 554.592 N and F_Q is calculated as 339.115 N. Then, the maximum bending moment is calculated by creating a bending moment diagram. A cut is made between each new force and in the distributed load to find the reaction bending moment. Equation 12, 13, 14, and 15 show the equations for finding the bending moment at cut 1, cut 2, cut 3, and cut 4, respectively.

$$\sum M = 0 = -0.02285F_B + M_1 \qquad \text{Eq. 12}$$

$$\sum M = 0 = -0.02285F_B + 10{,}369.36x(x + 0.03986) + M_2 \qquad \text{Eq. 13}$$

$$\sum M = 0 = -0.02285F_B + 0.1115F_h + M_3 \qquad \text{Eq. 14}$$

$$\sum M = 0 = -0.02285F_B + 0.1115F_h - 0.1998F_Q + M_4 \qquad \text{Eq. 15}$$

Plugging in the known values and solving equations 14 through 17, the bending moments are found as: 12.672 Nm for M_1, 12.672-10,369.36x(x+0.03986) Nm for M_2, -100.205 Nm for M_3, and -32.450 Nm for M_4.

Finally, the diameter of the drive shaft was calculated using equation 16 below (Khurmi & Gupta, 2005):

$$d^3 = \frac{16n}{\pi S_s}\sqrt{[K_b M_b]^2 + [K_t M_t]^2} \qquad \text{Eq. 16}$$

Here, d is the diameter of the drive shaft in m, n is the factor of safety, S_s is the allowable shear stress of the material in N/m^2, K_b is the combined shock and fatigue factor applied to bending moment, and K_t is the combined shock and fatigue factor applied to torsional moment. K_b and K_t are taken as 1.5 and 1 respectively for a rotating shaft with a gradually applied or steady load (Khurmi & Gupta, 2005). The maximum bending moment, M_b, is -100.205 Nm and the torsional moment, M_t, is 8.256 Nm. The allowable shear stress of the material was found using the ASME code that says the permissible shear stress for a shaft should be 30% of the yield strength (Jindal, 2010). The following equation was used to calculate S_s:

$$S_s = 0.3\sigma_{yt} \qquad \text{Eq. 17}$$

Where σ_{yt} is the yield strength of the material, taken as 75,000 pounds per square inch or 517,107,000 N/m^2 for the carbon steel shaft. This gives an allowable shear stress value of 155,132,100 N/m^2. Then solving for the diameter using equation 16, the minimum drive shaft diameter necessary is 0.02208 m or 0.869 inches. Therefore, a 1-inch diameter, carbon steel drive shaft was chosen to satisfy the minimum diameter calculated.

4.3 Manufacturing Procedure

A prototype of the final hammer mill design was manufactured in WPI's Washburn Labs. The engineering drawings that guided the manufacturing and assembly can be found in *Appendix D.* Materials were purchased, plasma cut, and welded before finally being assembled with the remaining parts.

4.3.1 Materials for Grinder

For the prototype, the following materials were purchased at a total cost of $527.60. There was a minimum purchase on the steel that included more steel than was needed for the prototype, so that also increased the cost. This did not include the cost of the motor, or the battery pack and inverter that is necessary for use in Agbogbloshie, so the overall cost would be higher for the waste processors to implement. More details on the materials and where they were ordered from can be found in *Appendix C*.

- 1 4 foot by 8 foot gauge 12 steel sheet
- 1 ¼ inch by 8 inch hot rolled steel flat , 10 feet long
- 1 2 inch by 1 ½ inch by 0.083 inch steel rectangular tubing, 20 feet long
- 1 1 inch diameter, 12 inch long 1566 carbon steel rotary shaft
- 4 0.5 inch diameter, 12 inch long 1566 carbon steel rotary shaft
- 2 mounted ball bearings with nickel-plated iron housing for 1 inch shaft diameter
- 1 7/8 inch fixed bore standard V-belt pulley, 3 inch outer diameter
- 1 1 inch fixed bore standard V-belt pulley, 6 inch outer diameter
- 1 A58 V-Belt, outside length 60 inches
- 1 Steel hinge without holes, 3 inch by 1 inch door leaf, 0.75 inches thick
- 1 10 pack of hex head screws, ½"-13 thread size, 1 ¼" long
- 1 10 pack of hex head screws, ½"-13 thread size, 7/8" long
- 1 25 pack of 316 stainless steel washers, for ½" screw size, 0.531" ID, 1.25" OD
- 1 50 pack of steel hex nuts, ½"-13 thread size

4.3.2 Plasma Cutting the Steel

The hammers and rotor discs were cut from the ¼ inch by 8 inch hot rolled flat and the outer casing, mesh, and motor stand were cut from the gauge 12 steel sheet. To cut these parts out, a Crossfire V1.1 CNC Plasma table was used, powered by the Hypertherm Powermax 1000 G3 Series. This machine cuts metal up to ½ inch thick in the x and y directions. This system uses the Mach3 application to read the G-code for the desired cut.

To create the G-code, Autodesk Fusion 360 was used following the guidance of Liam Hemmerling's (2020) Plasma Cutter Manual. The SolidWorks files for each part was converted to a 2D drawing file and uploaded to Fusion 360. Before setting up the desired cut path, the tool was added to the tool library. This step was important, as it set the kerf width for the plasma cutter. The approximate kerf width depends on the cutting speed, current, material, and consumable wear. Following an approximation for a 60 A shielded process, the kerf width was 0.063 inches for the ¼ inch thick steel and 0.056 inches for the 12-gauge steel. Then, the cutting process can be set up using the "manufacture" process in Fusion 360. A feed rate of 86 inches per minute (ipm) and a pierce delay of 0.25 was used for the ¼ inch thick steel. The 12-gauge steel used a feed rate of 308 ipm and a pierce delay of 0 (Hemmerling, 2020). For the order of the cuts, any inner holes were cut first, then the outer cut. After the cut process was set up, it was converted to G-code to be used in the Mach3 software (Hemmerling, 2020).

The G-code was them loaded into the Mach3 software on the plasma table's computer. *Figure 32* shows the setup of the plasma table and how it cuts out the parts following the G-code on the computer. After running the first cuts on each material, it was determined that the feed rates were too fast to cut completely through the steel. These original feed rates could have been off because the chart from the manufacture is old and material properties have slightly changed since then (Hemmerling, 2020). The feed rate for the ¼" steel was decreased to 60 ipm and the feed rate for the 12-gauge steel was decreased to 250 ipm. *Figure 33* shows some of the parts after being cut out by the plasma table.

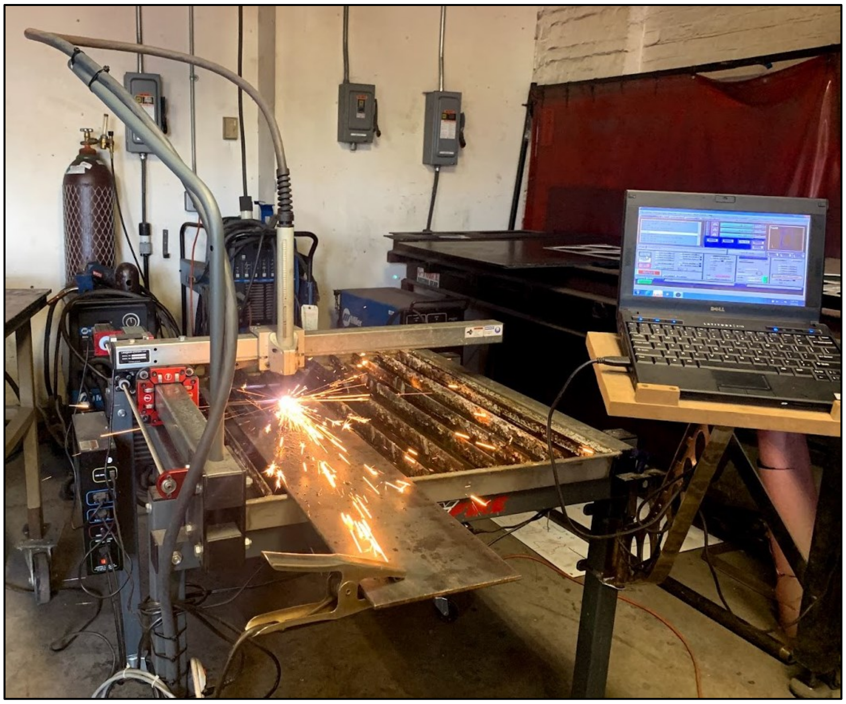

Figure 32: Crossfire V1.1 CNC Plasma table

Figure 33: Hammers and rotor discs plasma cut out of the 1/4" thick steel plate

As can be seen on the parts in *Figure 33,* the plasma table leaves imperfections of melted steel on the edges of the cuts. An angle grinder was used to smooth out the surfaces and ensure the shafts would fit. The edges of the crushing chamber pieces were also grinded to improve the surface for welding.

4.3.3 Drilling Holes in the Steel

A drill press was used to cut the holes in the steel for the bolts. The holes were first marked by a marker, then a drill tap was used to punch a hole in the center of the hole. This helps ensure the drill bit is properly aligned and stays in place when beginning the cut.

Before cutting, the drill press had to be set to the appropriate federate. Using the chart given for the machine and shown in *Figure 34*, the feed rate for uncoated, low carbon steel was 100 surface feet/minute. Converting this to RPM using a diameter of 0.5”, the feed rate became approximately 764 rpm. *Figure 35* shows the available feed rates listed on the machine. The closest feed rate, 640 rpm, was used.

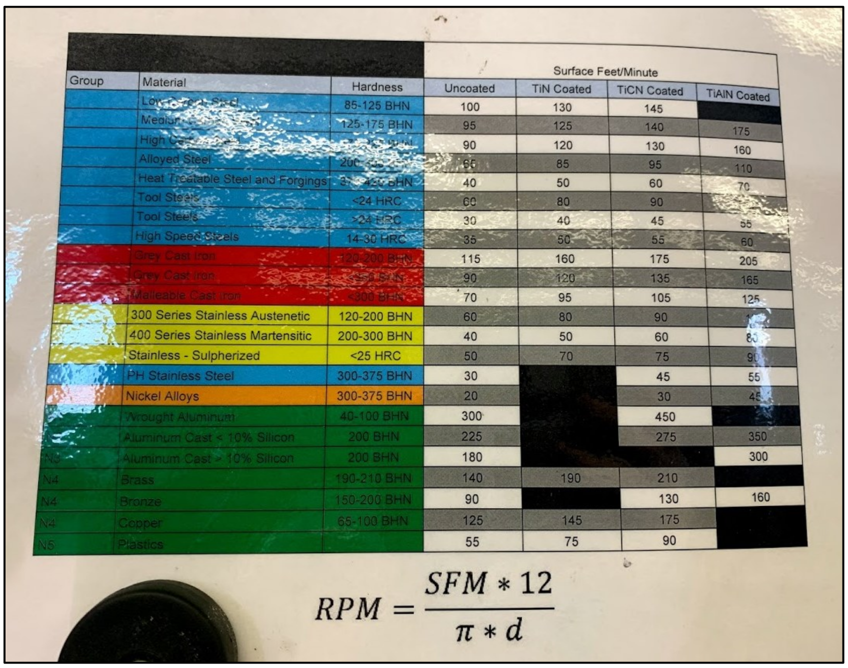

Group	Material	Hardness	Surface Feet/Minute: Uncoated	TiN Coated	TiCN Coated	TiAlN Coated
	[illegible]	85-125 BHN	100	130	145	
	[illegible]	125-175 BHN	95	125	140	175
	[illegible]	[illegible]	90	120	130	160
	Alloyed Steel	[illegible]	65	85	95	110
	Heat Treatable Steel and Forgings	[illegible]	40	50	60	70
	Tool Steels	<24 HRC	60	80	90	[illegible]
	Tool Steels	>24 HRC	30	40	45	55
	High Speed Steels	14-30 HRC	35	50	55	60
	Grey Cast Iron	120-200 BHN	115	160	175	205
	Grey Cast Iron	[illegible]	90	120	135	165
	Malleable Cast Iron	<300 BHN	70	95	105	125
	300 Series Stainless Austenetic	120-200 BHN	60	80	90	[illegible]
	400 Series Stainless Martensitic	200-300 BHN	40	50	60	[illegible]
	Stainless - Sulpherized	<25 HRC	50	70	75	[illegible]
	PH Stainless Steel	300-375 BHN	30		45	55
	Nickel Alloys	300-375 BHN	20		30	[illegible]
	Wrought Aluminum	40-100 BHN	300		450	
	Aluminum Cast < 10% Silicon	200 BHN	225		275	350
N3	Aluminum Cast > 10% Silicon	200 BHN	180			300
N4	Brass	190-210 BHN	140	190	210	
N4	Bronze	150-200 BHN	90		130	160
N4	Copper	65-100 BHN	125	145	175	
N5	Plastics		55	75	90	

$$RPM = \frac{SFM * 12}{\pi * d}$$

Figure 34: The drill press feed rate chart

Figure 35: Front face of the drill press, showing the available feed rates and their settings

Next, the size of the hole was determined. The bolts used are a ½”-13 thread size. The size of the hole was determined using a tap and clearance drill size chart. A free fit was desired to ensure the bolt would easily fit and give some more leeway in the alignment of holes in the assembly. A free fit clearance drill for a ½” bolt was 17/32” (Tap and Clearance Drill Sizes, n.d.). The step bit used in the drill press, as seen in *Figure 36*, did not have a 17/32” size. Therefore, the next closest size, 9/16”, was used to drill the holes. It was also necessary to place wood underneath the steel sheet, as seen in *Figure 36*, to ensure the drill bit could go through the sheet up to the 9/16” size. From the drilling, there were sharp edges on the back of the steel sheets. To remove these, the sheets were deburred with a hand drill.

Figure 36: Using the drill press to cut holes in the outer casing

4.3.4 Bending the Crushing Chamber Steel

After the plasma cutting and drilling, the parts were ready to be bent. This was done using a sheet metal slip roller and brake. First, the locations of the bend were marked on the pieces with a marker. Then, the two side pieces of the upper crushing chamber casing were curved using the slip roller. Starting with the roller flat, the sheet metal was fed through the rollers. The radius of curvature created by the rollers was then slightly increased and the sheet metal was fed through again. This process continued until the sheet metal was curved to the correct radius, when the roller lined up at approximately 2.85 inches.

Next, the sheet metal brake, shown in *Figure 37,* was used to make the bends. The bend lines were lined up with the brake and locked into place, allowing some room for the bend radius. Then, the brake was pushed upwards until the bend was at the correct angle.

Figure 37: Sheet metal brake used in Washburn Shops

The two flanges on the bottom crushing chamber casing were not able to be bent using the brake, due to the other bent pieces obstructing the way. Therefore, the piece was instead heated up and bent using a different method. First, as seen in *Figure 38*, the upper flange needs to sit flush with the top of the front side, to ensure the top and bottom casings fit snuggly. To allow for this, a hack saw was used to cut slightly into the sheet metal on each side of the flange, about ¼”. Then, the location of the bend was heated up using an oxy-acetylene flame. After the metal began to look red hot, it was clamped to the table with a piece of metal at the location of the bend, as seen in *Figure 39*. The metal was then bent upwards at a 90-degree angle. This was done for the flange on the top and bottom of both bottom casing pieces.

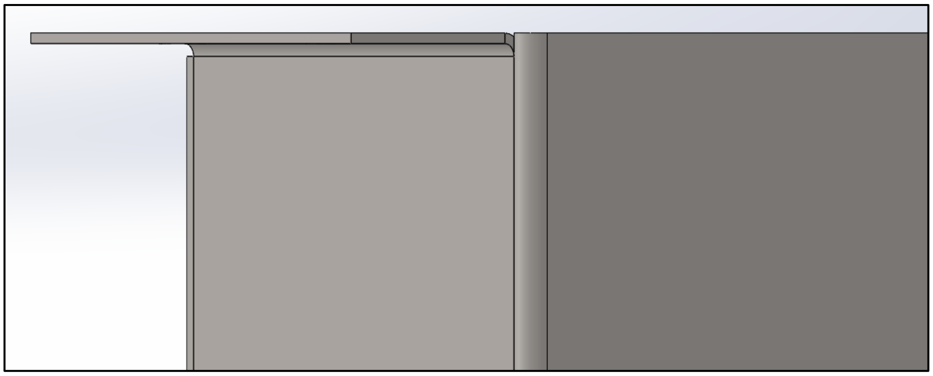

Figure 38: The upper flange on the bottom crushing chamber casing sitting flush with the front face

Figure 39: Outer casing clamped to the table, ready to bend the flanges

4.3.5 Cutting the Stand Tubing

The 2” x 1 ½” x 0.083” rectangular tubing was used to build the stand to support the hammer mill and bearings. The tubing was measured to the correct sizes and then cut using the table saw, seen in *Figure 40*. This process created sharp edges where the tubing was cut. The angle grinder was used again to remove these sharp edges and prepare it for welding.

Figure 40: Table saw used to cut the rectangular steel tubing

After being cut, holes were drilled into four of the pieces, two to hold the hammer mill and two to hold the bearings. The locations of these holes were determined by simply placing either the bearing or outer casing piece on top of them and tracing the hole. Then, the same steps were followed to use the drill press and create the holes.

The table saw was used again to cut the hammer pins. The shafts purchased for the hammer pins were 12 inches long. These had to be cut down into 8, 4.05" long shaft. These were measured out and then cut with the table saw just as the rectangular tubing was.

4.3.6 Welding the Crushing Chamber

After cutting the six outer casing pieces out of the gauge 12 steel and bending them to the desired shapes, MIG welding was used to connect them. MIG, or metal inert gas, welding is an arc welding process in which a continuous solid wire electrode is fed through a welding gun and into the weld pool, joining the two base materials together. A shielding gas is sent through the welding gun and protects the weld pool from contamination (MIG Welding: The Basics for Mild Steel, 2020).

We used the welding machine's associated chart, shown in *Figure 41,* to determine the wire speed and voltage settings, beginning with the type of material we were using. A mixture of 75% Argon and 25% Carbon dioxide was used for the shielding gas. This mixture of Argon and Carbon dioxide produces less spatter than a 100% Carbon dioxide shielding gas. 12-gauge steel is closest to 1/8 of an inch on the chart, so we used 1/8 of an inch was used for the thickness of the material being welded. The wire size diameter in Washburn shops was .035 inches. Based on the selections chart, 16 Volts and a 235 ft/min were chosen as a starting point. To fine tune the welding so that there were no bumps in the welding stream, the voltage was increased to 17.8 Volts and the wire speed was reduced to 199 ft/min.

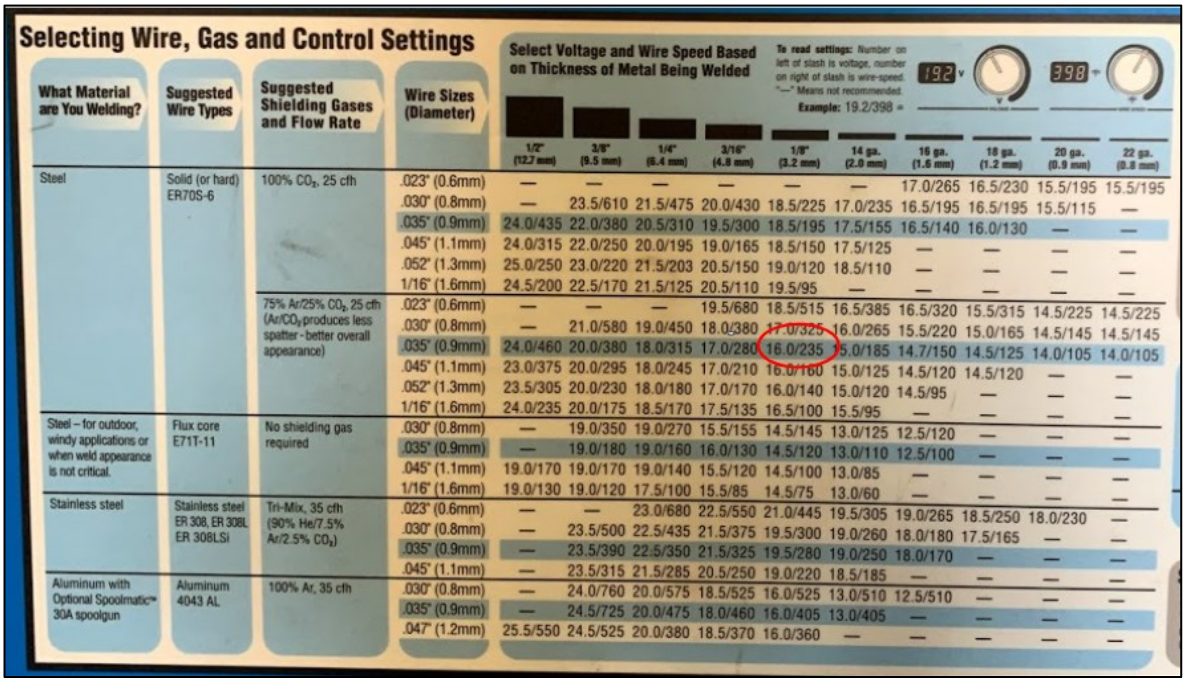

Selecting Wire, Gas and Control Settings

Select Voltage and Wire Speed Based on Thickness of Metal Being Welded

To read settings: Number on left of slash is voltage, number on right of slash is wire-speed. "—" Means not recommended. Example: 19.2/398 =

What Material are You Welding?	Suggested Wire Types	Suggested Shielding Gases and Flow Rate	Wire Sizes (Diameter)	1/2" (12.7 mm)	3/8" (9.5 mm)	1/4" (6.4 mm)	3/16" (4.8 mm)	1/8" (3.2 mm)	14 ga. (2.0 mm)	16 ga. (1.6 mm)	18 ga. (1.2 mm)	20 ga. (0.9 mm)	22 ga. (0.8 mm)
Steel	Solid (or hard) ER70S-6	100% CO_2, 25 cfh	.023" (0.6mm)	—	—	—	—	—	—	17.0/265	16.5/230	15.5/195	15.5/195
			.030" (0.8mm)	—	23.5/610	21.5/475	20.0/430	18.5/225	17.0/235	16.5/195	16.5/195	15.5/115	—
			.035" (0.9mm)	24.0/435	22.0/380	20.5/310	19.5/300	18.5/195	17.5/155	16.5/140	16.0/130	—	—
			.045" (1.1mm)	24.0/315	22.0/250	20.0/195	19.0/165	18.5/150	17.5/125	—	—	—	—
			.052" (1.3mm)	25.0/250	23.0/220	21.5/203	20.5/150	19.0/120	18.5/110	—	—	—	—
			1/16" (1.6mm)	24.5/200	22.5/170	21.5/125	20.5/110	19.5/95	—	—	—	—	—
		75% Ar/25% CO_2, 25 cfh (Ar/CO_2 produces less spatter - better overall appearance)	.023" (0.6mm)	—	—	—	19.5/680	18.5/515	16.5/385	16.5/320	15.5/315	14.5/225	14.5/225
			.030" (0.8mm)	—	21.0/580	19.0/450	18.0/380	17.0/325	16.0/265	15.5/220	15.0/165	14.5/145	14.5/145
			.035" (0.9mm)	24.0/460	20.0/380	18.0/315	17.0/280	16.0/235	15.0/185	14.7/150	14.5/125	14.0/105	14.0/105
			.045" (1.1mm)	23.0/375	20.0/295	18.0/245	17.0/210	16.0/160	15.0/125	14.5/120	14.5/120	—	—
			.052" (1.3mm)	23.5/305	20.0/230	18.0/180	17.0/170	16.0/140	15.0/120	14.5/95	—	—	—
			1/16" (1.6mm)	24.0/235	20.0/175	18.5/170	17.5/135	16.5/100	15.5/95	—	—	—	—
Steel – for outdoor, windy applications or when weld appearance is not critical.	Flux core E71T-11	No shielding gas required	.030" (0.8mm)	—	19.0/350	19.0/270	15.5/155	14.5/145	13.0/125	12.5/120	—	—	—
			.035" (0.9mm)	—	19.0/180	19.0/160	16.0/130	14.5/120	13.0/110	12.5/100	—	—	—
			.045" (1.1mm)	19.0/170	19.0/170	19.0/140	15.5/120	14.5/100	13.0/85	—	—	—	—
			1/16" (1.6mm)	19.0/130	19.0/120	17.5/100	15.5/85	14.5/75	13.0/60	—	—	—	—
Stainless steel	Stainless steel ER 308, ER 308L ER 308LSi	Tri-Mix, 35 cfh (90% He/7.5% Ar/2.5% CO_2)	.023" (0.6mm)	—	—	23.0/680	22.5/550	21.0/445	19.5/305	19.0/265	18.5/250	18.0/230	—
			.030" (0.8mm)	—	23.5/500	22.5/435	21.5/375	19.5/300	19.0/260	18.0/180	17.5/165	—	—
			.035" (0.9mm)	—	23.5/390	22.5/350	21.5/325	19.5/280	19.0/250	18.0/170	—	—	—
			.045" (1.1mm)	—	23.5/315	21.5/285	20.5/250	19.0/220	18.5/185	—	—	—	—
Aluminum with Optional Spoolmatic™ 30A spoolgun	Aluminum 4043 AL	100% Ar, 35 cfh	.030" (0.8mm)	—	24.0/760	20.0/575	18.5/525	16.0/525	13.0/510	12.5/510	—	—	—
			.035" (0.9mm)	—	24.5/725	20.0/475	18.0/460	16.0/405	13.0/405	—	—	—	—
			.047" (1.2mm)	25.5/550	24.5/525	20.0/380	18.5/370	16.0/360	—	—	—	—	—

Figure 41: The welding machine voltage and wire speed selection chart

First, corner and lap joints were practiced on scrap metal. Then, two parts of the upper assembly were secured into the shape visualized in the CAD using triangular shaped magnets. Several spot welds, or small and quick welds, were added to the straight edges of the two sheet metal pieces. After the spot welds, the straight edges of the two upper assembly parts were corner welded together. For the corner weld, one team member held the two pieces together while the other team member spot welded from the top to the bottom of the curve. *Figure 42* shows a corner weld along the curved edge of the upper assembly. The same process was repeated for connecting a third piece of the upper assembly. In the future, the remining outer casing, stand, and shaft assembly pieces will be welded using the same process.

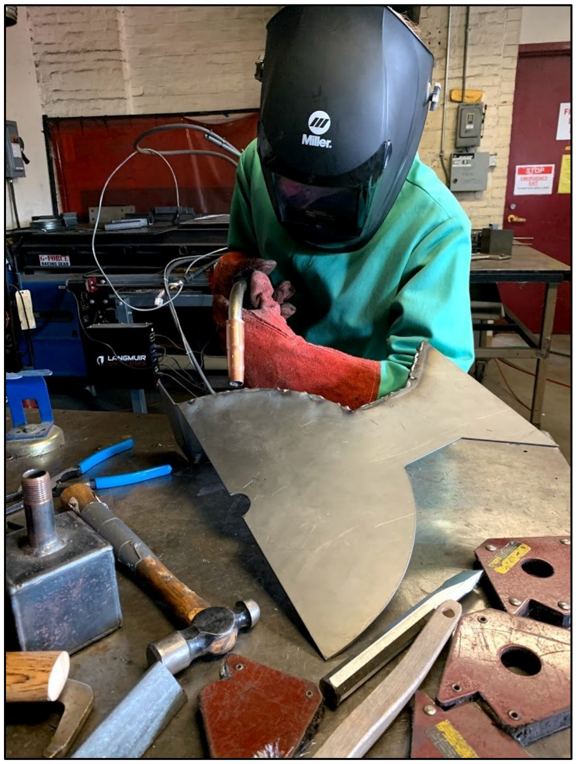

Figure 42: Welding the upper assembly together

4.3.7 Assembling the Final Prototype

After purchasing, cutting, bending, and welding all the parts, it was time to start the assembly. First, the shaft assembly was put together, where the hammer pins were put on a rotor disc, then four hammers added, and then a new rotor disc placed on top. Then, the new layer of hammers, in an alternating pattern, were placed. This was followed until all the hammers and rotor discs were assembled on the hammer pins. The main drive shaft was then put through the layers of rotor discs. Because the holes were not cut perfectly by the plasma cutter, they were filed down slightly to ensure the shaft could fit through. However, it was important not to file them down too much as a tight fit was still desired. After filing, the shaft was hammered through the holes using a rubber mallet. A bearing was then hammered onto each side of the shaft and screwed into place with two set screws. And finally, the drive pulley was hammered on and screwed into place to get the final shaft assembly show in *Figure 43*. In the future, the rotor discs will be welded to the hammer pins and drive shaft to ensure the design stays together when spinning at high speeds.

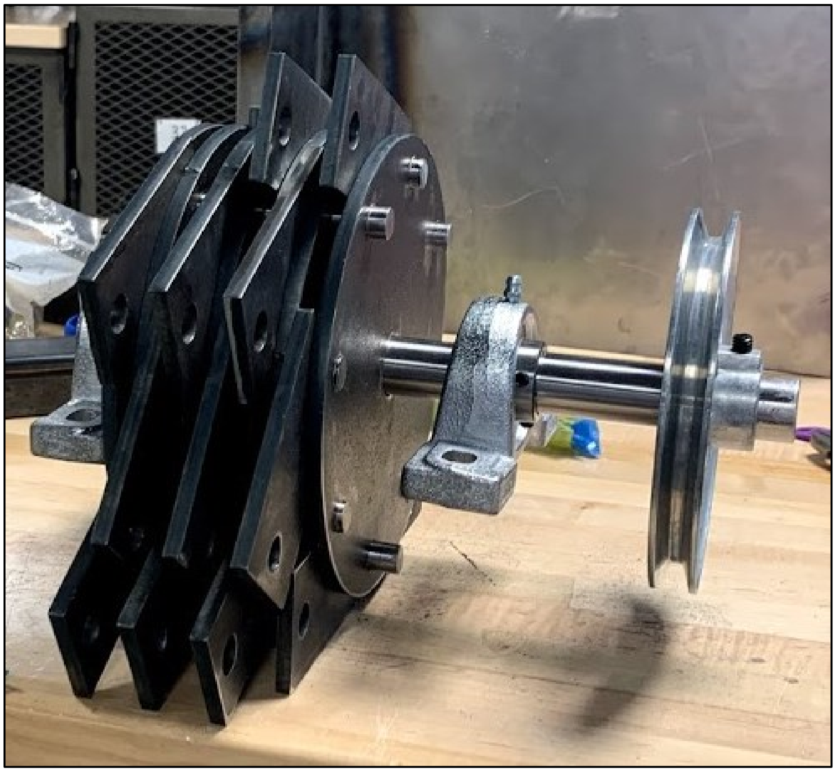

Figure 43: Final shaft assembly

Due to time constraints, the entire stand was not built. So, for proof-of-concept purposes, the shaft assembly was placed on top of just the bearing stand part of the full stand assembly. One half of the bottom casing was placed on the backside of the shaft assembly, while one half of the upper casing was placed on top of this. The two crushing chamber casing pieces were then bolted together. The final assembly made can be seen in *Figure 44*. Missing from this partial prototype is the front of the upper crushing chamber, the funnel cover, the other half of the bottom casing, the mesh, the stand, and the motor and pulley.

Figure 44: Final assembly of partial prototype

4.4 Testing the Hammer Mill Design

Because a full prototype was not completed, it could not be tested how well the design grinds the PCB. To support the design, a PCB was tested to determine is rupture energy, which shows that the hammer mill will in fact grind the PCB. ANSYS was also used to analyze the shaft and outer casing of the design. The shaft analysis showed that it would not fail under the given forces and reinforce the calculations done in Section 4.2.3.4. The outer casing analysis showed that if a hammer were to break off the shaft assembly and hit the outer casing during use, it would not pierce through the casing, ensuring that the design is safe. These tests support the use of the hammer mill, showing that it is safe and will work.

4.4.1 PCB Testing with an Instron

The specific rupture energy of the PCB can be compared to the specific energy of the hammer to determine if the hammer mill will efficiently break down the PCB, just as Ibrahim et. al. (2019) did for their agriculture hammer mill with corn. The rupture energy refers to the work required for rupture. The specific energy of one hammer should be higher than the specific rupture energy of the PCB to ensure the hammers will grind the PCBs. To test this, the specific energy of one hammer needs to be calculated. Based on *Figure 45*, which shows how the hammer crushes the PCB, two assumptions can be made. First, that the mass of the hammer is greater than the mass of one PCB particle. And second, that before impact, the linear velocity of the crushing hammer is more important than the velocity of the PCB particle. Therefore, kinetic energy of the PCB particles is negligible (Ibrahim, Omran, & Abd Elrhman, 2019).

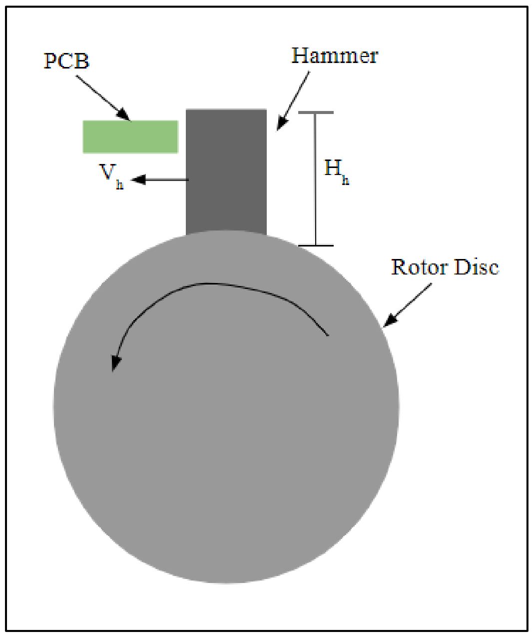

Figure 45: The mechanism of impact of how the hammer crushes the PCB

Because of these assumptions, the crushing effect is dependent on the kinetic energy of the hammer (Ibrahim, Omran, & Abd Elrhman, 2019). The kinetic energy of the hammer is calculated as the interchange of energy between the hammer and the particle. For a non-elastic collision and using the idea of conservation of linear momentum, the initial and final kinetic energy of the hammer are equal. The initial kinetic energy of the hammer is found using equation 18 (Ibrahim, Omran, & Abd Elrhman, 2019).

$$T_0 = \frac{1}{2} m_h V_h^2 \qquad \text{Eq. 18}$$

Where T_0 is the initial kinetic energy in Joules (J), m_h is the mass of one hammer in kg, and V_h is the velocity of the hammer, equal to the rotor velocity, in m/s. Using the mass of the hammer as 0.24858 kg and the velocity of the hammer as 13.421 m/s, the kinetic energy of one hammer is 22.387 J. Next, the mass of PCB impacting one hammer is calculated using equation 19 (Ibrahim, Omran, & Abd Elrhman, 2019).

$$m_I = m_p \frac{H_h}{W_h} \qquad \text{Eq. 19}$$

Where m_I is the mass impacting the hammer in g, m_p is the mass of the PCB in g, H_h is the height of the hammer in cm, and W_h is the width of the PCB in cm. Since this number varies as the PCB randomly moves inside the crushing chamber, the worst-case scenario is assumed. This is shown in *Figure 46,* where the entire hammer is interacting with vertically laid PCBs. Therefore, the width of the PCB is taken as 0.173 cm. Assuming a 2.54 cm by 2.54 cm piece (1 in^2), the mass is 2.39 g. Then, using the height of the hammer as 10.16 cm, the mass impacting the hammer is 140.36 g.

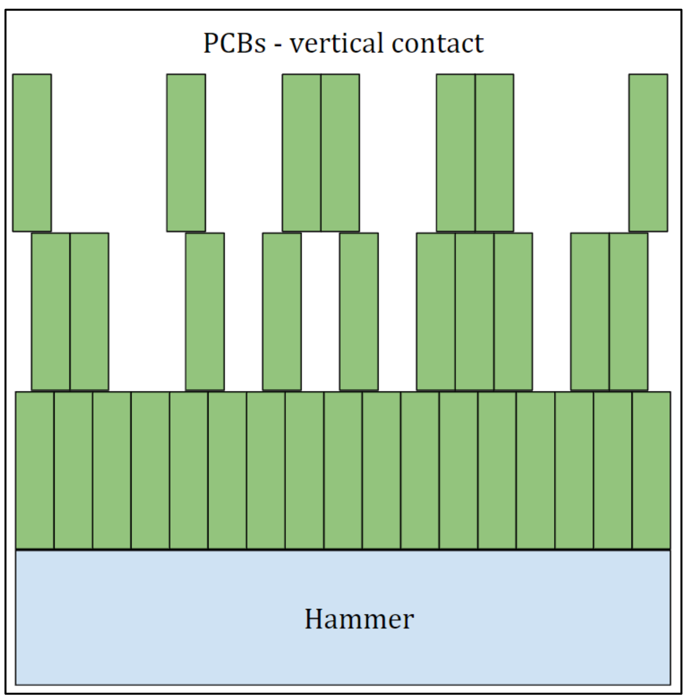

Figure 46: Maximum number of PCBs impacting the hammer

Finally, the specific kinetic energy of the hammer was found by dividing the kinetic energy by the mass impacting the hammer, shown in equation 20 (Ibrahim, Omran, & Abd Elrhman, 2019).

$$SE_h = \frac{T_0}{m_I} \qquad \text{Eq. 20}$$

Where SE_h is the specific energy of the hammer in J/kg. Using the specific energy of 22.387 J and mass impacting the hammer, now in kg, of 0.14037 kg, the specific energy of one hammer is 159.49 J/kg.

Next, the rupture energy can be calculated to compare to the specific energy of the hammer. The rupture energy is the work required for rupture which is determined from the area under the force-deformation curve, using equation 21 (Ibrahim, Omran, & Abd Elrhman, 2019).

$$RE = \frac{F_r D_r}{2} \qquad \text{Eq. 21}$$

Where RE is the rupture energy in Joules, F_r is the rupture force in Newtons and D_r is the deformation at the rupture point in m. This is then converted to the specific rupture energy, by dividing the rupture energy by the mass of the specimen tested.

An Instron machine was used to determine the force-deformation curve of the PCB we plan to grind. A three-point bending test, with a support span of 3 cm, was used as seen in *Figure 47*. A 10.16 cm by 10.16 cm piece of PCB was tested and the force-deformation curve calculated. The force-deformation curve can be found in *Figure 48*.

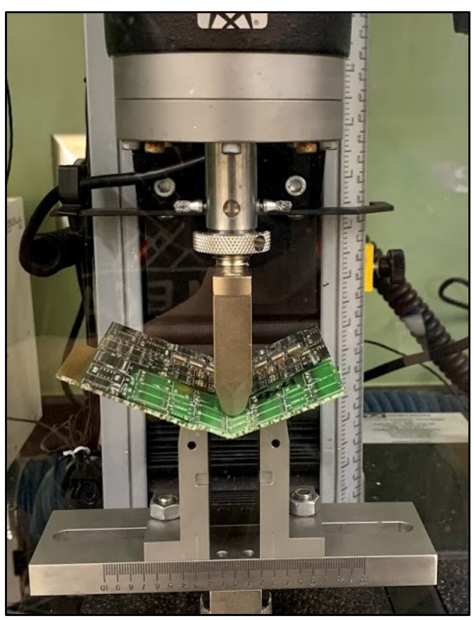

Figure 47: PCB three-point bending test on the Instron

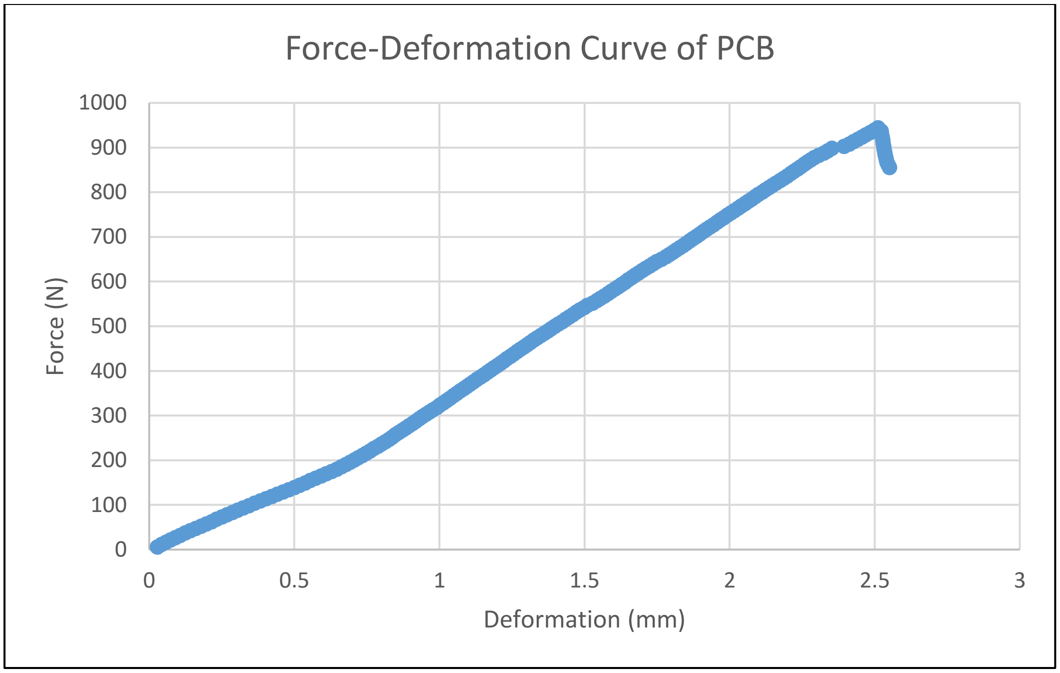

Figure 48: Force-deformation curve from the three-point bending of a PCB using the Instron

The rupture, or fracture, point is the maximum peak seen at a deformation of 2.522 mm and a force of 937.155 N. Using equation 21, the rupture energy is calculated as 1.182 J. The mass of the PCB specimen was 0.038 kg. Therefore, the specific rupture energy becomes 31.097 J/kg. Comparing this value to the specific kinetic energy of one hammer, 159.49 J/kg, the hammers will have sufficient force to break the PCB.

4.4.2 Shaft Analysis in ANSYS

To confirm the hand calculations for the shaft completed in Section 4.2.3.4, an ANSYS Static Structural analysis was run. The material of the shaft is 1566 Carbon Steel. So, the material settings were set to have a density of 7850 kg/m^3, a Poisson's ratio of 0.29, a shear modulus of 81 GPa, a Young's modulus of 209 GPa, a yield strength of 517 MPa, and an ultimate tensile strength of 689 MPa (ASTM A29 Grade 1566, n.d.). The shaft was split up into different sections as shown in *Figure 49*, to match the locations of where the forces are acting. Then, the forces were added in, using 1012.35 N for F_h, 118.646 N for F_P, 554.592 N for F_B, and 339.115 N for F_Q. A fixed support was placed at each end of the shaft.

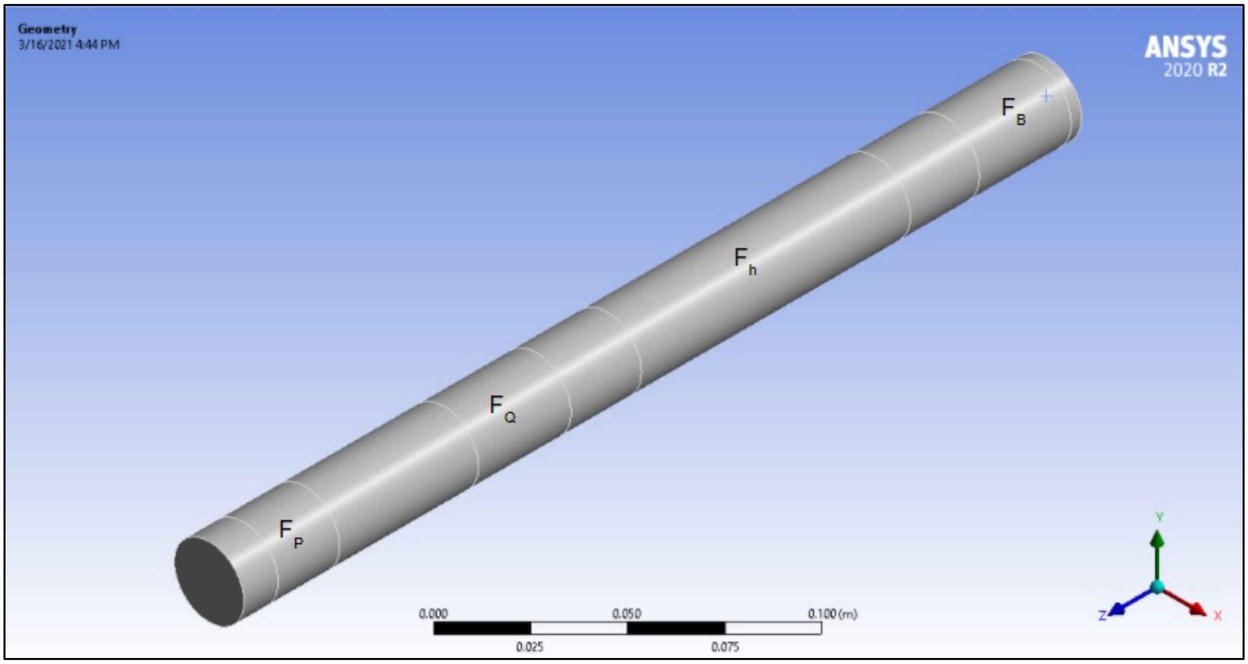

Figure 49: Shaft broken up into sections for each force

An equivalent von-mises stress was run on the shaft and the results are shown in *Figure 50*. This test showed that the maximum stress was 16.255 MPa, acting on the one end of the shaft. This stress is lower than the yield strength of the material, 517 MPa, so the shaft will not fail under the stresses.

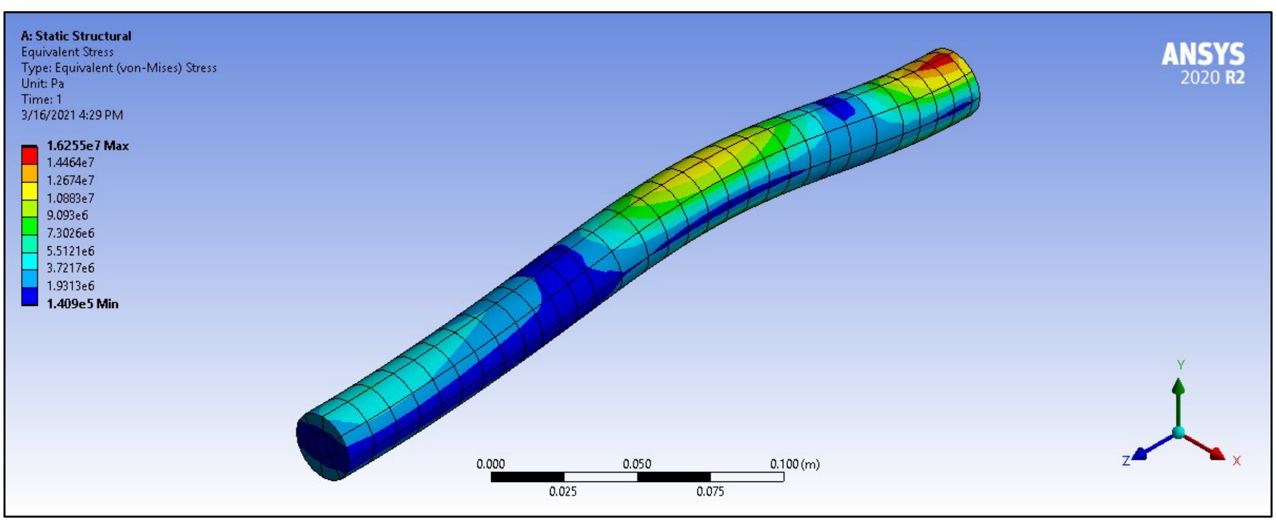

Figure 50: Equivalent von-mises stress on the drive shaft

4.4.3 Critical Failure of Crushing Chamber

An important design requirement was to ensure the grinder was safe to use. To ensure safety, the worst-case scenario must be considered. If a critical failure of the shaft assembly were to occur, a hammer could come flying off at a high speed into the crushing chamber casing. To protect the users of the grinder, the steel used for the grinder must be thick enough to withstand the force of the hammer and prevent it from breaking through. ANSYS Workbench was used to analyze if the force of the hammer would break through the gauge 12 steel chosen for the crushing chamber. The force of one hammer was found by dividing the centrifugal force by 24 hammers, to get 42.18 N of force. To consider how this force would affect the steel plate, two analyses were run. The first was with the force acting over a 2" by ¼" area as if the bottom part of the hammer were colliding with the middle of the casing. The equivalent stress caused by this is shown in *Figure 51*, where the maximum stress was 5.05 MPa.

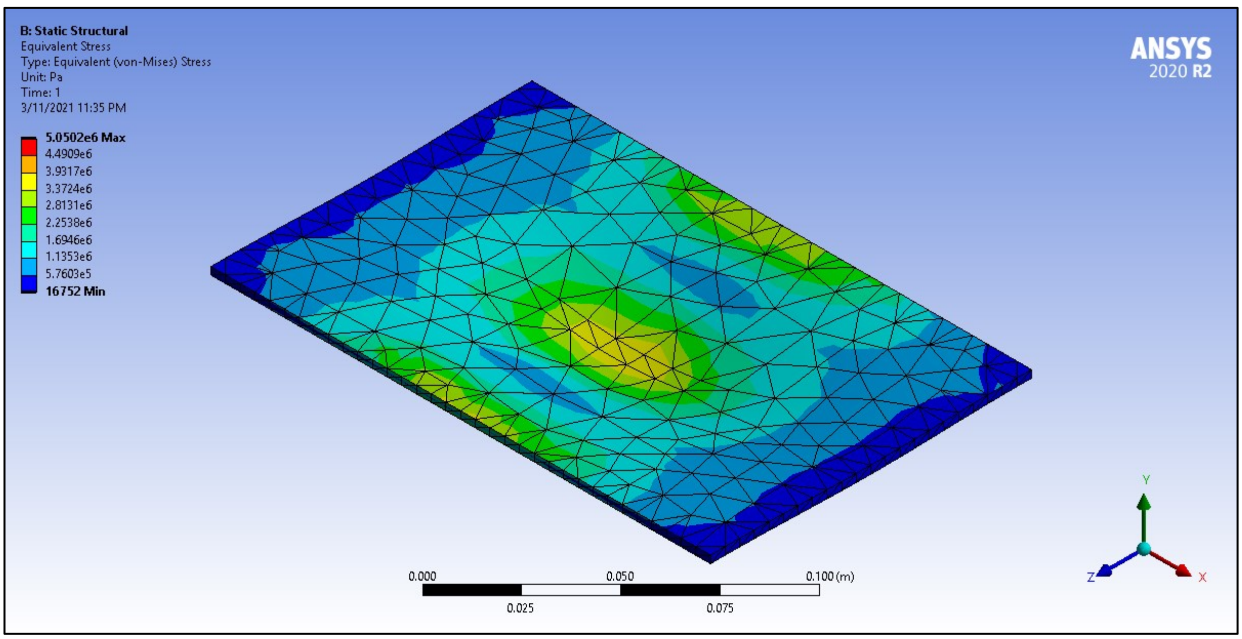

Figure 51: ANSYS equivalent stress analysis on impact of bottom of hammer on steel casing

The second test was run with the corner of the hammer, approximately ¼" by 0.01", hitting the outer casing in the corner of the plate. As seen in *Figure 52*, the maximum stress was higher at 13.76 MPa. Both values, however, were much smaller than the yield strength of the steel, around 520 MPa. This means that the hammer will not break through the crushing chamber casing if a catastrophic failure were to occur. Therefore, the design of the hammer mill meets the safety requirements.

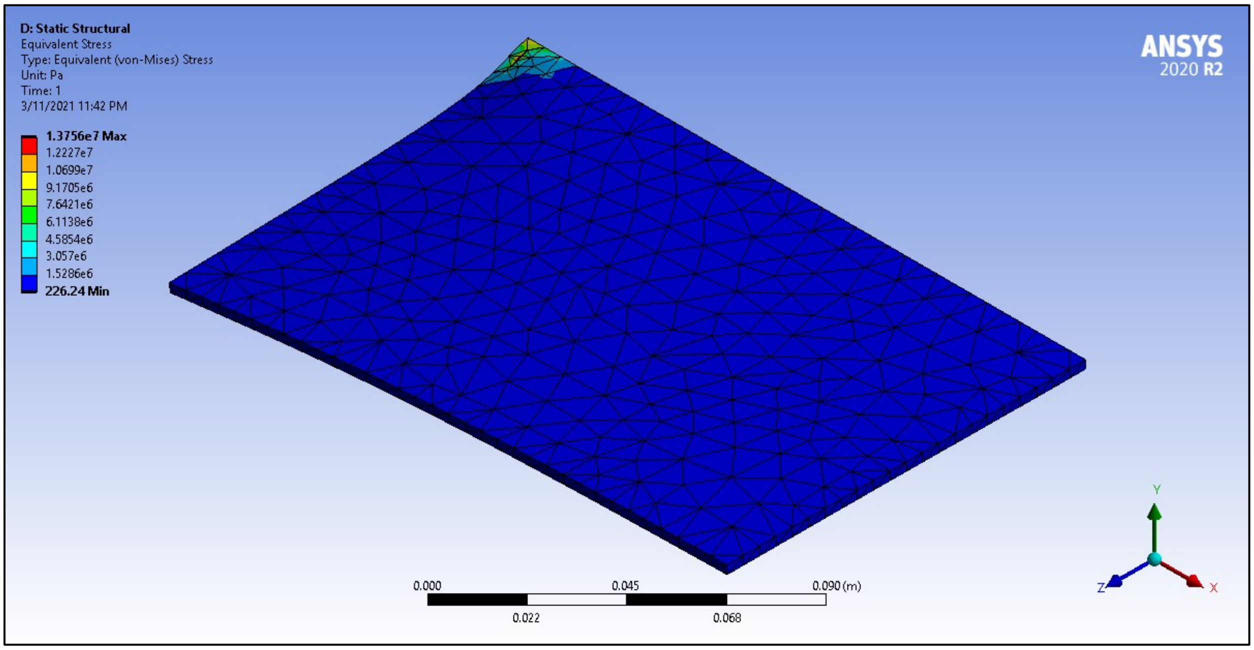

Figure 52: ANSYS equivalent stress analysis on impact of corner of hammer on steel casing

4.5 Recommendations for Deployment in Agbogbloshie

Deploying the grinder in Agbogbloshie provides a unique set of obstacles. First, the manufacturing capabilities are different than what is available at WPI's campus. However, there is a makerspace platform that can be used to successfully manufacture the grinder. There are also concerns about how to power the motor where the waste processes occur, since there is no electricity. However, a simple battery pack could be the solution. And lastly, the PCB grinder is a new idea that the waste processors may be weary of. If introduced correctly, the grinder can help fully realize the value of the PCBs. The following sections explain how the grinder can be adapted to fit the context of Agbogbloshie.

4.5.1 Manufacturing in Agbogbloshie

To manufacture the hammer mill grinder, the Agbogbloshie Makerspace Platform (AMP) can be utilized. DK Osseo-Asare and Dr. Yasmine Abbas developed the AMP spacecraft, a small-scale and low-cost craft space to enable makers with limited resources (Warner, 2018). The first spacecraft was launched in Agbogbloshie and is shown in *Figure 53*. The spacecraft creates a community makerspace with tools, paired with an app that can provide training and other scrap and trading information. Welders, seamstresses, technicians, machinists, and more make use of the makerspace (Warner, 2018).

Figure 53: AMP spacecraft in Agbogbloshie (Agbogbloshie Makerspace Platform, AMP_Spacecraft_2, 2017)

The makerspace and Agbogbloshie in general have many of the tools necessary for building the grinder. When researching how the makerspace spacecraft was built, drill presses and angle grinders can be seen, in *Figures 54 and 55*. There are also carts of tools in the makerspace, such as hammers, screw drivers, and saws, that can be checked out and either used in the space or taken somewhere else for use. Recently, they have also been working on adding ceiling-mounted CNC bots to these makerspaces. While there is no current update on if these have been installed yet or what they can be used for, it is possible the crushing chamber and shaft assembly parts can be machined here. If not, these parts can be outsourced and then assembled using the makerspace tools. There are also many artisanal welders within Agbogbloshie, who build their own welding machines with recycled copper wires and other parts and are skilled in using the machines.

Figure 54: Worker using a drill press while building the AMP spacecraft (Agbogbloshie Makerspace Platforms, 2014)

Figure 55: Worker using an angle grinder while building the AMP spacecraft (Agbogbloshie Makerspace Platform, DSC_0410, 2014)

Many parts, such as the shafts, bearings, pulleys, and motors may need to be outsourced if a suitable part cannot be recycled. However, the rest of the grinder likely can be manufactured and then assembled in the AMP spacecraft.

4.5.2 Power Recommendation for Agbogbloshie

A lead-acid battery bank paired with a sine wave power inverter may work best for using the grinder on site in Agbogbloshie because there is a lack of AC power. This will allow e-waste operators to run the grinder for 4-5 hours at a time without needing to recharge the batteries. *Figure 56* below shows an example of a sine wave power inverter with the following specifications: Input 12 V, Output 120 VAC, 60 Hz, 600 W / 1200 W Continuous / Source (Reid, 2017). This inverter was used to power a 400 W AC laser printer in an off-grid location with solar batteries. Reid (2017) recommends ensuring cable lengths between the DC battery and the inverter are as short as possible to reduce loss in the wires. Power inverters pull a huge amount of current on the DC battery side, so thick (larger than 6 gauge) and short wires tend to work best between the battery and power inverter.

Figure 56: Pure Sine Power Inverter (Reid, 2017)

To calculate how long the battery will last, the battery's capacity and how much current will be drawn by the motor are considered. Batteries measure their capacity in milliamp hours (mAh). This refers to how many hours the battery can supply 1 mA of current, or how many mA of current it can supply for one hour (Tips For Powering Motors With Batteries, 2020). To calculate how long a battery will last, the following formula was used:

$$Running\ Time\ (h) = \frac{Battery\ Capacity\ (mAh)}{Operating\ Current\ (mA)} \qquad \text{Eq. 22}$$

The battery capacity is measured under very specific test conditions and does not represent all scenarios. In real applications, the battery may perform to its rating with low and intermittent current draws, however, it will discharge much quickly with higher current draws. A battery with

1600 mAh rating will provide 1 mA for close to 1600 hours, however, it will not provide 1.6A for a full hour. Adding a second battery in parallel will keep the supply voltage the same but increase the capacity. Laptop batteries commonly use 4 cells in series to increase the voltage, and two parallel sets of the 4 series cells to increase the capacity (Tips For Powering Motors With Batteries, 2020). Usually, the battery capacity should be no more than 12 times the charging current that can be provided by the inverter. For example, a 5A charger can accommodate only 60AH (5A*12=60AH). In addition, the charging current provided by the inverter should be below the limiting current of the battery to ensure the battery does not get damaged during charging (Utility, 2020).

The battery power required for a 2HP Motor AC at 60 Hz that can run at approximately 1500-2000 rpm is calculated using Ohms Law and the running time formula. The stakeholders will be using an inverter to convert DC (12V) to AC (220v)(60Hz). When considering a 12 V battery the current required is given by:

$$I = \frac{P}{V} = \frac{2300\ Watts}{12\ V} \approx 200\ A \qquad \text{Eq. 23}$$

Where I is the current in Amps, P is the power in Watts, and V is the voltage in Volts. For a 5-hour run time, our stakeholders would need 1000 Ah capacity with a 100% efficiency inverter. Assuming the stakeholders use an 80% efficient inverter, and the batteries are discharged by 75 % to prolong their life, the required battery capacity is given by:

$$Ah = \frac{1000\ Ah}{80\% \times 75\%} = \frac{1000\ Ah}{0.8 \times 0.75} = 1666\ Ah \qquad \text{Eq. 24}$$

Ah represents battery capacity in Amperage hours. This means if a 12 V battery pack is used, it must be rated for at least 1666 Ah. When designing high-powered inverters and UPS the standard technique is to use a high voltage battery bank rather than a 12 V bank. The advantages of a high voltage battery bank are as follows: the current is lower, conductor sizes can be reduced, and the power loss through the switching devices (e.g., transistors) is less because of the reduced current (Battery Power Required for a 2HP Motor AC at 1800 rpm, 2016). Reduced power loss also reduces the heatsinking requirements, which is especially important to consider for the climate in Ghana.

4.5.3 Implementation and Use in Agbogbloshie

To implement the grinder into Agbogbloshie, the waste processors must understand the value it can create. When speaking with Hector Boye, he spoke about how it will be hard at first to introduce the PCB grinder because it is a completely new process to them. For them to adopt the process of extracting gold from PCBs, the waste processor must fully understand the value it can add. Currently, the waste processors make about $20 a week from various recycling techniques, including selling PCBs to other countries at a low cost. By grinding the PCBs and extracting the gold, the waste processors would be able to increase the amount of money they make. Traveling to Agbogbloshie, speaking with the waste processors, and improving the grinder design through co-design will greatly improve the implementation. This will ensure the waste processors understand the use and value creation and further tailor the design to something that can be manufactured and used by them.

Once the waste processors understand the purpose of the grinder and manufacture it, they can begin using it. This process will start by breaking down the PCB into smaller pieces, around 4 cm by 4 cm. Then, the smaller PCB pieces can be fed into the funnel of the grinder, while it is spinning at 1725 rpm. Once the PCB is grinded enough, it will fall through the mesh into the collection bucket. The gold will then be extracted from the PCB powder through Mohammed Mohammed's suggested process.

4.6 Summary

The design iterations were described in detail so that a future project can understand design decisions. The manufacturing procedure, including the materials purchased, plasma cutting, drilling holes, bending parts, cutting stand tubing, welding, and assembling was explained in detail. Testing of the hammer mill design, including Instron testing and ANSYS analysis, proved that the hammer mill will be able to crush PCBs. Manufacturing the prototype at WPI informed many opportunities for future work, as describes in the next chapter. The final chapter describes project limitations, achievements throughout the term, future co-design opportunities, and recommendations for improved design.

Chapter 5: Conclusions & Future Work

5.1 Limitations Throughout the Term

Throughout the project, there were several limitations that affected the projects outcome. One of the biggest limitations was not being able to travel to Ghana and instead working on WPI's campus. Because of this, it was difficult to fully co-design the grinder with input from the waste processors. Hector Boye, a PhD student living in Ghana, provided helpful insight from his visit to Agbogbloshie. His knowledge allowed the grinder to be tailored towards the waste processors wants and needs. The notes from this meeting can be found in *Appendix B*. However, there is much room to improve the design through direct co-design with the Agbogbloshie waste processors.

Another constraint was the project budget. The project had a budget of \$500, which was quickly surpassed as strong materials and a powerful motor was needed. Due to the minimum purchase sizes for the steel, more steel than was needed had to be purchased. Many of the parts purchased were also expensive to ensure they would not break under the forces of the grinder. Fortunately, an old motor was able to be borrowed which saved money. If not, this would have added another \$200+ to the cost. In the end, the budget was exceeded by ~\$30.

As this was a 7-week, term long MQP, time also proved to be a difficulty. With the on-going pandemic, campus was restricted and there was no access to the labs for the first 3 weeks. This pushed back the manufacturing and testing schedule. It also took longer to manufacture the prototype than expected, due to the learning curve in many of the processes. Due to the time constraints, a partial prototype was built. This meant it could not be physically tested to find the efficiency. As well, the prototype could not be redesigned to make improvements, as with normal engineering processes.

Another limitation was working at the same time as the partner chemistry MQP. Because the projects relied on each other but had a strict time constraint, a definite size of ground PCB was not able to be determined. Since Mohammed was working on his project at the same time, he did not get to fully test out his methods until the last couple weeks. Therefore, a best estimate was made of what size to aim to grind the PCB to.

5.2 Achievements Throughout the Term

Although there were difficulties along the way, there were still many successes. One of the biggest success was being able to build a partial prototype. Due to the time constraints, the original goal was to manufacture one or two parts of the overall design. So although there was not time to complete or test the prototype, it was still helpful to create almost a full prototype. Being able to make a full-scale proof of concept prototype for each part showed that the design can work and will be helpful for future groups who may take on this project. They will have a design to start with, be able to finish building and then test it, and finally redesign to improve the prototype.

Another success was working to simplify the design. As can be seen from the first design to the last design, the final design had less parts and was made to be easier to manufacture, assemble, and maintain. Removing the spacers allowed for a smaller design and also saved a lot of money. Splitting the crushing chamber into two parts and having the shaft assembly be supported by the stand allowed for the design to be easily assembled and taken apart when necessary. Attaching the mesh with bolts so that it can be removed without taking anything else apart helped to make the piece easier to replace or maintain.

Ensuring the design was safe was another success. To make sure there are no PCB pieces could fly out of the funnel, a hinged flap was added to the top. This allowed the funnel opening to be covered in between adding PCB. Another safety feature was ensuring the crushing chamber would not break either from the PCBs or a catastrophic failure of the shaft assembly. If a hammer were to break off the shaft assembly, the 12-gauge steel would be strong enough to stop the force of the hammer and contain it within the crushing chamber. This will ensure those working with the grinder do not get injured.

5.3 Recommendations for Improved Design

There are many ways to improve the PCB grinder design in the future. Future MQPs could investigate how much money the waste processors can make with the grinder and how long it would take to pay off fees to build grinder. Based on this, they could then work to lower the cost of producing the design and increase the amount made with it. Students can also explore ways to reduce the overall weight of the prototype, including determining whether or not using thinner rotor discs are possible. During the manufacturing, it was determined these pieces were very heavy and it could be cheaper to use thinner steel. For manufacturing, it is also recommended that the next student team drills test holes into the hammers and rotor discs to ensure that the shafts can fit through the holes. This provides an opportunity to test out how the tolerancing of the plasma cutter compares to the recommended tolerancing for typical holes and shafts. Future MQPs can also improve design through a comprehensive safety inspection, specifically paying attention to how the funnel can be best redesigned to prevent projectiles. If co-design feedback reveals that waste processors view fast processing as a priority, future work could include exploring the benefits of a rotary pocket feeder, as described in Section 3.4.2. This would allow for easier and faster grinding, but also complicate the design. Future students could also identify the specific sine wave power inverter specifications required to connect the three-phase motor to the battery bank. Then, they could test out how it works and if it is sufficient for powering the grinder and for how long. While significant progress was made on the grinder this year, there is always room to improve the design.

5.4 Future Co-Design Opportunities

Due to the pandemic, the co-design relationship with the community was not as strong as it might have been if the team had travelled to Ghana. This grinder design is presented as an idea for others to absorb and build upon through more extensive co-design. Future revisions of the e-waste recycling grinder could scale a manufacturing plan based on the final design, design the shredding and separation processes, and determine a grinder integration plan for Agbogbloshie. Future MQP students can refine the design with co-design participation from e-waste processors. For example, the next student team to travel to Ghana can redesign and manufacture the grinder in Ghana to test the prototype in the Ghanaian cultural context. These students could develop a cost-effective plan to source the shafts, bearings, pulleys, and motors necessary to build the number of grinders requested by the waste processors. Additionally, future work can include identifying what discarded parts from Agbogbloshie can be found and refurbished to build the grinder. Waste processors possess valuable insight into current e-waste recycling processes, so building a strong co-design relationship with them is crucial in order to ensure that the grinders can be easily maintained long after the students leave Ghana.

Future Interactive Qualifying Projects (IQPs) can aim to translate the e-waste recycling grinder MQP across cultures so that it can be introduced appropriately in Agbogbloshie. To ensure the grinder can be used in Agbogbloshie, local Ghanaian expertise must guide the project's focus on manufacturing and sustainable maintenance. IQP students could interview waste processors in Ghana to determine the best plan to integrate and maintain the grinder based on the existing recycling processes. The Agbogbloshie Makerspace Platform and the many artisanal welders within Agbogbloshie are great resources for building an integrative manufacturing plan. The GRATIS Foundation of Ghana can also be interviewed and used for a manufacturing plan, as they research, design, develop, manufacture and market appropriate technology-based products and services for socio-economic and industrial development in Ghana (GRATIS, 2020). IQP students may benefit from reaching out to this organization to gain a different perspective on product and process development in Ghana.

References

2 HP - TEFC - 3500 RPM. (2020). *Motor Boss US*. Retrieved from http://ecatalog.motorboss.com/Catalog/Motors/FD85

Adanu, S., Gbedemah, S., & Attah, M. (2020). Challenges of adopting sustainable technologies in e-waste management at Agbogbloshie, Ghana. *Heliyon*. Retrieved from http://www.sciencedirect.com/science/article/pii/S240584402031392X

Adekomaya, S. O., & Samuel, O. O. (2014). Design and Development of a Petrol-Powered Hammer Mill for Rural Nigerian Farmers. *Journal of Energy Technologies and Policy*, 65-72.

Advantages & Disadvantages in Particle Reduction Techniques. (2021). Retrieved from CPM: https://www.cpmroskamp.com/downloads/Advantages%20and%20Disadvantages%20of%20Particle%20Size%20Reduction%20Techniques.pdf

Agbogbloshie Makerspace Platform. (2014, October 23). DSC_0410. Accra, Ghana: Flickr. Retrieved from https://www.flickr.com/photos/qampnet/15206734253/in/album-72157649303276906/

Agbogbloshie Makerspace Platform. (2017, October 2017). AMP_Spacecraft_2. Retrieved from https://www.flickr.com/photos/qampnet/37738877702/in/album-72157649303276906/

Agbogbloshie Makerspace Platforms. (2014, October 23). DSC_0406. Accra, Ghana: Flickr. Retrieved from https://www.flickr.com/photos/qampnet/15206734253/in/album-72157649303276906/

Amoyaw-Osei, Y., Agyekum, O., Pwamang, J., Mueller, E., Fasko, R., & Schluep, M. (2011). Ghana e-Waste Country Assessment. *SBC e-Waste Africa Project*.

ASTM A29 Grade 1566. (n.d.). Retrieved from Matmatch: https://matmatch.com/materials/minfc21863-astm-a29-grade-1566

Azar, K., & Graebner, J. (1996). Experimental Determination of Thermal Conductivity of Printed Wiring Boards. *Proceedings of the Twelfth IEEE SEMI-THERM Symposium*, 169-182.

Ball Mills. (2020). *Retsch*. Retrieved from https://www.retsch.com/products/milling/ball-mills/

Ball Mills. (2021). *Grupa Wolff Safety and Innovations*. Retrieved from https://www.grupa-wolff.com/industrial-equipment/mills-for-powders/ball-mills/

Bank, T. W. (2016). Ghana: Mini-Grids for Last-Mile Electrification. *Energy Sector Management Assistance Program*. Retrieved from https://www.eca-uk.com/wp-content/uploads/2017/08/ESMAP-Ghana_Mini_grids_for_last_Mile_Electrification_Optimized.pdf

Battery Power Required for a 2HP Motor AC at 1800 rpm. (2016). *Electrical Engineering Stack Exchange*. Retrieved from https://electronics.stackexchange.com/questions/252652/battery-power-required-for-a-2hp-motor-ac-at-1800-rpm-56hz

Belt Disc Sander. (2021). *Tool Lots*. Retrieved from https://www.toolots.com/1-2hp-combo-4-36-belt-6-disc-sander-csa-listed.html?cid=9952931480&gclid=Cj0KCQjw0caCBhCIARIsAGAfuMwlILjo9iUKxn8qsrUQ3n5HXEUuObs7O-rR9e_Z0BlNVwDl8SUE4qEaAou6EALw_wcB

Boye, H., & Amoako-Gyimah, K. G. (2020). Ghana E-waste Recovery and Recycling Project.

Carvill, J., & Cullum, R. (1994). 10 - Power units and transmission . In *Mechanical Engineer's Reference Book (Twelfth Edition)* (pp. 10-1, 10-3-10-51). doi:https://doi.org/10.1016/B978-0-7506-1195-4.50014-2

Collins, D. (2017, November 1). *What are V-belt pitch length and datum length?* Retrieved from Linear Motion Tips: A Design World Resource: https://www.linearmotiontips.com/v-belt-pitch-length-datum-length/#comments

Csanyi, E. (2011). 5 steps to choose the best motor for your application. *Electrical Engineering Portal*. Retrieved from https://electrical-engineering-portal.com/5-steps-to-choose-best-motor-for-your-application

Cutting Mills. (2020). *Retsch*. Retrieved from https://www.retsch.com/products/milling/cutting-mills/

Cutting Mills. (2021). Retrieved from Retsch: https://www.retsch.com/products/milling/cutting-mills/

Daum, K. (2017). Toward a More Sustainable Trajectory for E-Waste Policy: A Review of a Decade of E-Waste Research in Accra, Ghana. *International Journal of Environmental Research and Public Health*. Retrieved from www.mdpi.com/1660-4601/14/2/135/html

Donadkar, M., & Solanke, S. (2016). Review of E-Waste Material Used in Making of Concrete. *JSTOR*. Retrieved from www.ijste.org/articles/IJSTEV2I7065.pdf

EPA, U. (2020). Cleaning Up Electronic Waste (E-Waste). *Environmental Protection Agency*. Retrieved 12 2020, from www.epa.gov/international-cooperation/cleaning-electronic-waste-e-waste

Escobar, A. (1995). *Encountering Development: The Making and Unmaking of the Third World.* Princeton University Press.

Ezurike, B. O., Osazuwa, O. J., Okoronkwo, C. A., & Okoji, K. I. (2018). Design, Construction and Performance Evaluation of a Flat Screen Hammer Mill Machine. *African Journal of Science, Technology, Innovation and Development*. doi:10.1080/20421338.2018.1491675

Francioli, D. M. (2015). Effect of Operational Variables on Ball Milling. Retrieved from http://monografias.poli.ufrj.br/monografias/monopoli10013290.pdf

Goosey, M., & Kellner, R. (2003). Recycling technologies for the treatment of end of life printed circuit boards (PCB) . *Circuit World*, 33-37.

GRATIS, F. (2020). Providing Technological Support for Industrial Grinding. *GRATIS Foundation*. Retrieved from http://gratis.gov.gh/

Hammer Mills. (2020). *Feed Machinery*. Retrieved from https://www.feedmachinery.com/glossary/equipment/hammer_mill/

Haque, T. (2019). Introduction to Electronics (E-Waste) Recycling. *The Balance*. Retrieved from www.thebalancesmb.com/introduction-to-electronics-e-waste-recycling-4049386

Hemmerling, L. (2020, October 20). Plasma Cutter CNC Table User Manual.

How to Choose the Right Motor. (2020). *Jameco Electronics*. Retrieved from https://www.jameco.com/Jameco/workshop/ProductNews/motor-buyers-guide.html

Hulse, J. (2007). *Sustainable Development at Risk: Ignoring the Past.* Foundation Books. doi:doi:10.1017/UPO9788175968356

Ibrahim, M. M., Omran, M. S., & Abd Elrhman, E. N. (2019). Design and Evaluation of Crushing Hammer Mill. *Farm Machinery and Power, 36* (1), 1-24. Retrieved from https://www.researchgate.net/publication/331963135_Design_and_Evaluation_of_Crushing_Hammer_mill

Intro Into Ball Mill. (2014). *Intro Into*. Retrieved from https://www.introinto.com.au/intro-into-ball-mill/

Jindal, U. C. (2010). *Machine Design.* Pearson India.

Kakuk, G., Zsoldos, I., Csanády, Á., & Oldal, I. (2009). Contributions to the modelling of the milling process in a planetary ball mill. *Reviews on Advanced Materials Science, 22*(2), 21-38.

Khurmi, R. S., & Gupta, J. K. (2005). *A Textbook of Machine Design.* Ram Hagar, New Dehli, India: Eurasia Publishing House (PVT.) LTD.

Lee, J., Kim, Y., & Lee, J. (2012). Disassembly and physical separation of electric/electronic components layered in printed circuit boards (PCB). *Journal of Hazardous Materials*, 387-394. Retrieved from http://www.sciencedirect.com/science/article/pii/S03

Liu, G. (2017). Hammer Milling and Jet Milling Fundamentals. *American Institute of Chemical Engineers (AIChE)*. Retrieved from https://www.aiche.org/resources/publications/cep/2017/june/hammer-milling-and-jet-milling-fundamentals

MCC. (1996). Electronics Industry Environmental Roadmap. *Microelectronics and Computer Technology Corporation*. Retrieved from https://www.iloencyclopaedia.org/part-xiii-12343/microelectronics-and-semiconductors/item/922-printed-circuit-board-and-computer

McElvaney, K. (2014). Agbogbloshie: the world's largest e-waste dump – in pictures. *The Guardian*. Retrieved from https://www.theguardian.com/environment/gallery/2014/feb/27/agbogbloshie-worlds-largest-e-waste-dump-in-pictures

McFadden, C. (2020). How Much Gold Is in Your Computer and How Efficient It Is to Reclaim It. *Interesting Engineering*. Retrieved from http://www.interestingengineering.com/how-much-gold-is-in-your-computer-and-how-efficient-it-is-to-reclaim-it.

Michaud, D. (2015). Grinding Circuit and Mill Safety. *911 Metallurgist*. Retrieved from https://www.911metallurgist.com/blog/grinding-circuit-and-mill-safety

Michaud, L. (2016). Hammer Mill Operating Principle. *911 Metallurgist*. Retrieved from https://www.911metallurgist.com/blog/hammermill-operating-principle

MIG Welding: The Basics for Mild Steel. (2020). Miller. Retrieved from https://www.millerwelds.com/resources/article-library/mig-welding-the-basics-for-mild-steel#:~:text=MIG%20welding%20is%20an%20arc,stands%20for%20metal%20inert%20gas

Minter, A. (2016). The Burning Truth Behind an E-Waste Dump in Africa. *Smithsonian Magazine*. Retrieved from www.smithsonianmag.com/science-nature/burning-truth-behind-e-waste-dump-africa-180957597/

Mohamed, T. H., Radwan, H. A., & Adly, M. (2015). Design and Evaluation of a Small Hammer Mill. *Research Gate, 93*(5). Retrieved from https://www.researchgate.net/publication/294893239_DESIGN_AND_EVALUATE_OF_A_SMALL_HAMMER_MILL

Motors and Pulley Selection. (2009). *The Engineering Toolbox*. Retrieved from https://www.engineeringtoolbox.com/pulley-motor-speed-d_1475.html

Neikov, O. D. (2009). Chapter 2 - Mechanical Crushing and Grinding. In S. S. Naboychenk, I. V. Murashove, V. G. Gopienko, I. V. Fishberg, D. V. Lotski, & O. D. Neikov, *Handbook of Non-Ferrous Metal Powders* (pp. 47-62). Elsevier. doi:10.1016/B978-1-85617-422-0.00002-1

Omrom Industrial Automation. (2021). *Can I Control Single-phase Motor with Inverter with Single-phase 100V Input?* Retrieved from https://www.omron.com.au/service_support/FAQ/FAQ00684/index.asp#:~:text=No%2C%20a%20single%2Dphase%20motor%20cannot%20be%20used.&text=In%20addition%2C%20if%20the%20Inverter,Use%20a%20three%2Dphase%20motor

Prakash, S., & Manhart, A. (2010). Socio-Economic Assessment and Feasibility Study on Sustainable e-Waste Management in Ghana. *Ministry of Housing, Spatial Planning and the Environment of the Netherlands (VROM-Inspectorate) and the Dutch Association for the Disposal of Metal and Electrical Products (NVMP)*. Retrieved from ressourcenfieber.org/publications/reports/2010-105-en.pdf

Princewell, N. C. (2017). Development and Performance Evaluation of Improved Hammer Mill. *Journal of Scientific and Engineering Research*, 4(8): 159-164. Retrieved from https://www.researchgate.net/publication/326546889

Prosino. (2020). Double shaft shredder with shearing blades. Retrieved from https://www.sinoshredder.com/shredders/double-shaft-shredder-single-motor/

Rapezzi, C. (2020). The Informal e-Waste and Metal Recyclers of Agbogbloshie. *Equal Times*. Retrieved from www.equaltimes.org/the-informal-e-waste-and-metal?lang=en#.X8cODchKiMo

Reid, T. (2017). How To Connect Power Inverters To Off Grid Solar Batteries. *The Do It Yourself World*. Retrieved from https://www.thedoityourselfworld.com/articles/article.php?id=11438

Sanders, E., & Stappers, P. (2008). *Co-creation and the new landscapes of design* (Vol. 1). Co-Design. doi:10.1080/15710880701875068

Sépulveda, A., & Schluep, M. (2010). A review of the environmental fate and effects of hazardous substances released from electrical and electronic equipments during recycling: Examples from China and India. *Environmental Impact Assessment Review, 30*(1), 28-41.

Srigboh, R., Basu, N., Stephens, J., Asampong, E., Perkins, M., Neitzel, R., & Fobil, J. (2016). Multiple elemental exposures amongst workers at the Agbogbloshie electronic waste (e-waste) site in Ghana. *Chemosphere, 164*, 68-74. doi:https://doi.org/10.1016/j.chemosphere.2016.08.089

Steen, M., Manschot, M., & De Koning, N. (2011). Benefits of co-design in service design projects. *International Journal of Design, 5*(2), 53-60.

Tap and Clearance Drill Sizes. (n.d.). Retrieved from Little Machine Shop: https://littlemachineshop.com/reference/tapdrill.php

The Ultimate Guide for International Development. (2020). *Net Impact*. Retrieved from www.netimpact.org/careers/international-development/big-picture

Tips For Powering Motors With Batteries. (2020). *Precision Microdrives*. Retrieved from https://www.precisionmicrodrives.com/content/tips-for-powering-motors-with-batteries/

Uplaonkar, P. S., & Vagha, M. A. (2019). Battery Balancing For a Multilevel Inverter. *International Journal of Engineering and Advanced Technology, 8*(6), 297-301. doi:https://doi.org/10.35940/ijeat.E7630.088619

Utility, G. (2020). Can I connect any capacity/any number of batteries to an Inverter/UPS to increase its runtime? *Glowship Utility Solutions*. Retrieved from https://www.glowship.com/faqs/inverters-and-batteries/ups-how-many-batteries/

Warner, B. (2018, May 12). *Treasure in the most toxic place on earth: AMP (Agbogbloshie Makerspace Platform)*. Retrieved from Atlas of the Future: https://atlasofthefuture.org/project/amp-agbogbloshie-makerspace-platform/

What is a hammermill and what can it do for you? (2018). Retrieved from Eagle Crusher: https://eaglecrusher.com/blog-1/what-is-a-hammermill-and-what-can-it-do-for-you

Xuan, C., Cao, L., Wu, P., Ma, Y., & Han, D. (2012). Development on a Hammer Mill with Separate Sieving. *TELKOMNIKA Indonesian Journal of Electrical Engineering*.

Yeung, P. (2019). The Toxic Effects of Electronic Waste in Accra, Ghana. *Bloomberg CityLab*. Retrieved from https://www.bloomberg.com/news/articles/2019-05-29/the-rich-world-s-electronic-waste-dumped-in-ghana

Appendix A: Hand Drawings of Design 1 From Ideation

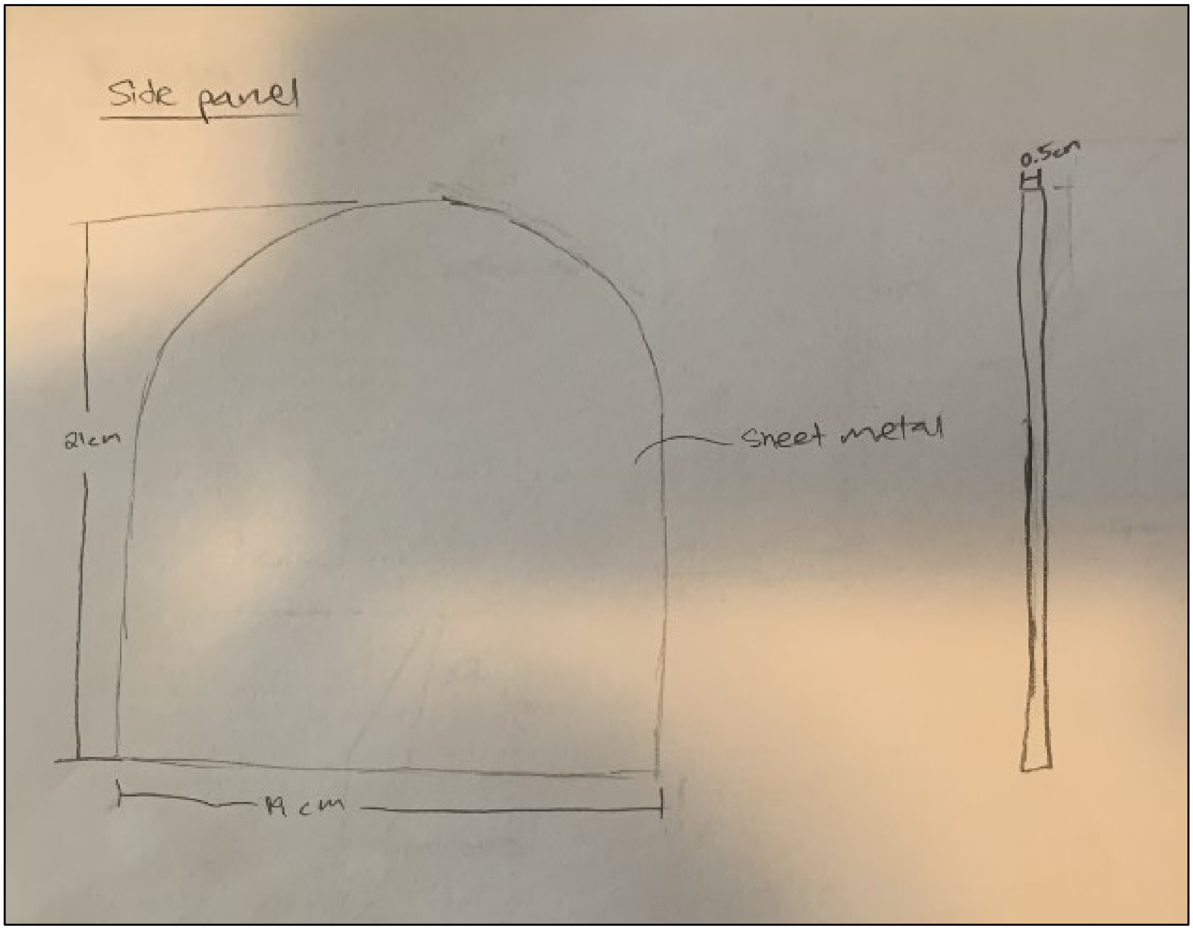

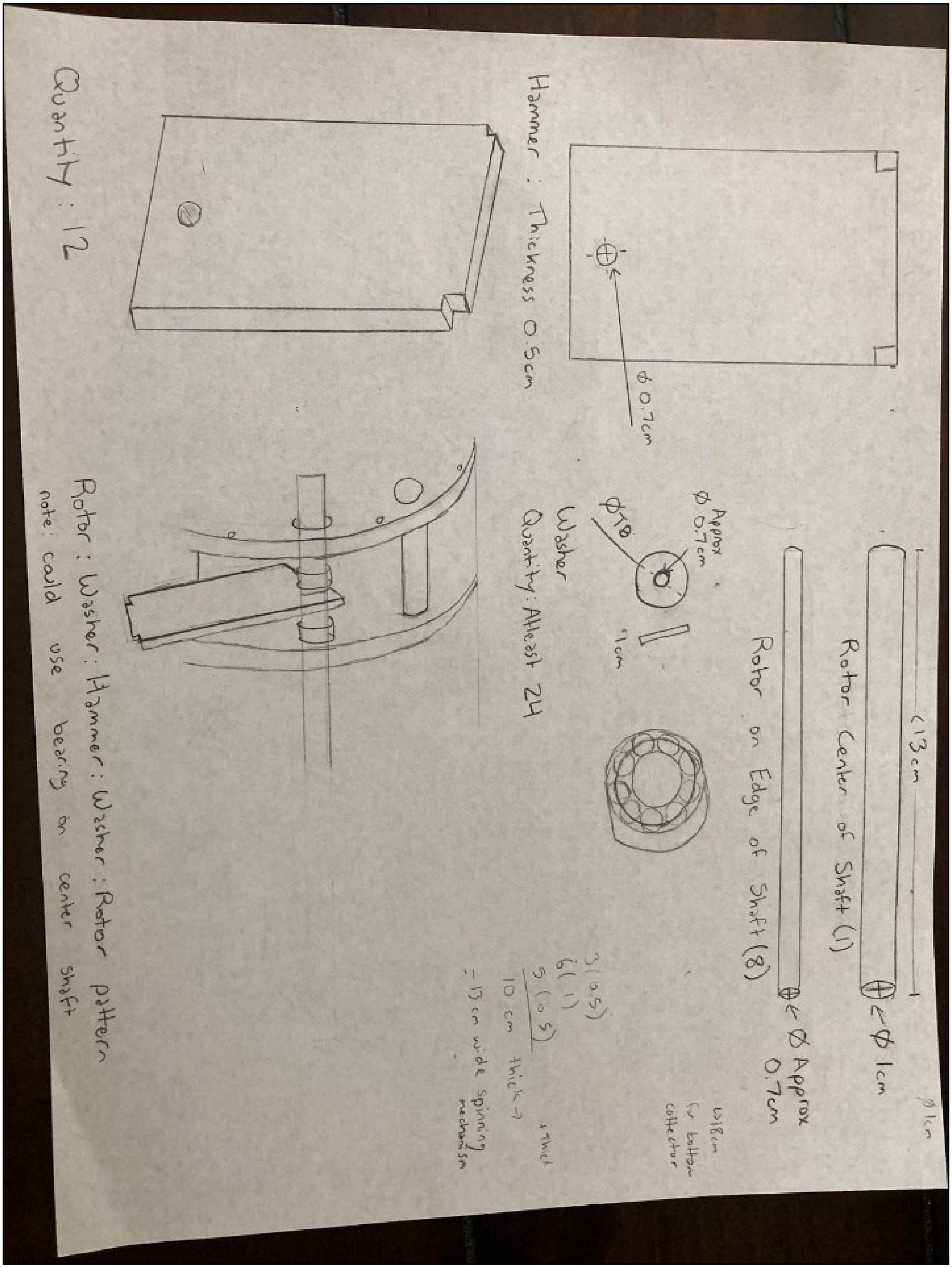

13cm
Rotor Center of Shaft (1)
← Ø 1cm
Rotor on Edge of Shaft (8)
← Ø Approx 0.7cm
Approx Ø 0.7cm
ØTB
1cm
Washer
Quantity: Atleast 24
Ø 0.7cm
Hammer : Thickness 0.5cm
Quantity : 12
Rotor : Washer : Hammer : Washer : Rotor pattern
note: could use bearing on center shaft

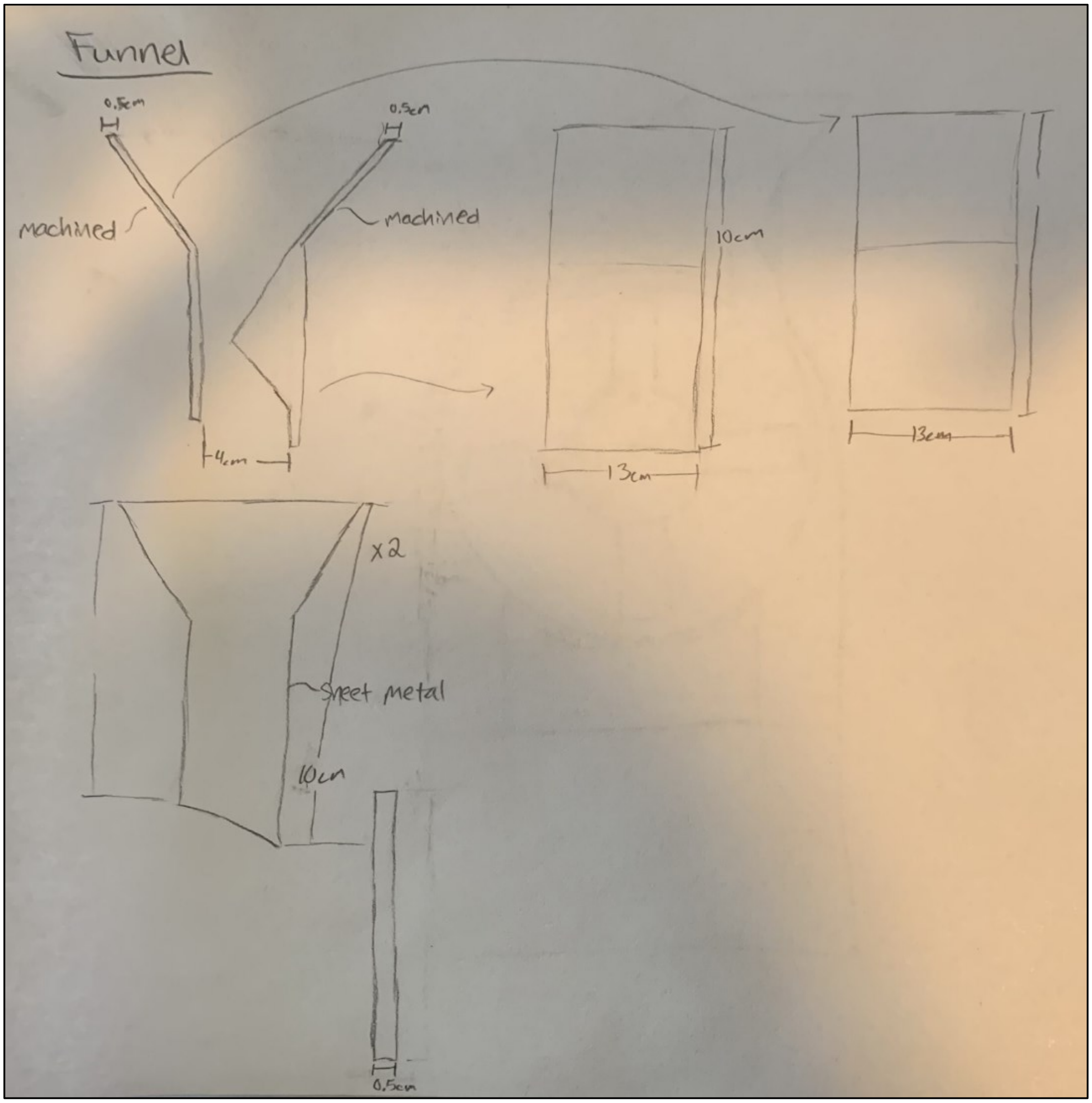
Funnel
0.5cm
0.5cm
machined
machined
10cm
4cm
13cm
13cm
x2
sheet metal
10cm
0.5cm

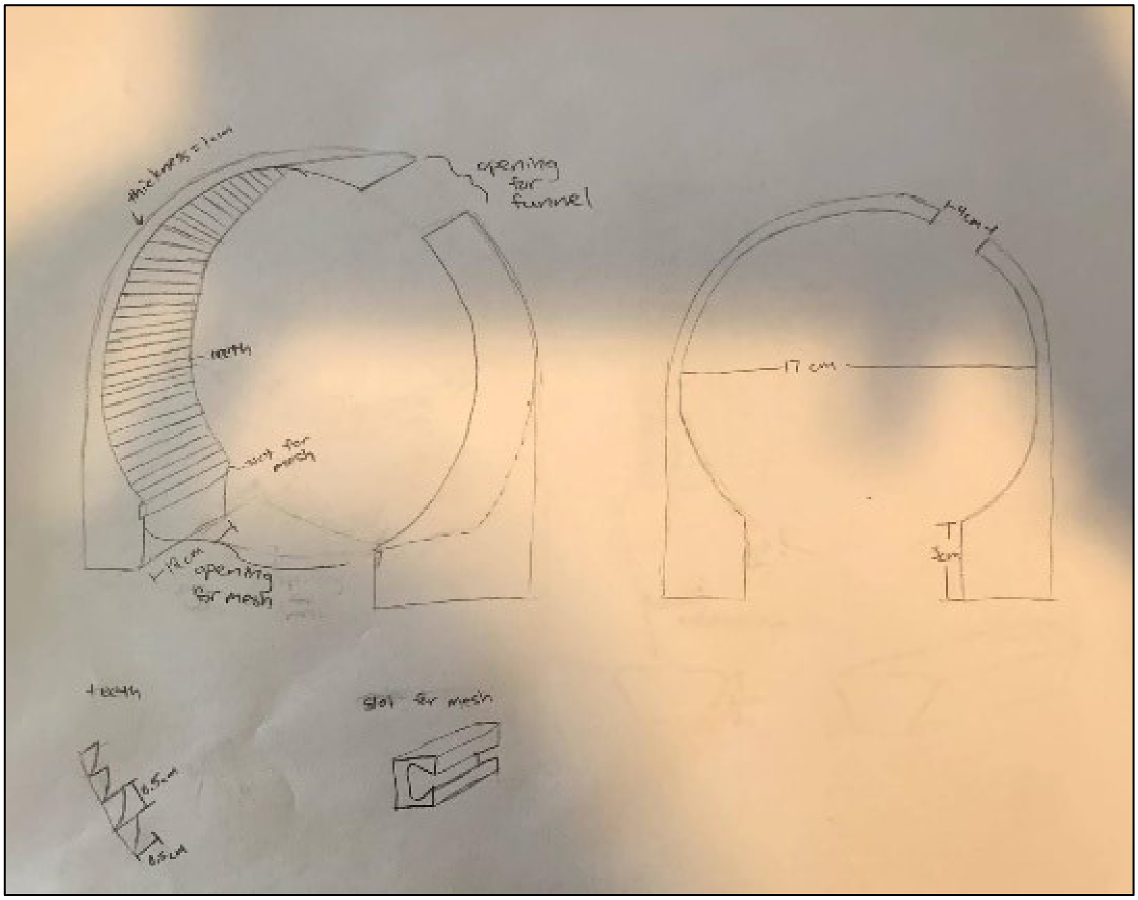
thickness = 1cm
opening for funnel
teeth
slot for mesh
opening for mesh
17 cm
teeth
0.5cm
0.5cm
slot for mesh

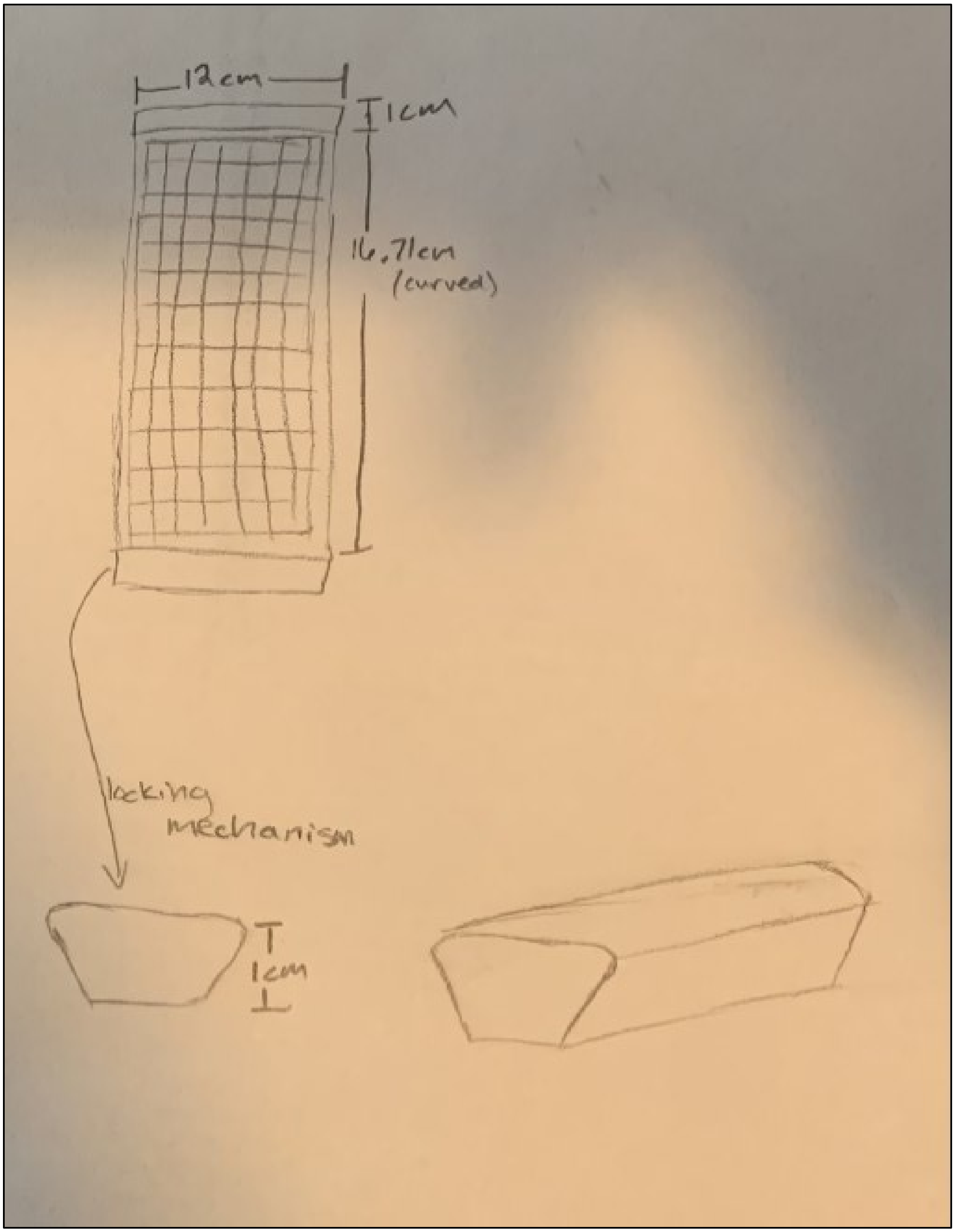
12cm
1cm
16.71cm
(curved)
locking
mechanism
1cm

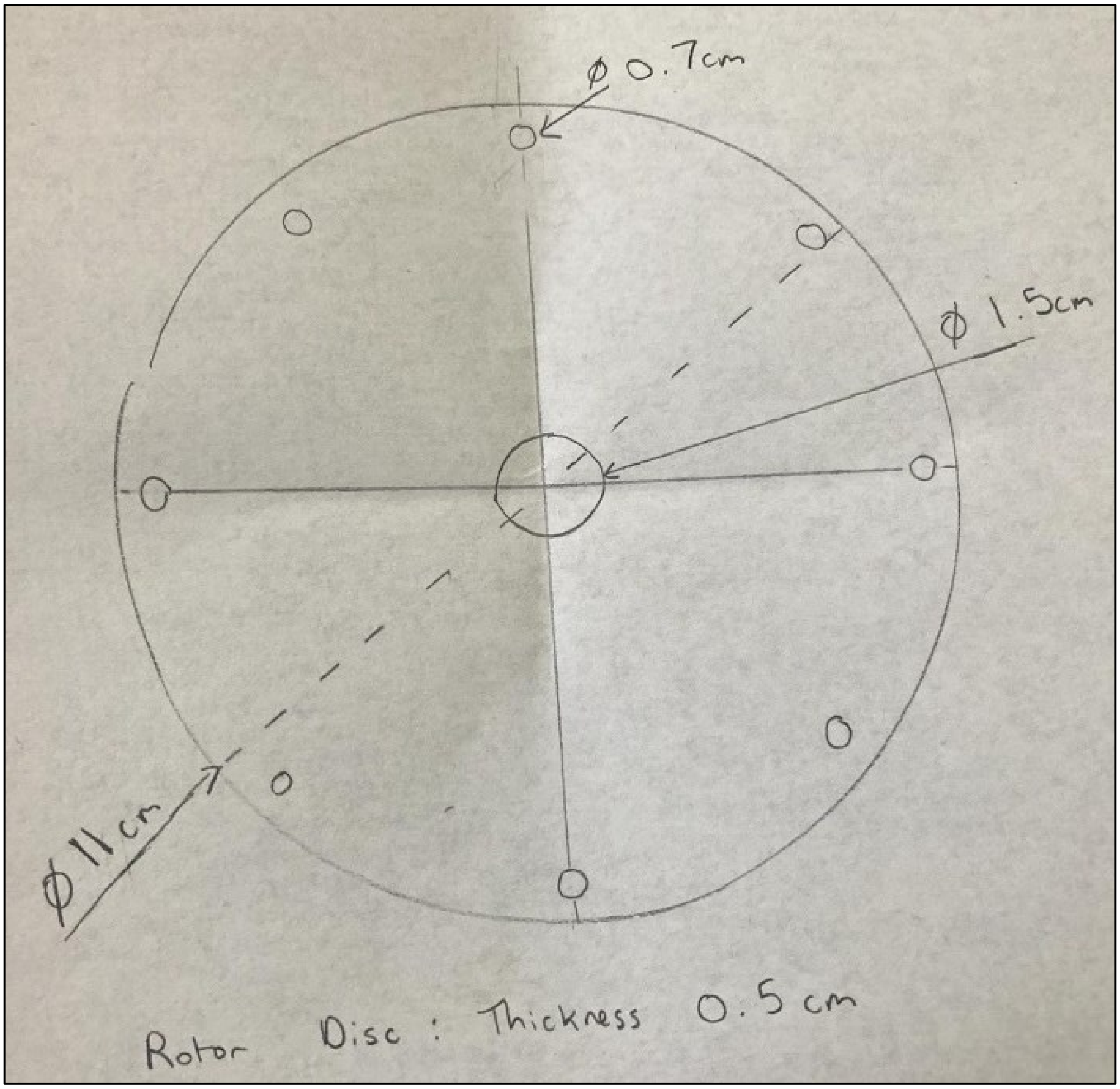
ϕ 0.7cm
ϕ 1.5cm
ϕ 11cm
Rotor Disc : Thickness 0.5 cm

Appendix B: Hector Boye

Questions prepared for meeting with Hector Boye:

- Can you tell us about your experience visiting Agbogbloshie?
- What is the typical recycling process of the e-waste processors?
- How much do the e-waste processors sell the PCBs for?
- What are the capabilities in Agbogbloshie for a PCB grinder like this?
    - What materials do they have access to for manufacturing?
    - What sources of power or electricity do they have?
    - Are there any old machines they have that parts can be salvaged from?
- Do you know anything about the Chang Fadongli grinding machine?
- Are there any recommendations you have for our design that the e-waste processors would like to see?

Notes from meeting with Hector Boye:

- 20-40 foot trailers filled with the secondhand and spare parts are sent to Agbogbloshie
    - All these parts have values because at the bare minimum, all these parts can be taken apart and used to fix other equipment
- At Agbogbloshie, they mainly process aluminum, phones, and DVD machines
- PCBs are typically sent to Nigeria for processing
- Current e-waste recycling process:
    - Sort and dismantle materials
    - Wires are incinerated to harvest copper
    - Phones and DVDs are burned to harvest aluminum
        - Molds are used to create aluminum pots
    - Other dismantled items are sold to places with scales
- It is important when introducing our e-waste grinder to the e-waste processors that we show the value creation
    - This is a completely new idea, and they need to have a reason to want to use it
- It is important to note that old PCBs tend to be more valuable than current ones, because they typically contain more gold

- For manufacturing, there are local machine shops
    - The Gratis Foundation in Accra helps with manufacturing from scratch
- The e-waste processors are secretive about how much their items sell for because of competition
    - Hector estimates they make $20 a week, so PCBs do not sell for much as that is a fraction of what they do
- There is electricity only on the outskirt of the e-waste site
    - To use the grinder on site where they are processing, a fuel powered motor would be necessary
    - Must be careful about the live wires where they are processing, because of their burning of wires

Appendix C: Bill of Materials

Part Name	Part Quantity	Unit Quantity	Purchase Quantity	Unit Cost	Total Cost	Link
Mounted Ball Bearing with Nickel-Plated Iron Housing for 1" Shaft Diameter	2	1	2	$39.74	$79.48	https://www.mcmaster.com/6494K14/
Rotary Shaft, 1566 Carbon Steel, 1" Diameter, 12" long	1	1	1	$23.46	$23.46	https://www.mcmaster.com/1346K37/
1" Fixed Bore Standard V-Belt Pulley, Outside Diameter 6"	1	1	1	$29.80	$29.80	https://www.grainger.com/product/CONGRESS-1-in-Fixed-Bore-Standard-V-54XN05
7/8" Fixed Bore Standard V-Belt Pulley, Outside Diameter 7/8"	1	1	1	$16.10	$16.10	https://www.grainger.com/product/CONGRESS-7-8-in-Fixed-Bore-Standard-3LC09
A58 V-Belt, Outside Length 60"	1	1	1	$17.20	$17.20	https://www.grainger.com/product/DAYTON-A58-V-Belt-3X547
Rotary Shaft, 1566 Carbon Steel, ½" Diameter, 12" Long	8	1	4	$8.92	$35.68	https://www.mcmaster.com/1346K17/

Zinc Yellow-Chromate Plated Hex Head Screw, Grade 8 Steel, ½"-13 Thread Size, 1 ¼" Long	4	10	1	$9.87	$9.87	https://www.mcmaster.com/92620A714/
Zinc Yellow-Chromate Plated Hex Head Screw, Grade 8 Steel, ½"-13 Thread Size, 7/8" Long	8	10	1	$7.08	$7.08	https://www.mcmaster.com/92620A710/
316 Stainless Steel Washer for ½" Screw Size, 0.531" ID, 1.25" OD	12	25	1	$8.16	$8.16	https://www.mcmaster.com/90107A033/
Medium-Strength Steek Hex Nut, Grade 5, ½"-13 Thread Side	16	50	1	$9.33	$9.33	https://www.mcmaster.com/95505A605/
Steel Hinge without Holes, Removable Pin, 3" x 1" Door Leaf, 0.075" Leaf Thickness	1	1	1	$4.72	$4.72	https://www.mcmaster.com/16175A61/
Rectangular Tubing – 2 x 1 ½ x 0.083 inch, 20 feet long	1	1	1	$48.93	$48.93	http://sullivanmetals.com/media/sullivan_stock_list.pdf
Hot Rolled Flat - ¼ x 8 inch, 24 feet long	1	1	1	$72.13	$72.13	http://sullivanmetals.com/media/sullivan_stock_list.pdf
Hot Rolled Sheet – 12 Gauge, 4 x 8 feet	1	1	1	$165.66	$165.66	http://sullivanmetals.com/media/sullivan_stock_list.pdf

Appendix D: Engineering Drawings

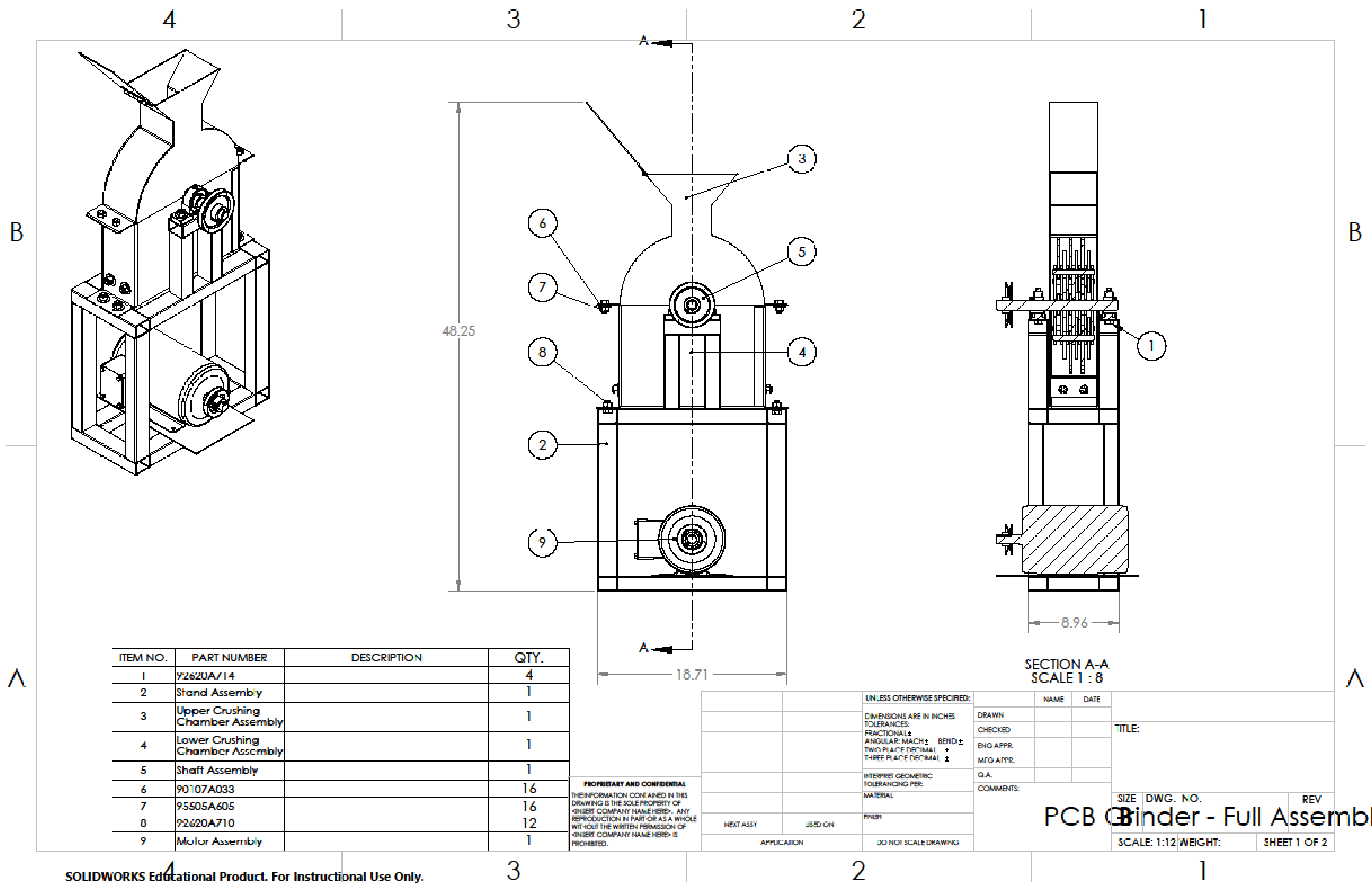

ITEM NO.	PART NUMBER	DESCRIPTION	QTY.
1	92620A714		4
2	Stand Assembly		1
3	Upper Crushing Chamber Assembly		1
4	Lower Crushing Chamber Assembly		1
5	Shaft Assembly		1
6	90107A033		16
7	95505A605		16
8	92620A710		12
9	Motor Assembly		1

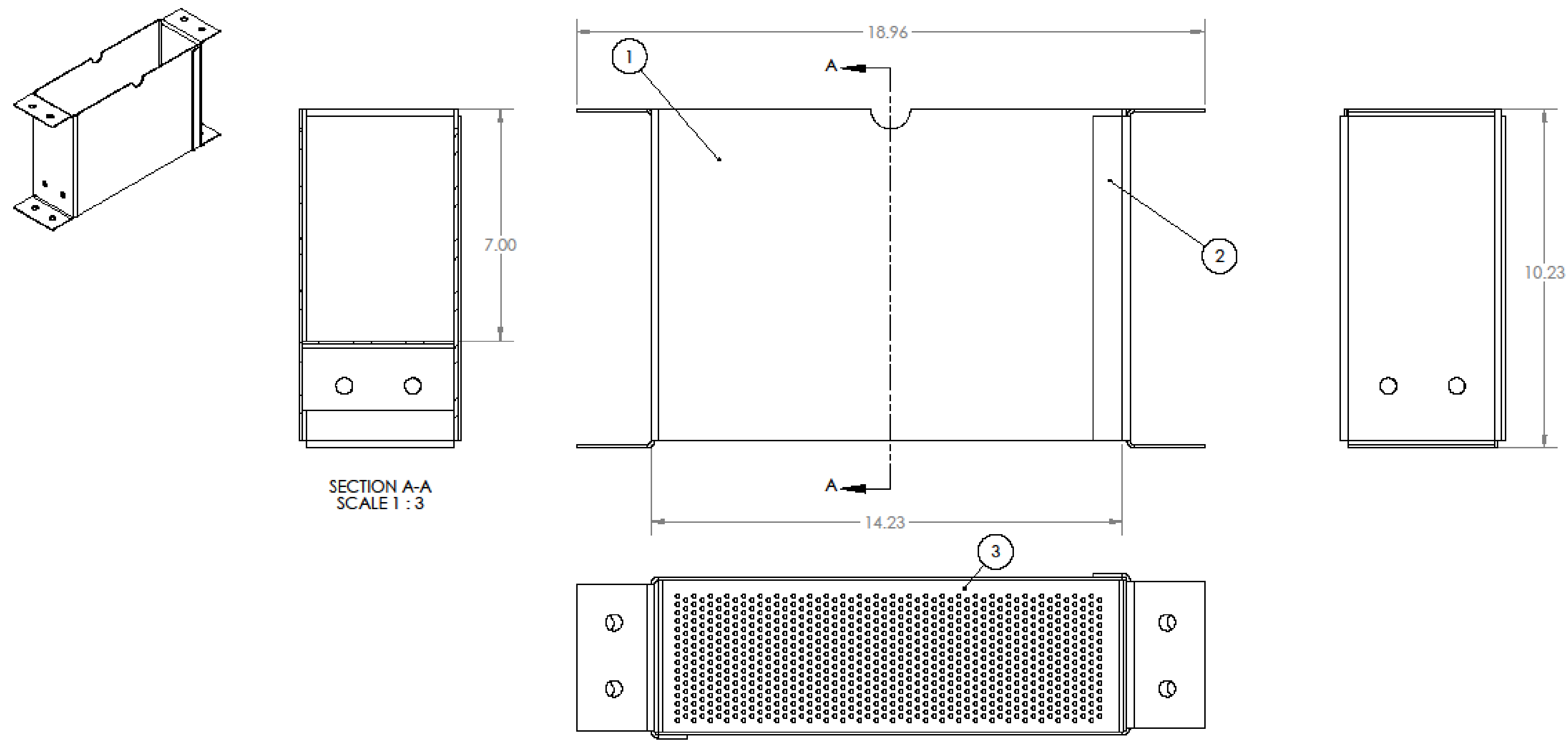

ITEM NO.	PART NUMBER	DESCRIPTION	QTY.
1	Outer Casing - Lower Side 1		1
2	Outer Casing - Lower Side 2		1
3	Mesh		1

PROPRIETARY AND CONFIDENTIAL

THE INFORMATION CONTAINED IN THIS DRAWING IS THE SOLE PROPERTY OF <INSERT COMPANY NAME HERE>. ANY REPRODUCTION IN PART OR AS A WHOLE WITHOUT THE WRITTEN PERMISSION OF <INSERT COMPANY NAME HERE> IS PROHIBITED.

NEXT ASSY | USED ON

APPLICATION

UNLESS OTHERWISE SPECIFIED:

DIMENSIONS ARE IN INCHES
TOLERANCES:
FRACTIONAL ±
ANGULAR: MACH ± BEND ±
TWO PLACE DECIMAL ±
THREE PLACE DECIMAL ±

INTERPRET GEOMETRIC TOLERANCING PER:

MATERIAL

FINISH

DO NOT SCALE DRAWING

	NAME	DATE
DRAWN		
CHECKED		
ENG APPR.		
MFG APPR.		
Q.A.		

COMMENTS:

TITLE:

SIZE B | DWG. NO. Lower Crushing Chamber Asse | REV

SCALE: 1:4 | WEIGHT: | SHEET 1 OF 1

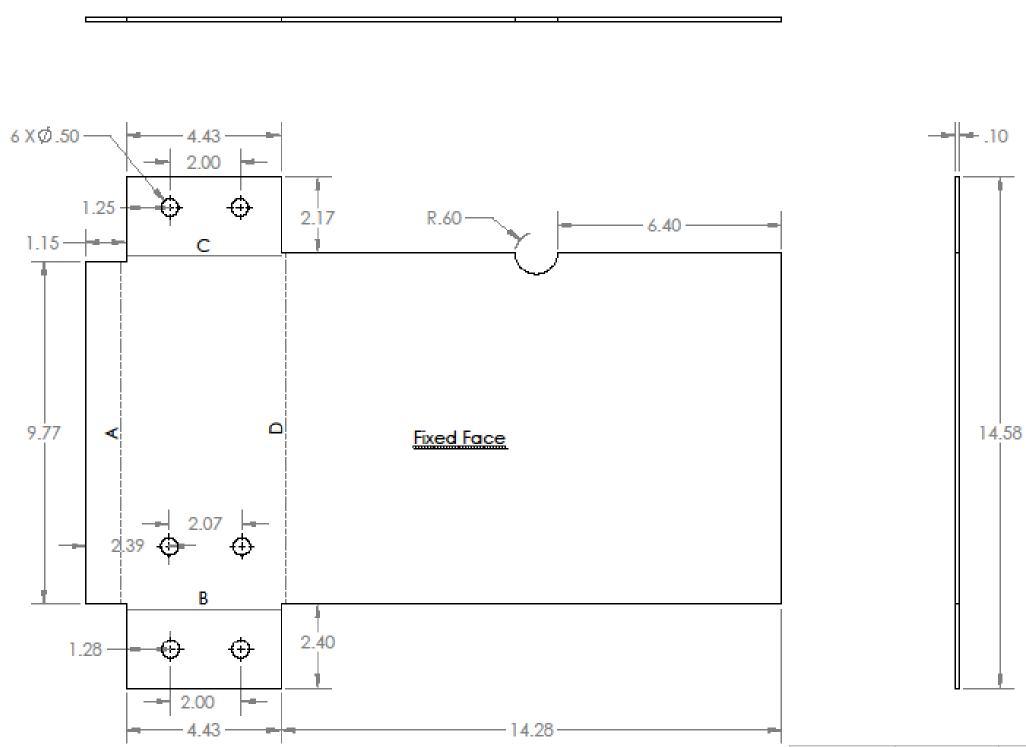

Tag	Direction	Angle	Inner Radius
A	DOWN	90°	0.13
B	UP	90°	0.13
C	UP	90°	0.13
D	DOWN	90°	0.13

UNLESS OTHERWISE SPECIFIED:
DIMENSIONS ARE IN INCHES
TOLERANCES:
FRACTIONAL ±
ANGULAR: MACH ± BEND ±
TWO PLACE DECIMAL ±
THREE PLACE DECIMAL ±

INTERPRET GEOMETRIC TOLERANCING PER:
MATERIAL
FINISH
DO NOT SCALE DRAWING

NEXT ASSY | USED ON
APPLICATION

	NAME	DATE
DRAWN		
CHECKED		
ENG APPR.		
MFG APPR.		
Q.A.		

COMMENTS:

TITLE:

SIZE B DWG. NO. REV

Outer Casing - Lower Side

SCALE: 1:4 WEIGHT: SHEET 1 OF 1

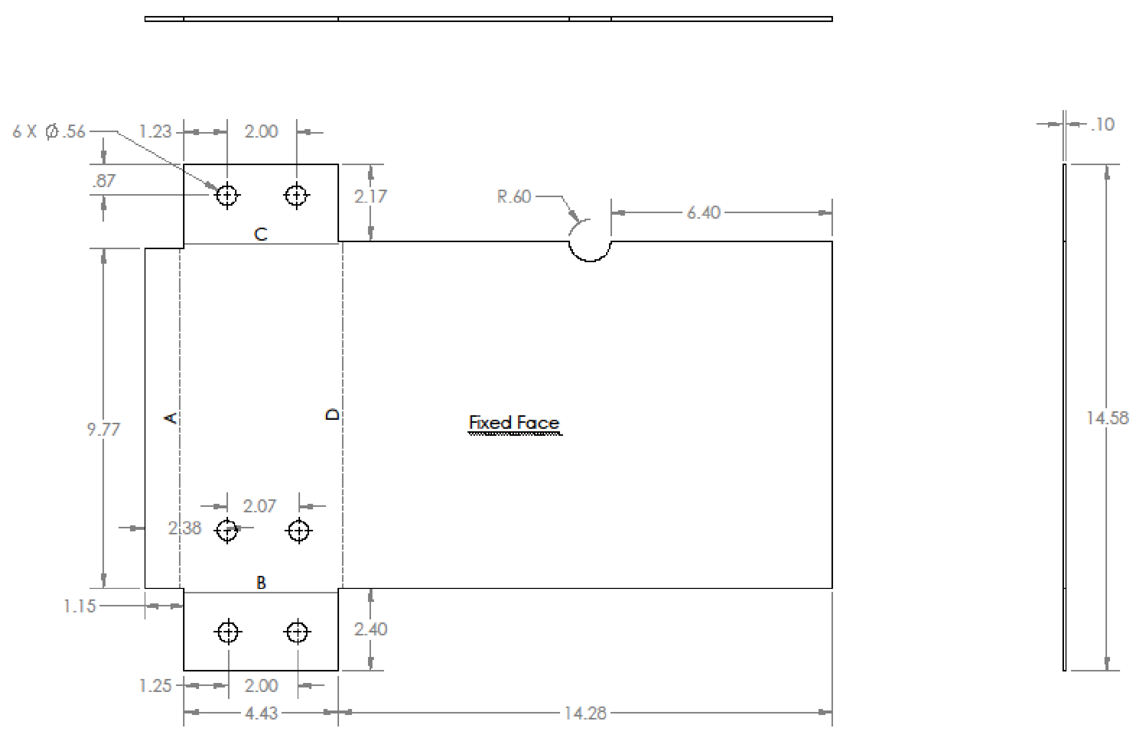

Tag	Direction	Angle	Inner Radius
A	DOWN	90°	0.13
B	UP	90°	0.13
C	UP	90°	0.13
D	DOWN	90°	0.13

PROPRIETARY AND CONFIDENTIAL

THE INFORMATION CONTAINED IN THIS DRAWING IS THE SOLE PROPERTY OF <INSERT COMPANY NAME HERE>. ANY REPRODUCTION IN PART OR AS A WHOLE WITHOUT THE WRITTEN PERMISSION OF <INSERT COMPANY NAME HERE> IS PROHIBITED.

NEXT ASSY | USED ON
APPLICATION

UNLESS OTHERWISE SPECIFIED:
DIMENSIONS ARE IN INCHES
TOLERANCES:
FRACTIONAL ±
ANGULAR: MACH ± BEND ±
TWO PLACE DECIMAL ±
THREE PLACE DECIMAL ±
INTERPRET GEOMETRIC TOLERANCING PER:
MATERIAL
FINISH
DO NOT SCALE DRAWING

	NAME	DATE
DRAWN		
CHECKED		
ENG APPR.		
MFG APPR.		
Q.A.		

COMMENTS:

TITLE:

SIZE B | DWG. NO. | REV

Outer Casing - Lower Side

SCALE: 1:4 | WEIGHT: | SHEET 2 OF 2

SOLIDWORKS Educational Product. For Instructional Use Only.

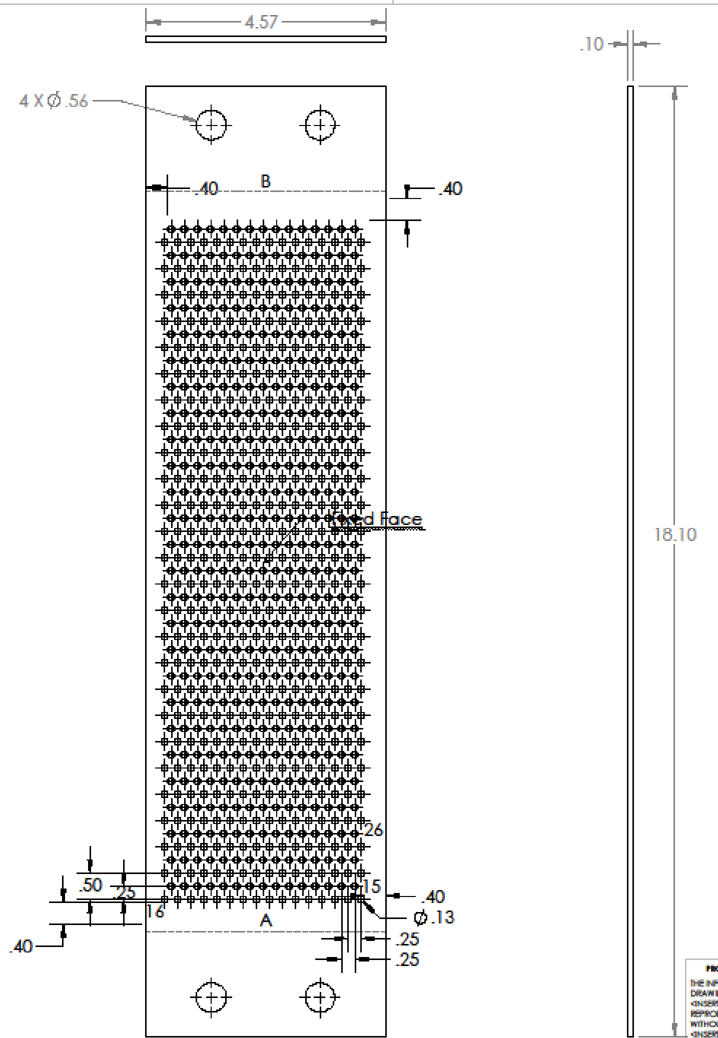

Tag	Direction	Angle	Inner Radius
A	DOWN	90°	0.13
B	DOWN	90°	0.13

	NAME	DATE
DRAWN		
CHECKED		
ENG APPR.		
MFG APPR.		
Q.A.		

COMMENTS:

UNLESS OTHERWISE SPECIFIED:
DIMENSIONS ARE IN INCHES
TOLERANCES:
FRACTIONAL ±
ANGULAR: MACH ± BEND ±
TWO PLACE DECIMAL ±
THREE PLACE DECIMAL ±

INTERPRET GEOMETRIC TOLERANCING PER:

MATERIAL

FINISH

NEXT ASSY | USED ON

APPLICATION

DO NOT SCALE DRAWING

TITLE:

SIZE B | DWG. NO. Mesh | REV

SCALE: 1:4 | WEIGHT: | SHEET 1 OF 1

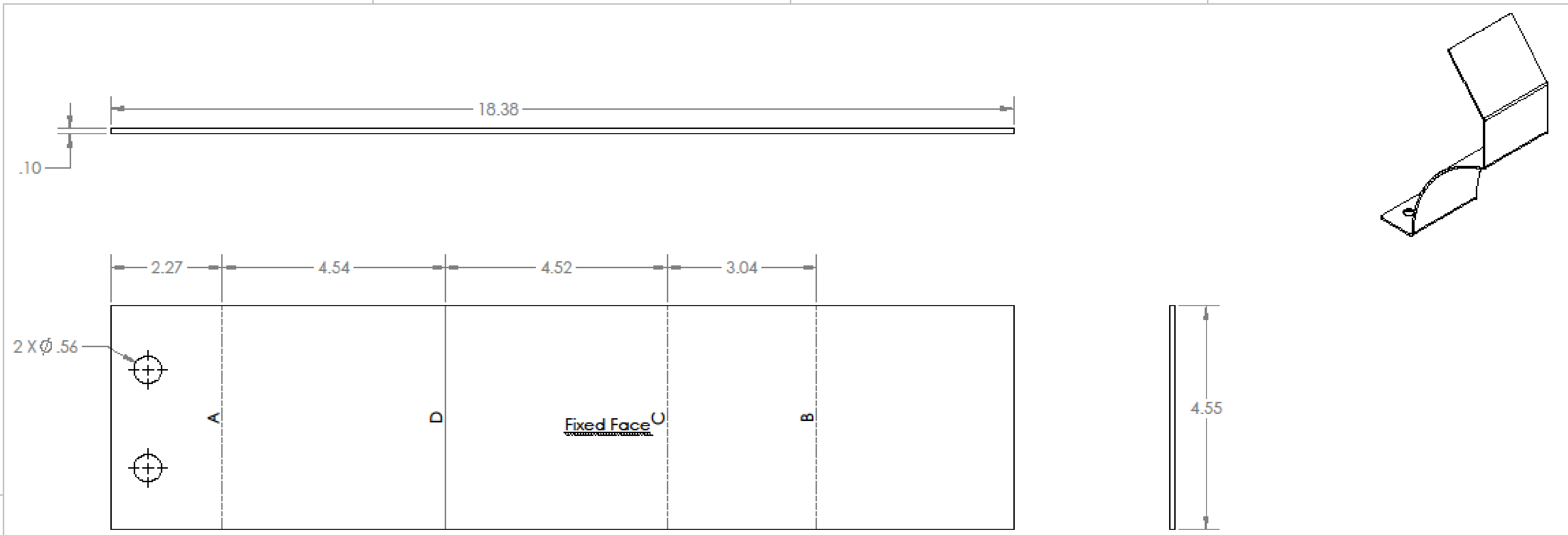

Tag	Direction	Angle	Inner Radius
A	DOWN	88.19°	0.13
B	DOWN	40°	0.13
C	DOWN	73.4°	0.13
D	UP	71.58°	7

PROPRIETARY AND CONFIDENTIAL

THE INFORMATION CONTAINED IN THIS DRAWING IS THE SOLE PROPERTY OF <INSERT COMPANY NAME HERE>. ANY REPRODUCTION IN PART OR AS A WHOLE WITHOUT THE WRITTEN PERMISSION OF <INSERT COMPANY NAME HERE> IS PROHIBITED.

NEXT ASSY | USED ON
APPLICATION

UNLESS OTHERWISE SPECIFIED:
DIMENSIONS ARE IN INCHES
TOLERANCES:
FRACTIONAL ±
ANGULAR: MACH ± BEND ±
TWO PLACE DECIMAL ±
THREE PLACE DECIMAL ±
INTERPRET GEOMETRIC TOLERANCING PER:
MATERIAL
FINISH
DO NOT SCALE DRAWING

	NAME	DATE
DRAWN		
CHECKED		
ENG APPR.		
MFG APPR.		
Q.A.		

COMMENTS:

TITLE:

SIZE | DWG. NO. | REV

Outer Casing - Upper Curve

SCALE: 1:4 | WEIGHT: | SHEET 1 OF 1

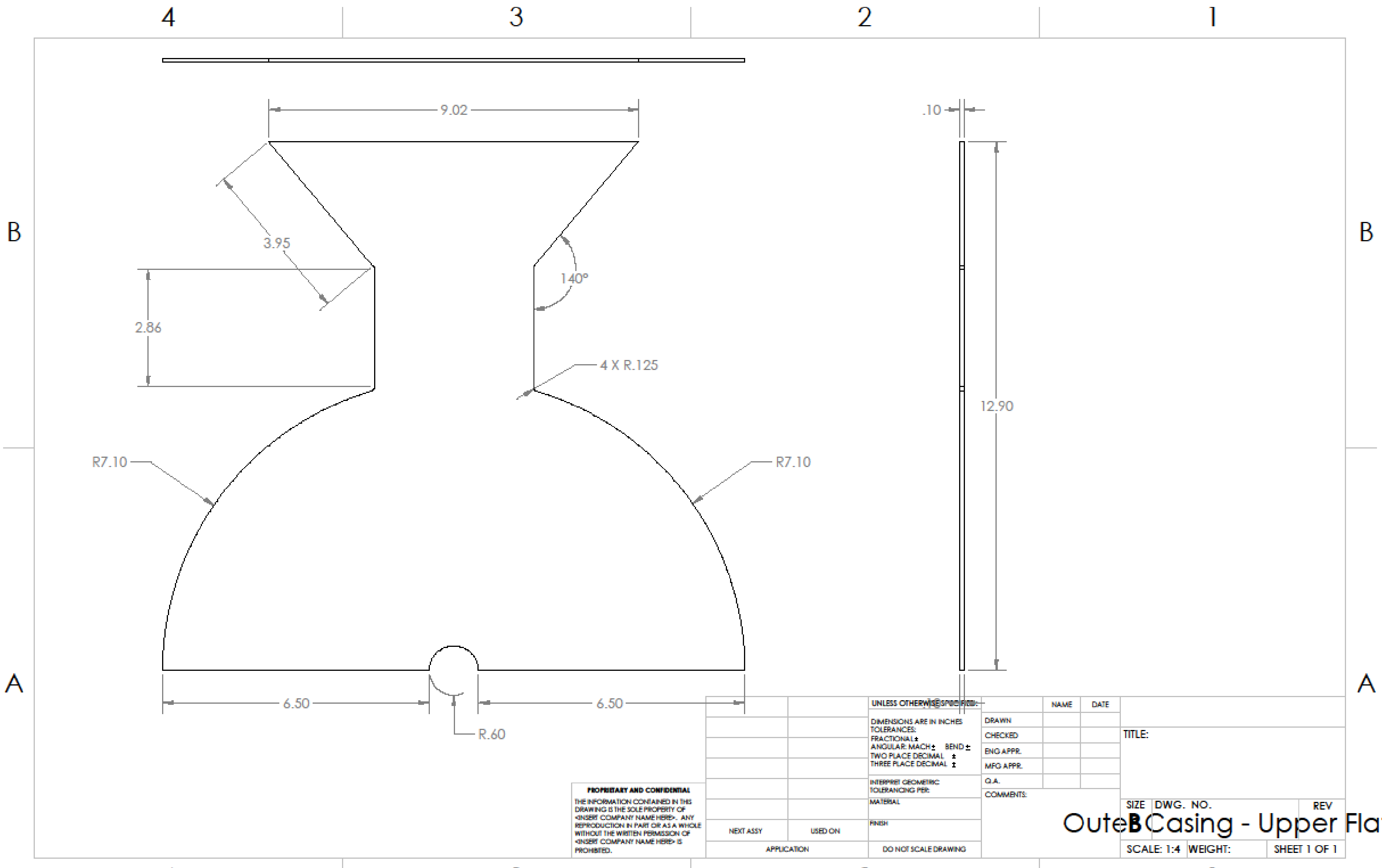
9.02
3.95
2.86
140°
4 X R.125
R7.10
R7.10
6.50
6.50
R.60
.10
12.90
PROPRIETARY AND CONFIDENTIAL
THE INFORMATION CONTAINED IN THIS DRAWING IS THE SOLE PROPERTY OF <INSERT COMPANY NAME HERE>. ANY REPRODUCTION IN PART OR AS A WHOLE WITHOUT THE WRITTEN PERMISSION OF <INSERT COMPANY NAME HERE> IS PROHIBITED.
NEXT ASSY
USED ON
APPLICATION
UNLESS OTHERWISE SPECIFIED:
DIMENSIONS ARE IN INCHES
TOLERANCES:
FRACTIONAL±
ANGULAR: MACH± BEND ±
TWO PLACE DECIMAL ±
THREE PLACE DECIMAL ±
INTERPRET GEOMETRIC TOLERANCING PER:
MATERIAL
FINISH
DO NOT SCALE DRAWING
NAME
DATE
DRAWN
CHECKED
ENG APPR.
MFG APPR.
Q.A.
COMMENTS:
TITLE:
SIZE
DWG. NO.
REV
B
Outer Casing - Upper Flat
SCALE: 1:4
WEIGHT:
SHEET 1 OF 1

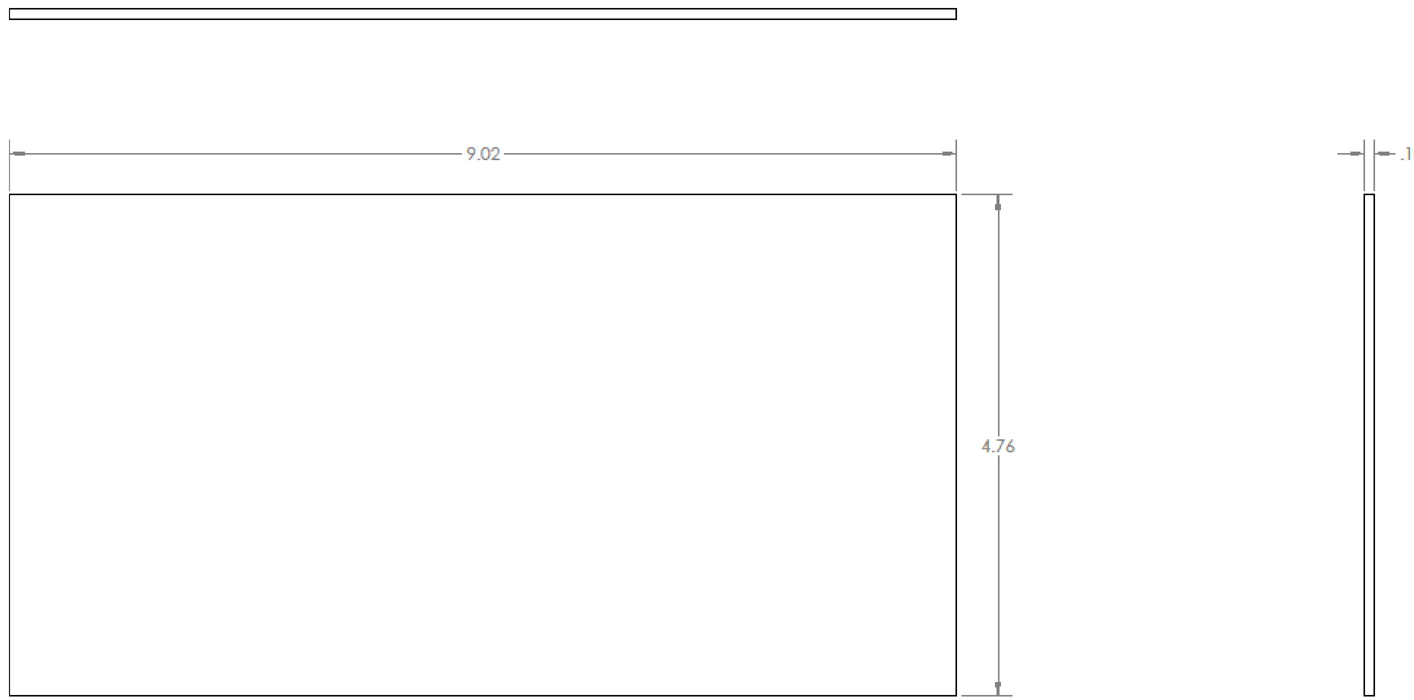

		UNLESS OTHERWISE SPECIFIED:		NAME	DATE	
		DIMENSIONS ARE IN INCHES TOLERANCES: FRACTIONAL± ANGULAR: MACH± BEND ± TWO PLACE DECIMAL ± THREE PLACE DECIMAL ±	DRAWN			TITLE:
			CHECKED			
			ENG APPR.			
			MFG APPR.			
		INTERPRET GEOMETRIC TOLERANCING PER:	Q.A.			
		MATERIAL	COMMENTS:			SIZE B DWG. NO. Funnel Cover REV
NEXT ASSY	USED ON	FINISH				
APPLICATION		DO NOT SCALE DRAWING				SCALE: 1:1 WEIGHT: SHEET 1 OF 1

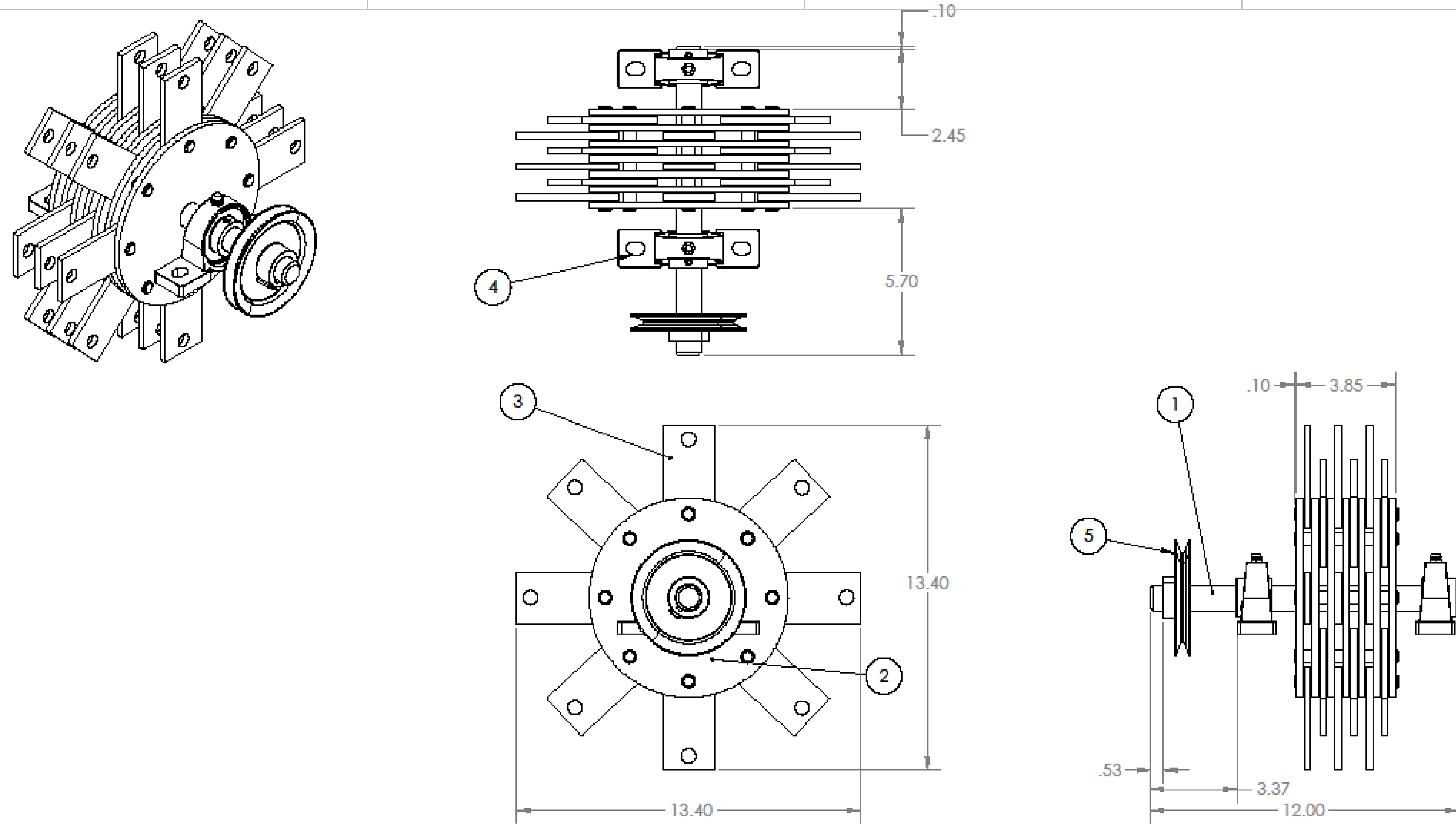

ITEM NO.	PART NUMBER	PART NAME	DESCRIPTION	QTY.
1	1346K31	Drive Shaft		1
2	Rotor Disc			7
3	Hammer Subassembly			8
4	6494K14	Bearing		2
5	Shaft Assembly - Pulley 1 in new			1

PROPRIETARY AND CONFIDENTIAL

THE INFORMATION CONTAINED IN THIS DRAWING IS THE SOLE PROPERTY OF <INSERT COMPANY NAME HERE>. ANY REPRODUCTION IN PART OR AS A WHOLE WITHOUT THE WRITTEN PERMISSION OF <INSERT COMPANY NAME HERE> IS PROHIBITED.

NEXT ASSY | USED ON

APPLICATION

UNLESS OTHERWISE SPECIFIED:

DIMENSIONS ARE IN INCHES
TOLERANCES:
FRACTIONAL±
ANGULAR: MACH± BEND ±
TWO PLACE DECIMAL ±
THREE PLACE DECIMAL ±

INTERPRET GEOMETRIC TOLERANCING PER:

MATERIAL

FINISH

DO NOT SCALE DRAWING

	NAME	DATE
DRAWN		
CHECKED		
ENG APPR.		
MFG APPR.		
Q.A.		

COMMENTS:

TITLE:

SIZE | DWG. NO. | REV

Bhaft Assembly

SCALE: 1:8 | WEIGHT: | SHEET 1 OF 1

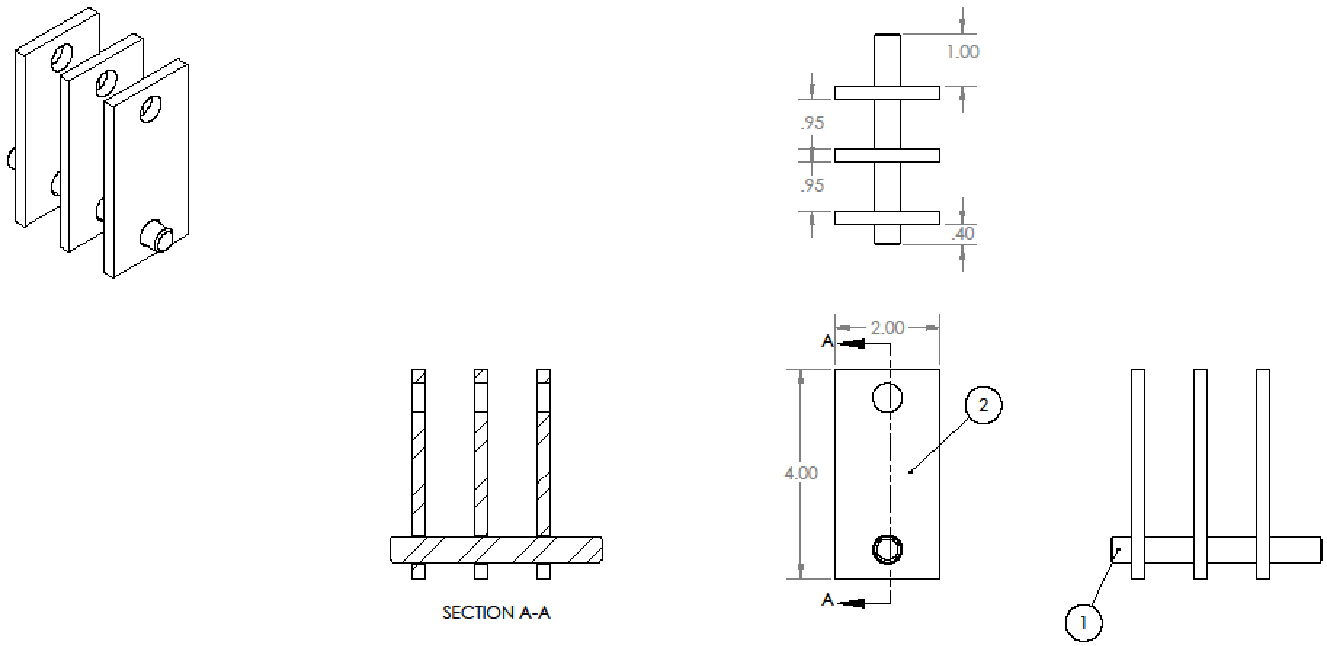

ITEM NO.	PART NUMBER	PART NAME	DESCRIPTION	QTY.
1	1346K11	Hammer Pin		1
2	Hammer			3

PROPRIETARY AND CONFIDENTIAL

THE INFORMATION CONTAINED IN THIS DRAWING IS THE SOLE PROPERTY OF <INSERT COMPANY NAME HERE>. ANY REPRODUCTION IN PART OR AS A WHOLE WITHOUT THE WRITTEN PERMISSION OF <INSERT COMPANY NAME HERE> IS PROHIBITED.

NEXT ASSY | USED ON

APPLICATION

UNLESS OTHERWISE SPECIFIED:
DIMENSIONS ARE IN INCHES
TOLERANCES:
FRACTIONAL ±
ANGULAR: MACH ± BEND ±
TWO PLACE DECIMAL ±
THREE PLACE DECIMAL ±

INTERPRET GEOMETRIC TOLERANCING PER:
MATERIAL
FINISH
DO NOT SCALE DRAWING

	NAME	DATE
DRAWN		
CHECKED		
ENG APPR.		
MFG APPR.		
Q.A.		

COMMENTS:

TITLE:

SIZE B | DWG. NO. Hammer Subassembly | REV

SCALE: 1:2 | WEIGHT: | SHEET 1 OF 1

SOLIDWORKS Educational Product. For Instructional Use Only.

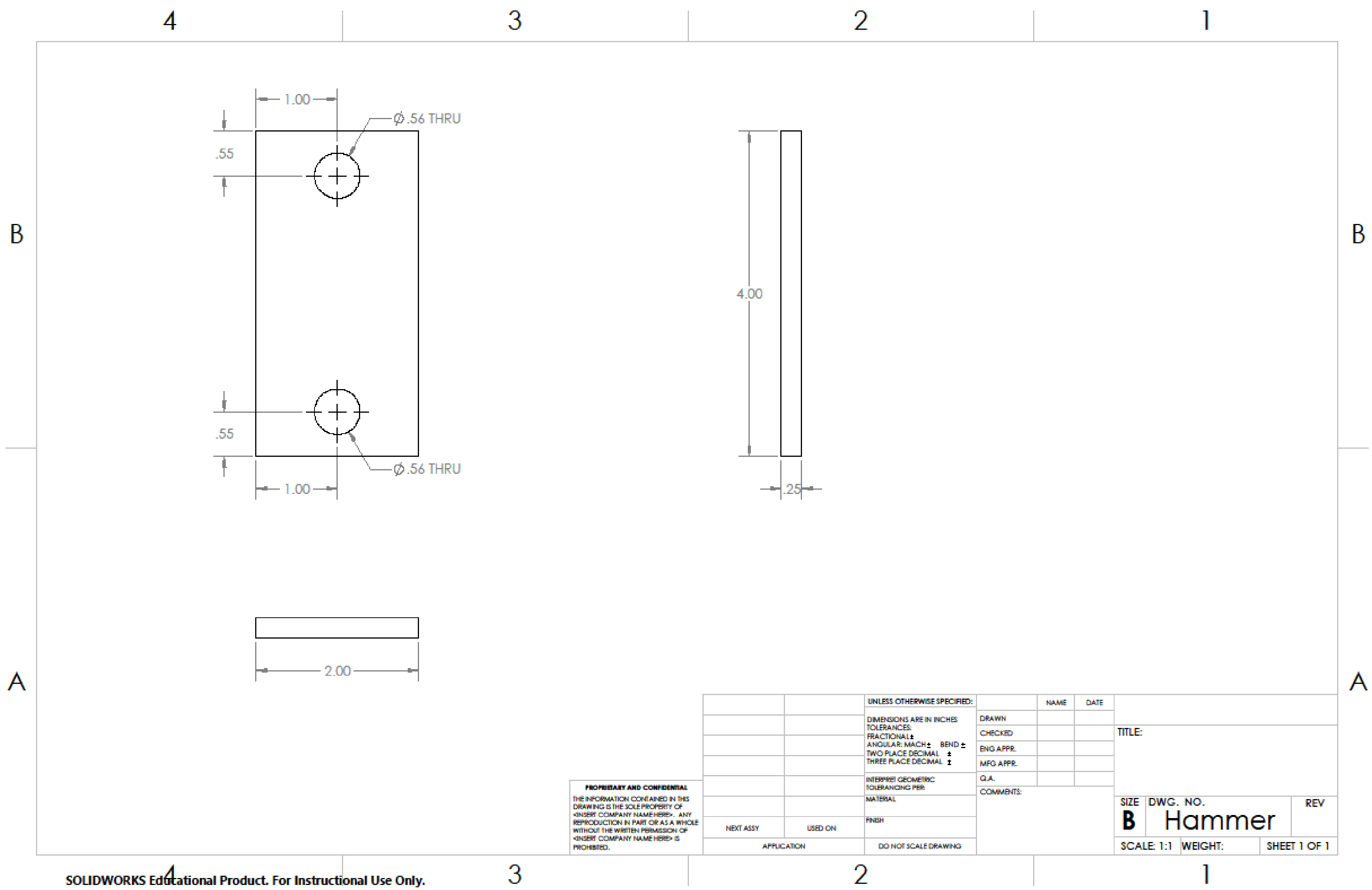

1.00
Ø.56 THRU
.55
4.00
.25
2.00
UNLESS OTHERWISE SPECIFIED:
DIMENSIONS ARE IN INCHES
TOLERANCES:
FRACTIONAL±
ANGULAR: MACH± BEND ±
TWO PLACE DECIMAL ±
THREE PLACE DECIMAL ±
INTERPRET GEOMETRIC TOLERANCING PER:
MATERIAL
FINISH
DO NOT SCALE DRAWING
NAME
DATE
DRAWN
CHECKED
ENG APPR.
MFG APPR.
Q.A.
COMMENTS:
TITLE:
SIZE
B
DWG. NO.
Hammer
REV
SCALE: 1:1
WEIGHT:
SHEET 1 OF 1
PROPRIETARY AND CONFIDENTIAL
THE INFORMATION CONTAINED IN THIS DRAWING IS THE SOLE PROPERTY OF <INSERT COMPANY NAME HERE>. ANY REPRODUCTION IN PART OR AS A WHOLE WITHOUT THE WRITTEN PERMISSION OF <INSERT COMPANY NAME HERE> IS PROHIBITED.
NEXT ASSY
USED ON
APPLICATION
SOLIDWORKS Educational Product. For Instructional Use Only.

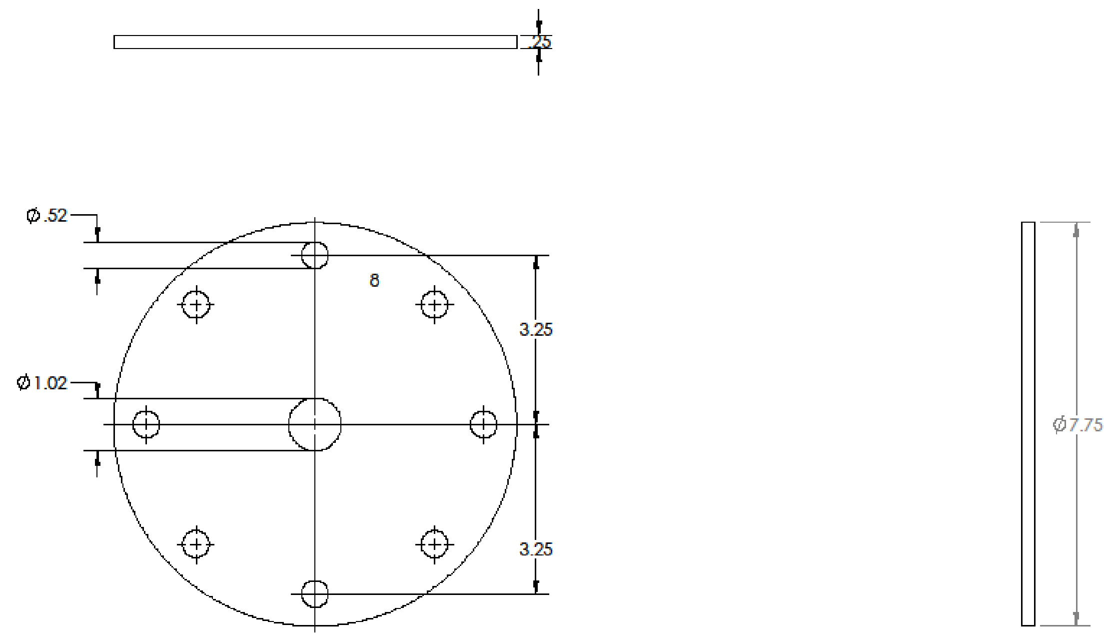

		UNLESS OTHERWISE SPECIFIED:		NAME	DATE	
		DIMENSIONS ARE IN INCHES TOLERANCES: FRACTIONAL± ANGULAR: MACH± BEND ± TWO PLACE DECIMAL ± THREE PLACE DECIMAL ±	DRAWN			TITLE:
			CHECKED			
			ENG APPR.			
			MFG APPR.			
		INTERPRET GEOMETRIC TOLERANCING PER:	Q.A.			
		MATERIAL	COMMENTS:			SIZE B DWG. NO. Rotor Disc REV
NEXT ASSY	USED ON	FINISH				
APPLICATION		DO NOT SCALE DRAWING				SCALE: 1:2 WEIGHT: SHEET 1 OF 1

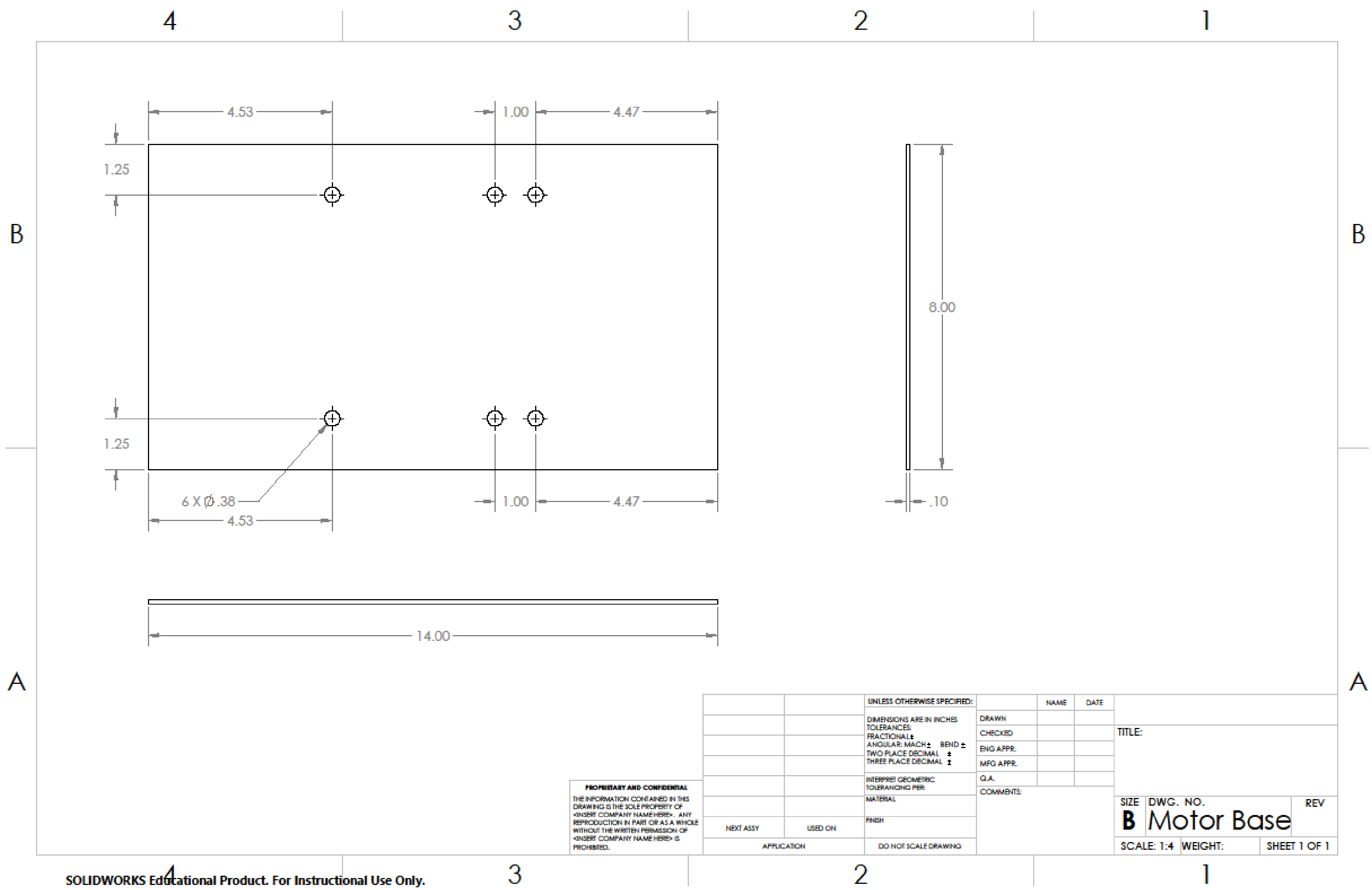
4.53
1.00
4.47
1.25
1.25
6 X Ø.38
8.00
.10
14.00
UNLESS OTHERWISE SPECIFIED:
DIMENSIONS ARE IN INCHES
TOLERANCES:
FRACTIONAL±
ANGULAR: MACH± BEND ±
TWO PLACE DECIMAL ±
THREE PLACE DECIMAL ±
INTERPRET GEOMETRIC TOLERANCING PER:
MATERIAL
FINISH
NEXT ASSY
USED ON
APPLICATION
DO NOT SCALE DRAWING
NAME
DATE
DRAWN
CHECKED
ENG APPR.
MFG APPR.
Q.A.
COMMENTS:
TITLE:
SIZE
B
DWG. NO.
Motor Base
REV
SCALE: 1:4
WEIGHT:
SHEET 1 OF 1
PROPRIETARY AND CONFIDENTIAL
THE INFORMATION CONTAINED IN THIS DRAWING IS THE SOLE PROPERTY OF <INSERT COMPANY NAME HERE>. ANY REPRODUCTION IN PART OR AS A WHOLE WITHOUT THE WRITTEN PERMISSION OF <INSERT COMPANY NAME HERE> IS PROHIBITED.
SOLIDWORKS Educational Product. For Instructional Use Only.